8-2018

Metabolic Plasticity in the Cellular Stress Response

Ying Li
East Tennessee State University

Metabolic Plasticity in the Cellular Stress Response

A dissertation

presented to

the faculty of the Department of Biomedical Sciences

East Tennessee State University

In partial fulfillment

of the requirements for the degree

Doctor of Philosophy in Biomedical Sciences

---

by

Ying Li

August 2018

Gary Wright, Ph.D., Co-Chair

Jonathan Peterson, Ph.D., Co-Chair

Kenneth Ferslew, Ph.D.

Krishna Singh, Ph.D.

Stacy Brown, Ph.D.

Douglas Thewke, Ph.D.

Keywords: hypoxic heart, cardioprotection, HIF-1α, glucose metabolism, metabolite, stable isotope, metabolomics, CTRP3, receptor, lipid metabolism

ABSTRACT

Metabolic Plasticity in the Cellular Stress Response

by

Ying Li

Changes to the metabolism of the cardiomyocyte are driven by complex signaling pathways in order to adjust to stress. For instance, HIF-1α is classically known to upregulate glycolytic metabolism to compensate for oxygen deficiency. Other important effects upon glucose metabolism, which we investigate here more extensively, were also observed. Hearts derived from mice with the cardiac-restricted expression of a stabilized form of HIF-1α are remarkably ischemia stress-tolerant. Here, stable isotope-resolved metabolomic analyses were utilized to investigate glucose cardiometabolism remodeling by HIF-1α during ischemia. We found that ^{13}C-lactate accumulation was significantly elevated in HIF-1α expressing hearts while paradoxically glycogen was maintained to a remarkable extent during an ischemic time course. These findings suggested an unexpected source of glucose in HIF-1α hearts during global ischemia. Accordingly, the presence of gluconeogenesis in hearts was evaluated. Indeed, gluconeogenic intermediates (i.e. m+3) including glucose-6-phosphate [m+3], fructose-6-phosphate [m+3], and fructose 1,6-bisphosphate [m+3] were observed at significantly elevated levels in the ischemic HIF-1α heart. Collectively, these data establish the surprising finding that HIF-1α supports active gluconeogenesis in the heart during ischemia.

As less is known regarding the effects of CTRP3 we first tested whether CTRP3 overexpression would protect the ischemic heart. Our data indicate that CTRP3 failed to confer ischemic tolerance in heart *ex vivo*. However, we were able to show that CTRP3 protected the liver from lipid-induced stress and prevented hepatic lipid accumulation. To further investigate the mechanisms of hepatic protective effect mediated by CTRP3, we identified the receptor and established that CTRP3 increases oxygen consumption in response to lipid overloaded.

In summary, these data indicate that targeted metabolic rearrangements within cardiomyocyte/hepatocyte holds promise for the alleviation of common pathological conditions.

TABLE OF CONTENTS

Page

LIST OF TABLES

LIST OF FIGURES

CHAPTER 1

INTRODUCTION

Metabolic disturbances have been commonly characterized in diverse diseases such as obesity, diabetes, ischemic heart disease, and nonalcoholic fatty liver disease (NAFLD) (Ahmed et al. 2012; Ballestri et al. 2016). The mortality rates of heart disease and stroke remain the top and third leading causes of death, respectively, in the United States over the last four decades (1975-2015).

During Myocardial infarction blood flow to the heart is stopped whereas during a stroke blood flow to the brain is inhibited. In both cases the resulting hypoxia is a major component involved in the severity of these diseases. Thus, identifying the cellular response to the low oxygen levels of great clinical importance.

HIF-1α

The transcription factor hypoxia inducible factor-1 (HIF-1) functions as a principal regulator of the cellular response to hypoxia. HIF-1 is a heterodimeric complex comprised of O_2-labile *α* subunit (120 kDa) and the constitutively expressed *β* subunit (91-94 kDa) (Wang and Semenza 1995; Wang et al. 1995). When oxygen is present, prolyl hydroxylase (PHDs) hydroxylate at the oxygen-dependent degradation (ODD) domain of HIF-1α at proline 402 and proline 564, which targets the protein for rapid degradation. Insufficient O_2 tension promotes HIF-1α stability by inhibiting the activity of PHDs (Salceda and Caro 1997; Huang et al. 1998; Maxwell et al. 1999; Ivan et al. 2001; Jaakkola et al. 2001). In addition, during hypoxia, HIF-1α transcription is stimulated. Briefly, when oxygen is present factor inhibiting HIF-1 (FIH-1) hydroxylates asparagine

803 at the c-terminal transactivation domains (TAD-C) of HIF-1α, which blocks HIF-1α from interacting with the coactivators CREB binding protein (CBP) and 300-kilodalton coactivator protein (p300) for its transcriptional activity (Mahon et al. 2001; Dames et al. 2002; Lando, Peet, Gorman, et al. 2002; Lando, Peet, Whelan, et al. 2002; Elkins et al. 2003; Freedman et al. 2002; Hewitson et al. 2002). However, during hypoxia HIF-1α accumulation facilitates the formation of functional heterodimeric transcription factor HIF-1 with the coactivators and binds to the core DNA recognition sequence 5′-RCGTG-3′ within hypoxia response elements (HRE), and activities full transcriptional activity (Forsythe et al. 1996; Semenza et al. 1996; Wang et al. 1995). Thus, the stability and activity of HIF-1α are closely regulated by oxygen availability. HIF-1α, in turn, initiates regulation of a wide variety of downstream target genes that mediate the cellular adaptation to hypoxia.

The role of HIF-1α was first established in erythropoiesis (Semenza and Wang, 1992; Wang and Semenza, 1996), and later in angiogenesis (Liu et al. 1995; Forsythe et al. 1996; Gerber et al. 1997), metabolism (Iyer et al. 1998; Seagroves et al. 2001), cell proliferation and apoptosis (Carmeliet et al. 1998). In many pathological settings, the HIF-1 signaling pathway is activated in order to cope with hypoxic stress. For instance, HIF-1α is essential factor for inflammatory pathogenesis mediated by the neutrophils and macrophages (Cramer et al. 2003). It has recently been revealed that inflammatory genes are promoted by HIF-1α-mediated metabolic reprogramming by in macrophages, dendritic cells (DCs), T-cells, and neutrophils (Corcoran and O'Neill 2016). HIF-1α is also associated frequently with cancer as a result of intratumoral hypoxia and genetic alterations (Semenza 2003). Evidence is observed that HIF-1α is

overexpressed in solid tumors (Semenza 2003; Bertout et al. 2008). Stabilized HIF-1α has also been described to induce the expression of vascular endothelial growth factor (VEGF) in atherosclerotic lesions (Vink et al. 2007).

HIF-1α has been shown to confer cellular protection in ischemic heart. For example, In the setting of ischemic preconditioning (IPC), short-episodes of ischemia and reperfusion confer cardioprotection during subsequent prolonged injury of ischemia-reperfusion (Murry et al. 1986; Rosenberg et al. 2018). The acute cardioprotection was lost in HIF-1α heterozygous-null or knockout mice, indicating that HIF-1α activity is essential for the potential benefits from IPC stimulus (Cai et al. 2008; Sarkar et al. 2012). Other downstream targets of HIF-1α such as nitric oxide synthase (NOS), vascular endothelial growth factor (VEGF), and heme oxygenase-1 (HO-1), have been shown to promote tolerance to ischemic stress in mice hearts or isolated cardiomyocytes (Guo et al. 1999; Jung et al. 2000; Ockaili 2005; Li et al. 2007).

In recent studies, we have utilized a transgenic adult mouse with a cardiac-specific, oxygen-stabilized, and doxycycline(Dox)-off HIF-1α expression (HIF-1α-PPN) to probe the roles of HIF-1α in ischemic tolerance. The results show that HIF-1α elicits robust protection in the mouse hearts subjected to the global ischemia, *ex vivo* (J. Wu et al. 2013). These studies also revealed evidence that glucose metabolism was remodeled in the HIF-1α hearts (J. Wu et al. 2013). We have previously identified several HIF-1α-induced metabolic pathways contributing to the ischemic cardioprotection.(J. Wu et al. 2015) In HIF-1α-expressing hearts, the purine nucleotide cycle (PNC) was found to be upregulated. The PNC preserves the adenylate energy

charge and protects myocardia from toxic accumulation of adenosine during ischemia. The nucleotide salvage enzyme hypoxanthine phosphoribosyl transferase (HPRT) was also found to be induced by HIF-1α. HPRT recycles the nucleotide degradation product hypoxanthine and prevents potential damage from hydrogen peroxide (H_2O_2) generated by xanthine oxidase during reperfusion of ischemic heart (J. Wu et al. 2015).

CTRP3

CTRP3 also functions as a metabolic regulator and has versatile effects in multi-type tissues (reviewed in chapter 3) (Li et al. 2017). C1q TNF-related protein-3 (CTRP3) is a distinctive member of highly conserved CTRP family that comprises a suite of paralogs of adiponectin (Wong et al. 2004). Several reports have suggested that CTRP3 contributes to cardio-metabolic regulation in cardiovascular diseases. For example, myocardial infarction (MI) was shown to lead to lower CTRP3 tissue expressions and plasma CTRP3 level (Yi et al. 2012; D. Wu et al. 2015). Infusions of globular CTRP3 or CTRP3 adenovirus improved functional recovery of the left ventricle and prevented pathological remodeling of fibrosis following MI injury in myocardia (Yi et al. 2012; D. Wu et al. 2015). The anti-fibrotic effect of CTRP3 was induced by inhibitions of phosphorylation of Smad-3 in post-infarct myocardia (D. Wu et al. 2015). The vessels formation in the infarcted border zone has been shown to be promoted through CTRP3-induced phosphorylations of Akt, HIF-1α, and VEGF in the myocardium (Yi et al. 2012). Finally recent studies showed that the treatment of CTRP3 ameliorates mitochondrial dysfunction after hypoxia-reoxygenation injury in neonatal cardiomyocytes (Zhang et al. 2017).

Taken together, these data suggested the potential of CTRP3 as a prospective modulator for ischemic heart disease. We therefore sought to probe the role of CTRP3 in cardioprotection. A transgenic mouse model of CTRP3 overexpression was used in this study. WT and CTRP3 overexpressing hearts were retrograde perfused via the aorta and subjected to 30 mins of ischemia followed by 30 mins of reperfusion, *ex vivo*. Subsequent recovery of function and tissue viability were assessed upon reperfusion of heart. Our results showed that recovery of left ventricular developed pressure (LVDP) in CTRP3 overexpressing hearts after ischemia, was not significantly better (22% vs 39%, $P>0.05$). (Figure 1.1) In addition, there are no significant differences in tissue viability after reperfusion between WT and CTRP3 overexpressing hearts. (Figure 1.2) These results indicated that CTRP3 does not confer specific cardioprotection at least in this model of hypoxic injury.

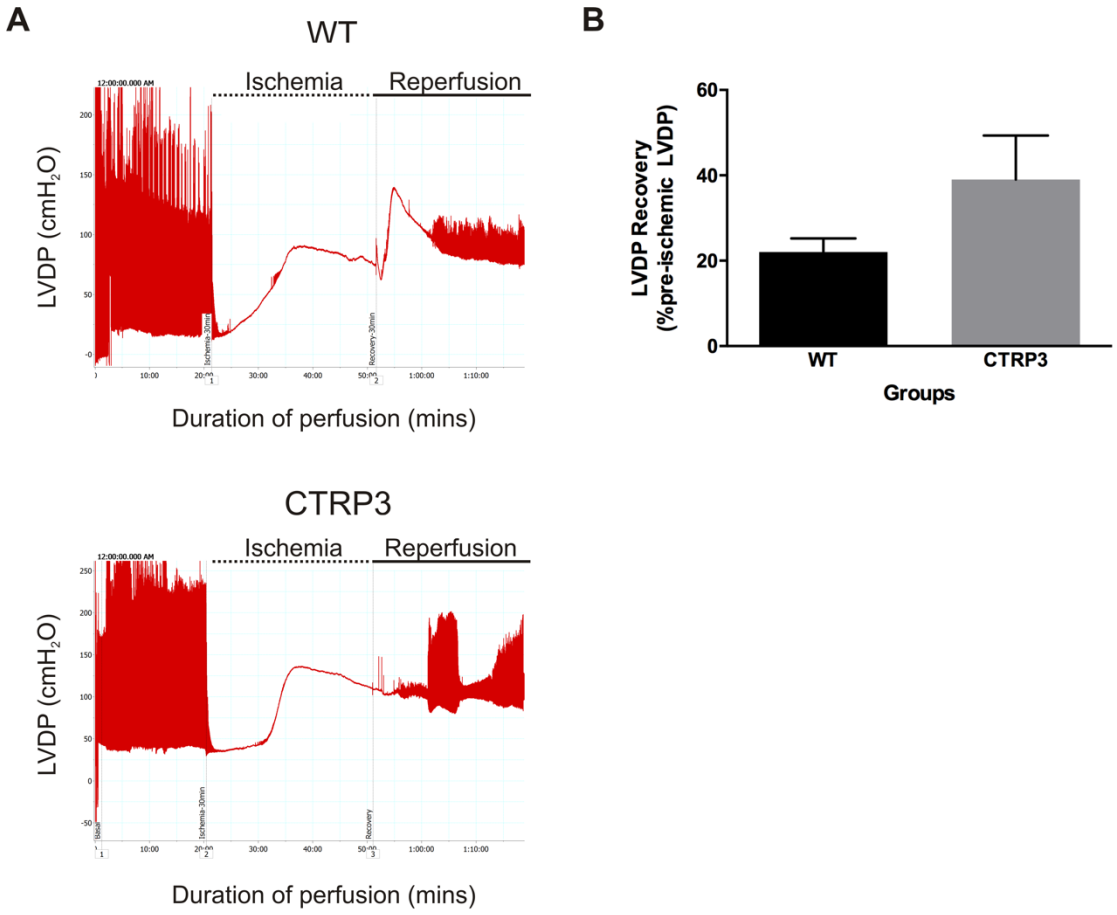

Figure 1.1: *Cardiac Response to Ischemic Stress*. A. condensed pressure tracings were shown from Langendorff-perfused hearts derived from wildtype (WT) and CTRP3 overexpressing (CTRP3) mice. Following 20 mins of pre-ischemic perfusion, hearts were subjected to 30 mins of ischemia and subsequently to 30 mins of reperfusion and left ventricular developed pressure (LVDP) was measured. B. quantification of the recovery of LVDP after ischemia, expressed as a percent of pre-ischemic LVDP is shown. $P > 0.05$ vs. WT; n = 3-5 hearts.

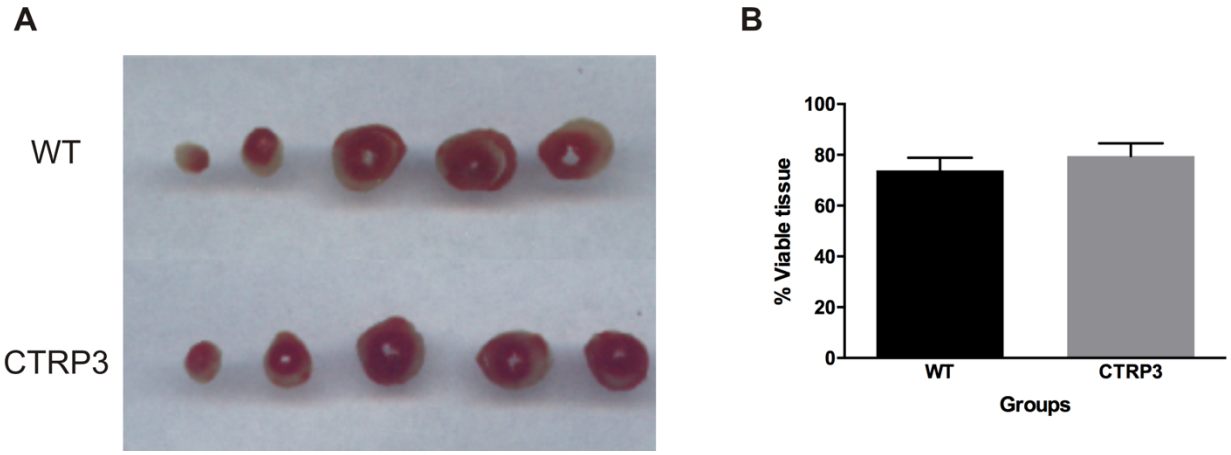

Figure 1.2: *Myocardial Ischemic Injury Indicated by Triphenyltetrazolium Chloride (TTC) Staining*. A. Langendorff-perfused hearts derived from wildtype (WT) and CTRP3 overexpressing (CTRP3) mice were collected following 30 mins of reperfusion after 30 mins of ischemia. Viable (red) and inviable tissue (pale) were shown in sectioned hearts. B. quantification of viable tissue, expressed as a percent of each heart tissue. $P > 0.05$ vs. WT; n = 3-5 hearts.

By comparison, CTRP3 appears to protect the liver from lipid-induced stress and regulate hepatic metabolism. For example, we initially established evidence that CTRP3 maintains glucose homeostasis by suppression of hepatic gluconeogenesis via protein kinase B (Peterson et al. 2010). Insulin resistance and dyslipidemia have emerged as the most predominant features and pathological basis of NAFLD. NAFLD refers to a spectrum of pathological phenotypes comprising simple steatosis, nonalcoholic steatohepatitis (NASH), fibrosis, and cirrhosis. Accumulation of hepatocellular lipid metabolites is recognized as the first “hit” of complex mechanisms of NAFLD to induce the ultimate liver injury (Perla et al. 2017). The net lipid flux is enhanced and causes dysregulation of lipid and lipoprotein metabolism, eventually developing into the overload of lipid in hepatocytes. The excessive lipid retention leads to insulin resistance via the stimulation of glucose secretion and inhibition of the

phosphorylation of the insulin receptor substrate (IRS)-1/ IRS-2 in liver (Perla et al. 2017).

Interestingly, we have found that CTRP3 overexpressing efficiently limits the development of high fat diet-induced hepatic steatosis and insulin resistance 48. This effect is associated with the suppression of hepatic triglyceride synthesis enzymes (Peterson et al. 2013). Consistent with *in vivo* data, rCTRP3 treatment reduced fatty acid synthesis and lipid accumulation in rat H4IIE hepatocytes (Peterson et al. 2013). In CTRP3 knockout mice, however, hepatic triglycerides were elevated after high fat diet fed.(Wolf et al. 2016) In contrast, these CTRP3-induced metabolic changes have not been found in mice fed with a low fat diet (Peterson et al. 2013; Wolf et al. 2016). Collectively, although these data indicate that CTRP3 regulate hepatic lipid metabolism in response to high fat diet-induced stress, the mechanisms deserve to be further investigated. Thus it needs to be clarified whether CTRP3 acts directly or is mediated by potential receptors in hepatocytes.

Overall Hypothesis and Specific Aims

The overall goal of this dissertation was to investigate mechanisms to manipulate the cellular response to stress to prevent/treat disease. Based on the discussion above, this study aimed to identify unique metabolic mechanisms induced by HIF-1α and CTRP3 that respond to stress conditions. Aim 1) was to determine the cardiometabolic flux, particularly as it relates to glucose metabolism and to further elucidate the mechanisms responsible for HIF-1α's ischemic protection. In chapter 2 we describe how we used metabolomics analysis to show that glucose metabolism was

different in the HIF-1α-expressing heart during ischemia. Specifically, we observed convincing evidence that HIF-1α induces gluconeogenic pathway. These studies have identified a number of potential mechanisms to explain the cardioprotective effects of HIF-1α. Aim 2) was to investigate the heart and hepatic protective effects of CTRP3 based upon remodeling of lipid metabolism to high fat diet-induced stress. In chapter 3 we review CTRP3 function and regulation. In chapter 4 we demonstrate that CTRP3 promotes fatty acid utilization following lipid overload *in vitro* and identified a putative receptor for CTRP3.

CHAPTER 2

HIF-1α IN HEART: EVIDENCE OF GLUCONEOGENESIS IN MYOCARDIUM DURING ISCHEMIA

Li Y [1], Warmoes MO [2], Lin PH [2], Peterson JM [1,3], Bolton NW [1] and Wright GL [1].

[1] Department of Biomedical Sciences, Quillen College of Medicine, East Tennessee State University, Johnson City, TN [2] Center for Environmental and Systems Biochemistry, Markey Cancer Center, University of Kentucky, Lexington, KY
[3] Department of Health Sciences, College of Public Health, East Tennessee State University, Johnson City, TN

ABSTRACT

Hypoxia inducible-1α (HIF-1α) is a transcription factor that directs multiple cellular changes to adapt to low oxygen conditions. Previously we have shown that hearts derived from mice with the cardiac-restricted overexpression of HIF-1α are remarkably ischemia stress-tolerant (4). The current studies are designed to further probe the metabolic rearrangements directed by HIF-1α, particularly as they relate to glucose metabolism. U-$^{13}C_6$ glucose was loaded into Wild-type (WT) and HIF-1α expressing hearts for 30 mins, *ex vivo*. Subsequently the hearts were subjected to global zero-flow ischemia (0, 5, 10, 15, and 30 mins) and flash frozen. Polar metabolites were subsequently extracted. In parallel, myocardial protein was collected for western blot analysis. The incorporation of ^{13}C in the metabolome reservoir of the heart was determined by Nuclear Magnetic Resonance (NMR) spectroscopy and Ion-Cyclotron Resonance coupled Mass Spectrometry (ICR-MS). Indicating enhanced glycolytic flux, ^{13}C-lactate accumulated in HIF-1α hearts and WT hearts as ischemia progressed but was significantly elevated in the HIF-1α hearts. Glucose reserves (i.e. glycogen) are maintained to a remarkable extent at 5, 10 and 30 mins of ischemia in HIF-1α hearts while, in stark contrast, glycogen is largely depleted after 5 mins of ischemia in WT hearts. ^{13}C-Glucose incorporation into

glycogen is maintained at pre-ischemic levels in HIF-1α hearts for up to 30 mins of ischemia while becoming undetectable in WT hearts. These findings suggested an unexpected source of glucose in the ischemic HIF-1α heart. Accordingly, the presence of gluconeogenesis in hearts was evaluated. Indeed, IC-MS detected gluconeogenic intermediates (i.e. m+3) including glucose-6-phosphate [m+3], fructose-6-phosphate [m+3], and fructose-1-6-bisphosphate [m+3] at statistically elevated levels in HIF-1α hearts during ischemia. Taken together, these data establish the surprising finding that HIF-1α supports active gluconeogenesis in the heart during ischemia.

INTRODUCTION

Hypoxia inducible factor-1α (HIF-1α) is "master regulatory" transcription factor that governs the expression of over 120 genes, including those functioning metabolic adaptation, angiogenesis, tumorigenesis, inflammation, and apoptosis (1). HIF-1α is functional as a heterodimer composed of the oxygen-regulated α-subunit and a constitutively expressed β-subunit (also known as ARNT). The heterodimers bind to hypoxia response elements (HREs) to regulate nuclear transcriptional activity of target genes.

The stability of HIF-1α is regulated by the proline hydroxylase domain-containing proteins (PHD) which serve as oxygen sensors. HIF-1α is subjected to hydroxylation which leads to its ubiquitination by the von Hipple-Lindau protein (pVHL) for consequent proteasomal degradation (2). The activity of the dioxygenase PHDs diminishes with oxygen shortage and the reduced post-translation hydroxylation of HIF-1α results in its stabilization. Hypoxia also lowers the activity of the factor inhibiting HIF (FIH), an

asparaginyl hydroxylase which inhibits HIF-1α transcriptional activity by preventing recruitment of co-activator (3). In these studies, we use a transgenic mouse model containing HIF-1α cDNA with alanine substitutions at Pro402, Pro564, and Asn803 as described in our previous studies (4, 5). This HIF-1α construct displays full transcriptional activity and the protein is stabilized under normoxic conditions. Moreover, HIF-1α protein (termed as "HIF-1α-PPN) is yoked to a TET-off γ-myosin promoter effecting cardiomyocyte-specific expression controlled by a doxycycline-diet.

Hypoxia is fundamental stimuli that initiates a number of cellular adaptive responses in the myocyte. In heart, it has been widely known that flux through glycolysis is stimulated and lactate production is preferred while fatty acid oxidation is actively suppressed during low oxygen availability. Glucose transportation is also increased by HIF-1α through an upregulation of GLUT-1 (6). During chronic hypoxia, reduced mitochondrial metabolism is a strategy to maintain redox homeostasis and cell survival against excessive levels of reactive oxygen species (ROS). For example, pyruvate dehydrogenase kinase 1 (PDK1) prevents the conversion from pyruvate to acetyl-CoA through the tricarboxylic acid (TCA) cycle, which allows the shift from oxidative to glycolytic metabolism. The gene encoding PDK1 protein is directly activated by HIF-1α, thus shifting glucose from the oxidative to the fermentative pathways (7, 8).

In a transgenic murine model where HIF-1α is stably expressed in heart, we previously demonstrated remarkable protection against ischemia-reperfusion injury, *ex vivo*, and anaerobic fumarate respiration which preserves mitochondrial polarization during anoxia (4). Further investigation revealed that AMP deaminase (AMPD), the entry

point of the purine nucleotide cycle (PNC), is upregulated by HIF-1α, which results in inhibiting production of adenosine in myocardium during ischemia and favors production of fumarate to support the above mentioned fumarate reductase activity (5). These results indicated that HIF-1α regulates nucleotide metabolism as a compensatory response to metabolic perturbations which provides fumarate and conserves the nucleotide pool during hypoxia (5). Despite these recent advances in understanding the mechanisms of cardioprotection induced by HIF-1α during ischemic stress, the role of remodeling of glucose metabolism by HIF-1α remains unclear. These studies were undertaken to further probe the cardio-specific role of HIF-1α in cardioprotection, especially as they are related to glucose metabolism.

Metabolomics is a platform enabling the simultaneous qualitative measurement of metabolites in biological samples. ^{1}H NMR and MS techniques are two popular analytical techniques applied to the analysis of the metabolic profile (9, 10). Here, a metabolomics approach based on ^{1}H NMR and MS was used to quantify metabolite levels in heart during ischemia and to probe the underlying metabolic mechanisms of cardioprotection elicited by HIF-1α. Studies were performed in perfused mouse hearts that had undergone ischemia following the incorporation of Uniform-$^{13}C_6$-(U-$^{13}C_6$) glucose, with subsequent determination of metabolites downstream in glucose metabolism.

EXPERIMENTAL PROCEDURES

Animals. Male B6C3F1 mice contain a doxycycline-restraining HIF-1α transgene (HIF-1α-PPN) that has been described previously (4). These HIF-1α-PPN mice are fed daily with a doxycycline-loaded diet (625 mg/kg, Harlan Research Laboratories, Madison,

WI). HIF-1α specific stably expressing in mouse heart is elicited after 5-7 days following switching to regular diet. All wildtype and HIF-1α-expressing mice were used for the study at 3.5-4.5 months of age. Procedures on animal experiments were performed in accordance with the regulations issued by the East Tennessee State University Committee on Animal Care.

Langendorff perfusion. Hearts were retrograde perfused through the aorta using methods described previously. [4] Krebs-Henseleit buffer containing (mM): 118.5 NaCl, 4.7 KCl, 1.2 $MgSO_4$, 1.2 KH_2PO_4, 24.8 $NaCHO_3$, 2.5 $CaCl_2$, and 10.6 glucose (U-$^{13}C_6$-glucose, Cambridge Isotope Laboratories, Inc. Andover, MA) that has been made and then warmed at 37°C using refrigerated circulating bath (VWR, Radnor, PA) during perfusion. The buffer was equilibrated with mix of 95% O_2/5% CO_2 for at least 20 mins. U-$^{13}C_6$-glucose was infused of 30 mins. Then hearts are subjected to global ischemia for 0, 5, 10, 15 or 30 mins, respectively. Hearts were flash-frozen by clamping with a set of Wollenberger tongs that were prechilling in liquid nitrogen, where upon the hearts were ground into a fine powder using a mortar and pestle with liquid N_2.

Preparation of sample. The frozen powdered heart samples were quenched in a cold cocktail of CH_3CN:ddH_2O=2:1.5 (CH_3CN: Sigma, St. Louis, MO) after which, polar compounds were extracted according to the lab protocols from Resource Center for Stable Isotope-Resolved Metabolomics (University of Kentucky, KY). Briefly, 1mL of $CHCl_3$ (Sigma, St. Louis, MO) was added to ensure the ratio in samples (CH_3CN:ddH_2O: $CHCl_3$=2:1.5:1), shaken vigorously and vortexed, then centrifuged at 3,500 g at 4°C for 20 mins. The polar fraction (upper layer) and protein (middle layer) were collected and

lyophilized for further experiments. Levels of metabolites in hearts were determined by NMR and ICR/MS Spectrometers (Resource Center for Stable Isotope-Resolved Metabolomics, University of Kentucky, KY).

1D ^{1}H and $^{1}H\{^{13}C\}$ HSQC NMR analyses. Polar extracts were reconstituted in D_2O (> 99.9%, Cambridge Isotope Laboratories, MA) containing 0.1 mM EDTA (Ethylenediaminetetraacetic acid, Sigma Aldrich, St. Louis, MO) and 0.5 mM d6-2,2-dimethyl-2-silapentane-5-sulfonate (DSS) (Cambridge Isotope Laboratories, Tewksbury, MA) as internal standard were performed on a DD2 14.1 Tesla NMR spectrometer (Agilent Technologies, CA) equipped with a 3 mm inverse triple resonance HCN cryoprobe. 1D ^{1}H spectra were acquired with standard PRESAT pulse sequence at 15°C. A total of 16384 data points were acquired with 2 s acquisition time, 512 transients, 12 ppm spectral width, and 4 s recycle delay time during which water peak was irradiated by soft pulse for suppression. The spectra were then linear predicted and zero filled to 128k points and apodized with 1 Hz exponential line broadening. 1D HSQC spectra were recorded with ^{13}C adiabatic decoupling scheme for broad range decoupling during proton acquisition time of 0.25 s. 1796 data points were collected each transient and a total of 1024 transients were acquired with 12 ppm spectral width. The HSQC spectra were zero filling to 16k data points before Fourier transformation and then apodized with unshifted Gaussian function and 4 Hz exponential line broadening. Metabolites were assigned by comparison with in-house (11) and public NMR databases. Metabolite and their ^{13}C isotopomers were quantified using the MestReNova software (Mestrelab, Spain) by peak deconvolution. The peak intensities of metabolites obtained were converted into nmoles by calibration against the peak intensity of internal standard DSS (27.5 nmoles) at 0 ppm

for 1H spectra and that of Lac-3 at 1.32 ppm (nmoles determined from 1D 1H spectra) for HSQC spectra before normalization to the dry residue weight of each sample extracted.

Ion Chromatography-Mass Spectrometry (IC-MS) analyses. Unless stated otherwise, ICMS analysis was performed as previously described (12, 13). In short, polar extracts were reconstituted in 20 µL nanopure water of which 10 µL was injected for analysis on a Dionex ICS-5000+ion chromatograph interfaced to an Orbitrap Fusion Tribrid mass spectrometer (Thermo Fisher Scientific, San Jose, CA, USA). MS1 mass spectra were acquired at a resolution setting of 500,000 (FWHM at m/z 200) and an m/z range from 80 to 700. The chromatograph was outfitted with a Dionex IonPac AG11-HC-4 µm guard and column (both 2 × 50 mm). MS1 peak areas for isotopologues were integrated and exported to Excel via the Thermo TraceFinder (version 3.3) software package. Peak areas were corrected for natural abundance as previously described (14).

Western Blotting. Protein samples were separated in Pierce Tris-HEPES-SDS 4–20% precast polyacrylamide gels (Thermo scientific). Proteins were transferred to polyvinylidene difluoride membranes (BioRad, Richmond, CA) at 300 mA for 1.5 hours. following transfer, Ponceau S (Sigma) staining was used to ensure complete transfer and equal protein loading. Membranes were blocked in 5% nonfat dry milk in 1xTBS with 0.1% Tween 20 (TBS-T) for 1 hour at room temperature. Phospho-glycogen synthase (Ser641) expression was probed with a rabbit monoclonal primary antibody (Cell signaling #3891) at 1:1,000 dilution in TBS-T. The membrane was incubated at 4°C overnight and washed for 10 mins x 3 times in TBS-T before incubation with goat anti-rabbit horseradish peroxidase-conjugated (HRP) secondary antibody. Protein

bands were detected using the Pierce supersignal chemiluminescence substrate (Thermo scientific) in the G:Box fluorescence and chemiluminescence imaging system (Syngene, Frederick, MD). Densitometry was performed using ImageJ (National Institutes of Health, Bethesda, MD).

Statistical Analysis. Quantified metabolite levels (umol or nmol/g protein) from each experiment were expressed as means±SEM. Independent replicates were combined and analyzed with a two-way ANOVA followed by Bonferroni's (for metabolomics data) or Sidak's (for western blot data) multiple comparisons analysis. Statistical analyses were performed in Graphpad Prism 6 (La Jolla, CA).

RESULTS

Enhanced glycolytic flux in HIF-1α-expressing heart in response to ischemia with the unexpected failure to deplete glycogen levels.

HIF-1α expression was specifically induced in murine cardiomyocytes through the removal of Doxy diet for 5-7 days prior to the experiment. Wild-type (WT) and HIF-1α expressing hearts were perfused with 10.6 mM U-$^{13}C_6$ glucose for 30 mins, *ex vivo* in the loading phase. Subsequently the hearts were subjected to global ischemia (for 0, 5, 10, 15 and 30 mins), flash frozen and metabolites were extracted following established procedures. Extracted metabolites were quantitated in spectra of ^{1}H heteronuclear single quantum coherence (HSQC) and ^{1}H spectra with presaturation (PRESAT), respectively. All quantitation is normalized to the dry residue protein weight (umol/g). In HSQC spectra, metabolites assessed are linked to ^{13}C directly, whereas it is linked to total amount of molecule in PRESAT spectra.

We found that in HSQC spectra, ^{13}C-labeled lactate production increased in both of WT and Doxy-off-induced HIF-1α hearts during ischemia (Figure 2.1B). However, the upward trend is interrupted in WT hearts at 15 mins, while ^{13}C-labeled lactate production continues and is significantly elevated in HIF-1α hearts at 30 mins of ischemia. This is consistent with the increased glycolytic flux that we and others, have previously noted accompanies HIF-1α expression (4, 22). Given that we are examining isolated hearts undergoing global ischemia, glycogen is the only acknowledged source of available glucose reserves. Accordingly, ^{13}C-labeled glycogen levels in WT and HIF-1α hearts were assessed at indicated ischemic times in HSQC spectra (Figure 2.1A). As expected glycogen glucose reserves are depleted rapidly in WT hearts during ischemia. In stark contrast, HIF-1α hearts maintained glycogen levels at pre-ischemic levels after 30 mins of ischemia. These striking results were followed by the assessment of PRESAT spectra glycogen levels (Figure 2.1C), which measures the total amount of glycogen (^{12}C and ^{13}C-labeled glycogen). ^{13}C-labeled glycogen levels of satellite B in PRESAT spectra were measured as well (Figure 2.1E). Similar to the HSQC spectra, ^{13}C-labeled glycogen levels are maintained to a remarkable extent in HIF-1α hearts during ischemia. Indicating enhanced glycolytic flux, ^{13}C-lactate production was elevated in the HIF-1α as compared to WT hearts, especially after 15 mins of ischemia where lactate levels continued to rise in the HIF-1α hearts while peaking within 5-10 mins of ischemia in WT hearts (Figure 2.1B, D, and F). In addition, lactate levels were confirmed to be significantly elevated in ^{13}C-labeled satellite A and satellite B in HIF-1α hearts at 30 mins of ischemia, compared to WT (Figure 2.1D and F).

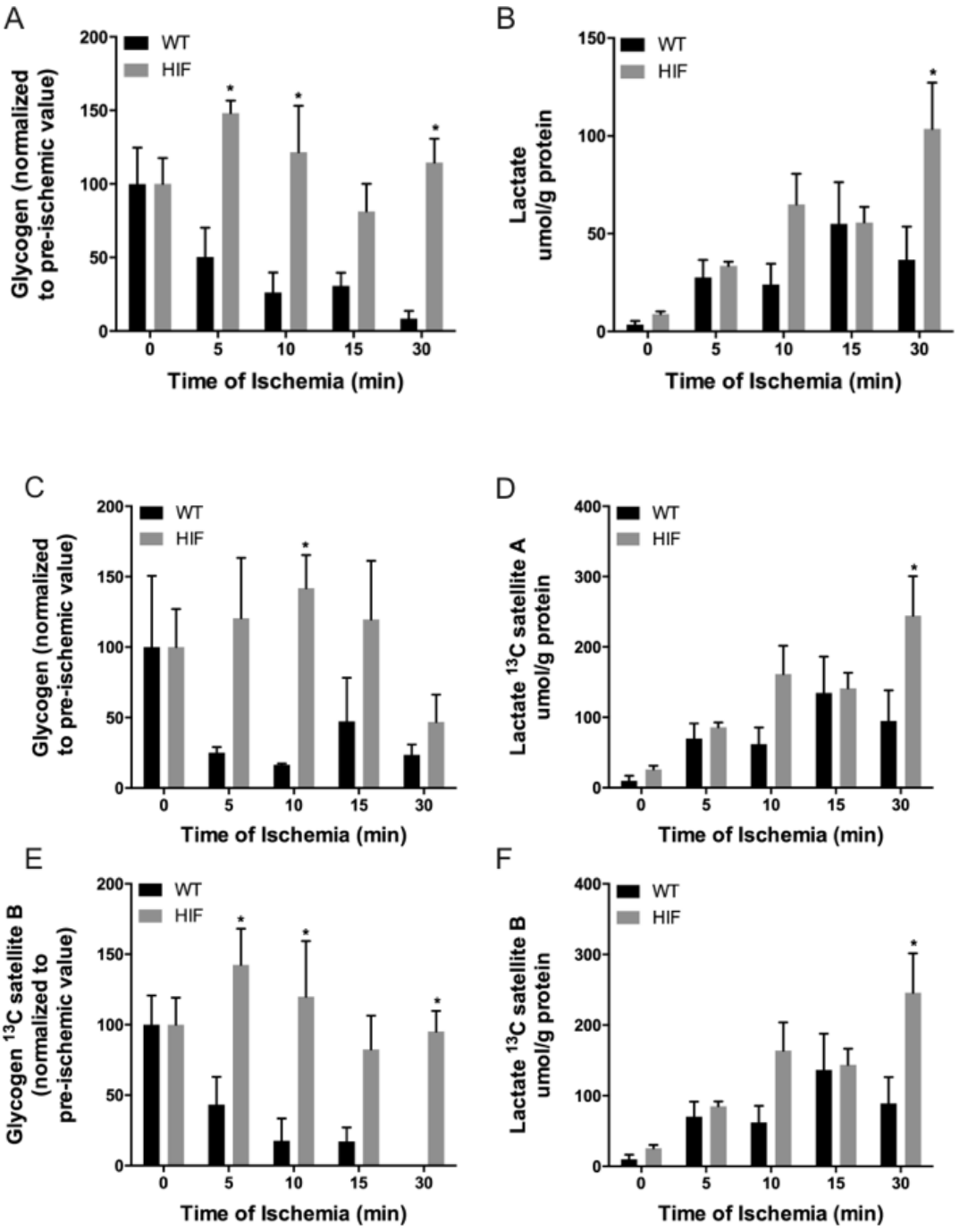

Figure 2.1: *Glycogen Reserves Maintained despite Increased Lactic Acid Production by HIF-1α-expressing Hearts for up to 30 mins of Ischemia.* Langerdorff perfused hearts were loaded with U-$^{13}C_6$ glucose for 30 mins and then subjected to the indicated times for ischemia. ^{13}C-labeled metabolites derived from WT and HIF-1α mouse hearts were quantitated in ^{1}H heteronuclear single quantum coherence (HSQC) spectra by NMR spectroscopy (Figure 1, A, B). Assessment

of (A) glycogen levels and (B) lactic acid production in heart tissues at corresponding ischemic times. The glycogen levels are expressed as the percentage of change relative to pre-ischemic value.

^{12}C- and ^{13}C-labeled metabolites are able to be determined synchronously in ^{1}H spectra with presaturation (PRESAT) by NMR spectroscopy (Figure 1, C-F). (C) ^{12}C-labeled glycogen levels, (E) ^{13}C-labeled glycogen levels, and (D, F) ^{13}C-labeled lactic acid production in WT and HIF-1α-PPN/tTA mouse hearts are shown at indicated ischemic times. All glycogen levels are expressed as the percentage change relative to pre-ischemic value. * $P<0.05$ vs WT at corresponding ischemic times; *n*= 3-5 hearts.

Active gluconeogenesis is responsible for the maintenance of glycogen levels and glucose:glycogen turnover at later times of ischemia in the HIF-1α-expressing heart.

We next investigated ^{13}C-labeled isotopologues of metabolites using IC-MS. ^{13}C-labeled metabolites of glucose are shown (Figure 2.3). During ischemia, glycolysis of ^{13}C-labeled glucose increases as a compensatory ATP source in hearts during ischemia, explaining the elevated lactate production in HIF-1α hearts, compared with WT. The maintenance of glycogen levels suggested an unexpected source of glucose is present in what is an essentially closed perfusion system. Accordingly, we investigated the presence of gluconeogenesis intermedates. That is, metabolites labeled with three carbons (^{13}C-[m+3]), such as Fructose 1,6-bisphosphate, Fructose 6-phosphate, Glucose 6-phosphate, and Glucose 1-phosphate, are considered as ^{13}C-labeled glyconeogenic intermediates (Figure 2.3). We found that Glucose 6-phosphate [m+3] and Fructose 6-phosphate [m+3] increased significantly in HIF-1α hearts at 30 mins of ischemia, compared with WT hearts. We also observed that Fructose 1,6-bisphosphate [m+3] was elevated significantly in HIF-1α hearts at 15 mins of ischemia, compared with WT (Figure 2.2).

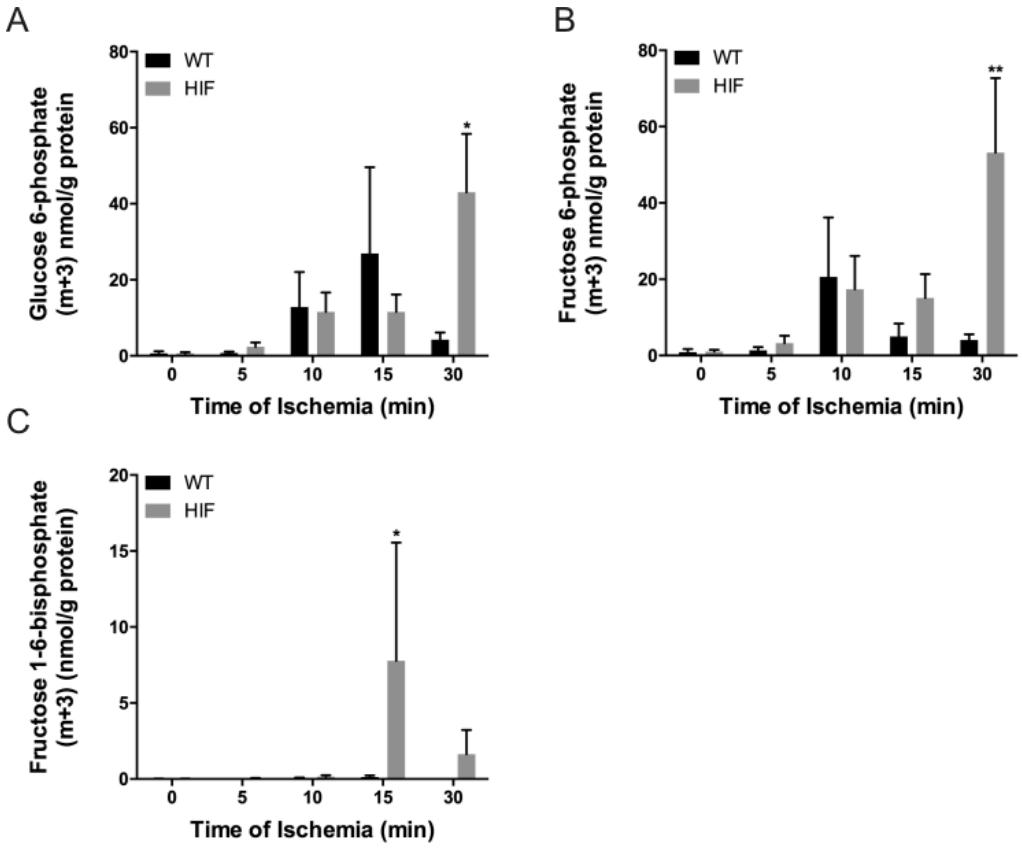

Figure 2.2*: Elevated ^{13}C-labeled Gluconeogenetic Intermediates [m+3] in HIF-1α Ischemic Hearts.* ^{13}C-labeled gluconeogenetic intermediates are determined using IC-MS. (A) glucose-6-phosphate, m+3 (G6P). (B) fructose-6-phosphate, m+3 (F6P). (C) fructose 1-6-bisphosphate, m+3 (F 1,6-BP). * P<0.05 vs WT at corresponding ischemic period; *n*= 3-5 hearts.

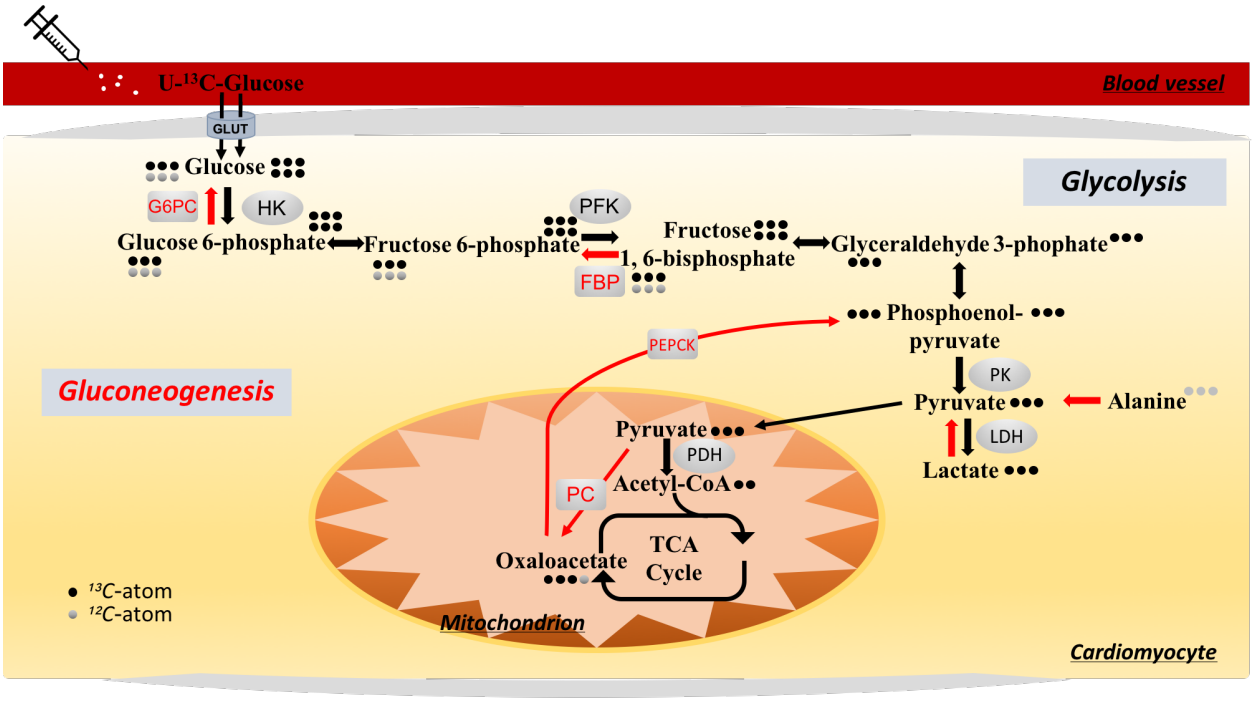

Figure 2.3: *Schematic viewing of U-^{13}C-glucose metabolism in heart.* Black dots indicate ^{13}C-atoms and grey dots indicate ^{12}C-atoms. In cytosol, U-^{13}C-labeled glucose is phosphorylated and converted to [m+6] ^{13}C-labeled G6P, F6P, F1,6-BP, then split up to [m+3] ^{13}C-labeled DHAP (not shown) and GAP. Eventually, [m+3] ^{13}C-atom will be passed into PEP and pyruvate that can be converted into [m+3] ^{13}C-labeled lactate and alanine under anaerobic condition. Pyruvate is actively transported into the mitochondria, thereafter in the matrix, there are 2 different routes. 1. pyruvate could be converted into [m+2] ^{13}C-labeled acetyl-CoA by the PDH complex. acetyl-CoA brings the acetyl group into the TCA cycle and then produce ATP by the oxidative phosphorylation under the aerobic conditions, acetyl-CoA is also precursors for *de novo* biosynthesis of fatty acids and cholesterol, [m+2] and [m+4] OAA will be produced by this way (not shown). 2. pyruvate could be converted directly by PC to [m+3] ^{13}C-labeled OAA. Since OAA is limited to across inner membrane of the mitochondria, so it needs to be transported by the malate-aspartate shuttle into the cytosol, there, PEPCK de-carboxylates and phosphorylates OAA for its conversion to [m+2] (not shown) and [m+3] ^{13}C-labeled PEP. Then 1-molecular [m+3] ^{13}C-labeled GAP combines with 1-molecular endogenous ^{12}C-labeled GAP to generate [m+3] ^{13}C-labeled F1,6-BP, F6P, G6P, and glucose through the gluconeogenesis. This glucose production could contribute to the increased glycogen level by glycogenesis in HIF-1α heart. (GULT: Glucose transporter, G6P: glucose 6-phosphate, F6P: Fructose 6-phosphate, F1,6-BP: Fructose 1,6-bisphosphate, DHAP: Dihydroxyacetone phosphate, GAP: Glyceraldehyde 3-phosphate, PEP: Phosphoenolpyruvate,

PDH: Pyruvate dehydrogenase, HK: Hexokinase, PFK: phosphofructokinase, PK: pyruvate kinase, LDH: Lactate Dehydrogenase, TCA cycle: tricarboxylic acid cycle, OAA: oxaloacetate, PC: pyruvate carboxylase, PEPCK: phosphoenolpyruvate carboxykinase, FBP: fructose 1,6-bisphosphatase, G6PC: glucose 6-phosphatase.)

HIF-1α-expressing hearts more effectively mobilize glycogen synthesis during Ischemia.

The continued incorporation of ^{13}C-glucose into glycogen even at late times of ischemia coupled to the continued accumulation of lactate suggests that the HIF-1α hearts were more effective at mobilizing glucose from glycogen. Accordingly, the status of glycogen synthase (GS) phosphorylation was examined. P-GS is inactivated and favors glucose mobilization (Figure 2.4). We observed that in hearts, the phosphor-glycogen synthase is dynamically regulated by ischemia and significantly induced by HIF-1α.

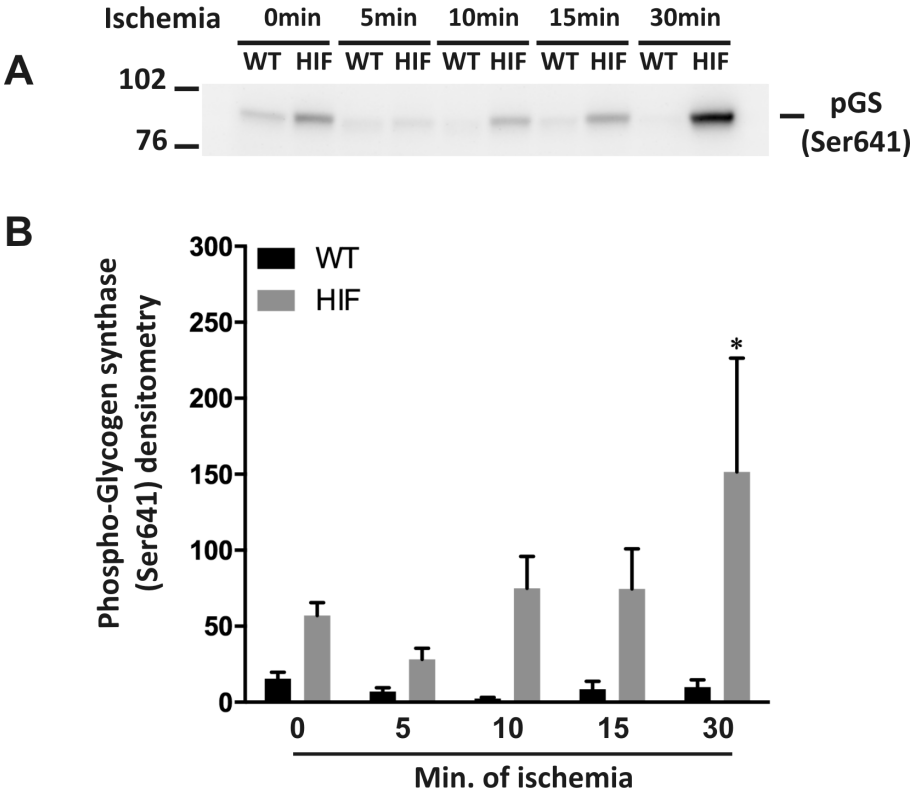

Figure 2.4: *Enhanced glycolytic flux in HIF-1α-expressing heart during ischemia.* Tissue samples from WT and HIF-1α mice hearts were collected following various ischemic periods (0, 5, 10, 15, and 30 mins) for Western Blotting analysis. (A) the protein expression of phosphor-glycogen synthase (pGS) as determined for these indicated heart groups. (B) quantification of band intensity was performed in imageJ. * $P<0.05$ vs WT at corresponding ischemic period; *n*= 4.

DISCUSSION

A considerable amount of research has demonstrated the protective effect of HIF-1α against ischemia in heart (4, 15, 16). During chronic myocardial ischemia, downregulation of fatty acids and ketone body oxidation is accompanied by upregulation of substrate preference toward glucose utilization (17). Hence it is of acute interest to understand the role of glucose metabolism in myocardial tolerance to hypoxic stress. It is well established that HIF-1α increases the glycolytic capacity by positively targeting glycolytic enzyme expression. Glyceraldehyde-3-phosphate dehydrogenase (GAPDH), Hexokinase 1/2 (HK1/2) and Triosephosphate isomerase (TPI) under anaerobic, or aerobic conditions (18, 19, 20). In these studies, we find that that lactate production is enhanced in HIF-1α hearts, and that ^{13}C incorporation of lactate continues for up to 30 mins of ischemia. This is consistent with our previous data where we showed that lactate production in 6D-induced HIF-1α-PPN mouse hearts following ischemia is significantly elevated (4). Taken together the findings indicate that HIF-1α hearts are more effective at maintaining glycolytic activity during total global heart ischemia. We will discuss the reasons for this below.

Our previous work has demonstrated that the purine nucleotide cycle (PNC), a AMP salvage pathway is upregulated by HIF-1α. The PNC generates fumarate from aspartate during instances where AMP levels rise, such as strenuous exercise or ischemia (31). We have also shown that the PHD-pathway/HIF-1α confers upon myocytes

the ability to perform anaerobic mitochondrial respiration using fumarate as an electron acceptor. In this scenario mitochondrial complex II reduces fumarate to succinate. This allows for continued electron flux through complex I when oxygen is absent. These mechanisms probably result in two major consequences that impact glycolysis. Firstly, during ischemia, NAD^+ continues to be regenerated, thus allowing glycolysis to proceed unimpeded. We believe that this accounts, in part, for the findings that lactate continues to accumulate and incorporate ^{13}C label even after 30 mins of global ischemia in the HIF-1α hearts. Secondly, AMP deaminase, the rate-limiting enzyme of the PNC that is upregulated by HIF-1α has been posited to positively regulate phosphofructokinase (31). Ammonium ions produced by AMP deaminase activate phosphofructokinase, which in turn, stimulates glycolysis. Clearly, HIF-1α exerts its effects through multiple regulatory mechanisms to many metabolic pathways in order to situate the myocyte to tolerate a low oxygen/substrate environment.

The most remarkable finding of this study is the extent to which ^{13}C-labeled and total glycogen levels were maintained in HIF-1α hearts at ischemic times of up to 30 mins. This surprising finding suggested an unexpected source of glucose in the un-perfused ischemic HIF-1α heart. Accordingly, we investigated the levels of gluconeogenic intermediates (i.e. [M+3] isotopologues of glycolytic intermediates; consult figure 2.2 and 2.3) in the HIF-1α hearts. Indeed, we find that the levels of gluconeogenic intermediate metabolites are highly elevated in the HIF-1α hearts during ischemia as compared to the WT hearts. Taken together these findings indicate that active gluconeogenesis accounts for the failure to deplete glycogen and glucose and fructose phosphate species in the HIF-1α hearts.

Two ATP equivalents are produced in anaerobic glycolysis. In contrast, 4 ATP and 2 GTP are consumed to produce glucose via gluconeogenesis. The HIF-1α heart does have sources of anaerobically produced high energy phosphates, including the aforementioned “fumarate respiration”, that are not available to the naïve WT hearts. Nonetheless, the question arises, what advantage might arise to expending scarce ATP to maintain glucose/glycogen levels and glycolytic activity. We believe the answer may lie in the nature of glycolytic ATP utilization versus oxidatively produced ATP. Unlike myocardial contractile function, which is supported primarily by energy derived oxidative phosphorylation, sarcolemma ion channel function (e.g. Na^+-K^+ pump) of the cardiomyocyte is preferentially fueled by glycolytic ATP production (28, 29). The functional compartmentalization is achieved through the location of key enzymes in the membrane or adjacent cytoskeleton region of cell (30). Loss of ionic homeostasis, either at the sarcolemma, or at the mitochondrial inner membrane is associated with irreversible cellular damage. In this view, continued glycolytic metabolism may represent a key requisite for cellular survival.

In summary, we show that HIF-1α upregulates and prolongs glycolytic flux in heart for longer periods (i.e. 30 mins) of ischemia via activating gluconeogenesis. The preservation of glycogen in the HIF-1α heart provides uninterrupted anaerobic energy supply that primarily fuels ionic homeostasis and, which may prevent cardiomyocyte injury mediated by ionic gradient dissolution in ischemia.

REFERENCES

1. **Majmundar, A. J., Wong, W. J. & Simon, M. C.** Hypoxia-Inducible Factors and the Response to Hypoxic Stress. *Mol. Cell.* **40**, 294-309 (2010).

2. **Kaelin, W. G. & Ratcliffe, P. J.** Oxygen Sensing by Metazoans: The Central Role of the HIF Hydroxylase Pathway. *Mol. Cell.* **30**, 393-402 (2008).

3. **Lando, D., Peet, D. J., Whelan, D. A., Gorman, J. J. & Whitelaw, M. L.** Asparagine hydroxylation of the HIF transactivation domain: A hypoxic switch. *Science.* **295**, 858-861 (2002).

4. **Wu, J. *et al.*** HIF-1α in heart: protective mechanisms. *Am. J. Physiol. Heart Circ. Physiol.* **305,** 821-828 (2013).

5. **Wu, J. *et al.*** HIF-1α in the heart: Remodeling nucleotide metabolism. *J. Mol. Cell. Cardiol.* **82**, 194-200 (2015).

6. **Hayashi, M. *et al.*** Induction of glucose transporter 1 expression through hypoxia-inducible factor 1alpha under hypoxic conditions in trophoblast-derived cells. *J. Endocrinol.* **183**, 145-154 (2004).

7. **Papandreou, I., Cairns, R. A., Fontana, L., Lim, A. L. & Denko, N. C.** HIF-1 mediates adaptation to hypoxia by actively downregulating mitochondrial oxygen consumption. *Cell. Metab.* **3**, 187-197 (2006).

8. **Kim, J. W., Tchernyshyov, I., Semenza, G. L. & Dang, C. V.** HIF-1-mediated expression of pyruvate dehydrogenase kinase: A metabolic switch required for cellular adaptation to hypoxia. *Cell. Metab.* **3**, 177-185 (2006).

9. **Deidda, M. *et al.*** Blood metabolomic fingerprint is distinct in healthy coronary and in stenosing or microvascular ischemic heart disease. *J. Transl. Med.* **15**, 112 (2017).

10. **Bekeredjian, R. *et al.*** Conditional HIF-1α expression produces a reversible cardiomyopathy. *PLoS One.* **5**, e11693 (2010).

11. **Fan, T. W. M. & Lane, A. N.** Structure-based profiling of metabolites and isotopomers by NMR. *Prog. Nucl. Magn. Reson. Spectrosc.* **52**, 69-117 (2008).

12. **Fan, T. W. *et al.*** Distinctly perturbed metabolic networks underlie differential tumor tissue damages induced by immune modulator beta-glucan in a two-case *ex vivo* non-small-cell lung cancer study. *Cold. Spring. Harb. Mol. Case. Stud.* **2**, a000893 (2016).

13. **Sun, R. C. *et al.*** Noninvasive liquid diet delivery of stable isotopes into mouse models for deep metabolic network tracing. *Nat. Commun.* **8**, 1646 (2017).

14. **Moseley, H. N. B.** Correcting for the effects of natural abundance in stable isotope resolved metabolomics experiments involving ultra-high resolution mass spectrometry. *BMC Bioinformatics.* **11**, 139 (2010).

15. **Semenza, G. L.** Hypoxia-Inducible Factor 1 and Cardiovascular Disease. *Annu. Rev. Physiol.* **76**, 39-56 (2014).

16. **Jianqiang, P. *et al.*** Expression of hypoxia-inducible factor 1 alpha ameliorate myocardial ischemia in rat. *Biochem. Biophys. Res. Commun.* **465**, 691-695 (2015).

17. **Shohet, R. V. & Garcia, J. A.** Keeping the engine primed: HIF factors as key regulators of cardiac metabolism and angiogenesis during ischemia. *J. Mol. Med.* **85**, 1309-1315 (2007).

18. **Iyer, N. V *et al.*** Cellular and developmental control of O_2 homeostasis by hypoxia-inducible factor 1 alpha. *Genes. Dev.* **12**, 149-162 (1998).

19. **Seagroves, T. N. *et al.*** Transcription factor HIF-1 is a necessary mediator of the pasteur effect in mammalian cells. *Mol. Cell. Biol.* **21**, 3436-3444 (2001).

20. **Del Rey, M. J. *et al.*** Hif-1α Knockdown Reduces Glycolytic Metabolism and Induces Cell Death of Human Synovial Fibroblasts under Normoxic Conditions. *Sci. Rep.* **7**, 3644 (2017).

21. **Valvona, C. J., Fillmore, H. L., Nunn, P. B. & Pilkington, G. J.** The Regulation and Function of Lactate Dehydrogenase A: Therapeutic Potential in Brain Tumor. *Brain Pathol.* **26**, 3-17 (2016).

22. **Semenza, G. L. *et al.*** Hypoxia response elements in the aldolase A, enolase 1, and lactate dehydrogenase a gene promoters contain essential binding sites for hypoxia-inducible factor 1. *J. Biol. Chem.* **271**, 32529-32537 (1996).

23. **Ullah, M. S., Davies, A. J. & Halestrap, A. P.** The plasma membrane lactate transporter MCT4, but not MCT1, is up-regulated by hypoxia through a HIF-1α-dependent mechanism. *J. Biol. Chem.* **281**, 9030-9037 (2006).

24. **Huang, Y. *et al.*** Cardiac myocyte-specific HIF-1α deletion alters vascularization, energy availability, calcium flux, and contractility in the normoxic heart. *FASEB J.* **18**, 1138-1140 (2004).

25. **Scheuer, J., & Stezoski, S. W.** Protective role of increased myocardial glycogen stores in cardiac anoxia in the rat. *Circ. Res.* 27, 835-849. (1970).

26. **Pelletier, J. *et al.*** Glycogen synthesis is induced in hypoxia by the hypoxia-inducible factor and promotes cancer cell survival. *Front Oncol.* **2**, 18 (2012).

27. **Cross, H. R., Opie, L. H., Radda, G. K. & Clarke, K.** Is a high glycogen content beneficial or detrimental to the ischemic rat heart? A controversy resolved. *Circ. Res.* **78**, 482-491 (1996).

28. **Weiss, J. & Hiltbrand, B.** Functional compartmentation of glycolytic versus oxidative metabolism in isolated rabbit heart. *J. Clin. Invest.* **75**, 436-447 (1985).

29. **Glitsch, H. G. & Tappe, A.** The Na+/K+ pump of cardiac purkinje cells is preferentially fuelled by glycolytic ATP production. *Pflügers Arch. Eur. J. Physiol.* **422**, 380-385 (1993).

30. **Weiss, J. N. & Lamp, S. T.** Glycolysis preferentially inhibits ATP-sensitive K+ channels in isolated guinea pig cardiac myocytes. *Science.* **238**, 67-69 (1987).

31. **Tornheim K, Lowenstein JM.** The purine nucleotide cycle. Control of phosphofructokinase and glycolytic oscillations in muscle extracts. *J Biol Chem.* 250(16):6304-14.

CHAPTER 3

C1Q/TNF-RELATED PROTEIN 3 (CTRP3) FUNCTION AND REGULATION

Li Y [1], Wright GL [1], and Peterson JM [1,2].

[1] Department of Biomedical Sciences, Quillen College of Medicine, East Tennessee State University, Johnson City, TN [2] Department of Health Sciences, College of Public Health, East Tennessee State University, Johnson City, TN

This review has been published in Li et al., Comprehensive Physiology, 7(3), 863-878, 2017

ABSTRACT

As the largest endocrine organ, adipose tissue secretes many bioactive molecules that circulate in the blood, collectively termed adipokines. Efforts to identify such metabolic regulators have led to the discovery of a family of secreted proteins, designated as C1q tumor necrosis factor (TNF)-related proteins (CTRPs). The CTRP proteins, adiponectin, TNF-alpha, as well as other proteins with the distinct C1q domain are collectively grouped together as the C1q/TNF superfamily. Reflecting profound biological potency, the initial characterization of these adipose tissue-derived CTRP factors finds wide-ranging effects upon metabolism, inflammation, and survival-signaling in multiple tissue types. CTRP3 (also known as CORS26, cartducin, or cartonectin) is a unique member of this adipokine family. In this review we provide a comprehensive overview of the research concerning the expression, regulation, and physiological function of CTRP3.

INTRODUCTION

Since the discovery of Leptin in 1994 and then later adiponectin there has been a fundamental shift in how adipose tissue is viewed within the medical and research community, as an active endocrine organ which effects human health and physiology (57, 87). In 2004 Wong *et al*. characterized a novel family of adipose tissue-derived

cytokines, collectively called adipokines, referred to as Complement C1q Tumor necrosis factor-Related Proteins (CTRPs) (76), like adiponectin and tumor necrosis factor (TNF) these CTRPs all contain a C1q globular domain and are characterized together as the C1q/TNF superfamily (62). To date, this superfamily has been documented to have a wide range and opposing effects on metabolism, food intake, inflammation, tumor metastasis, apoptosis, vascular disorders, ischemic injury, and even sexual reproduction (7, 8, 25, 29, 30, 49, 51, 57, 62, 64, 68, 69, 74-76, 81, 84, 89). The purpose of this review is to carefully summarize the research that has been accomplished on one of these proteins, CTRP3. A list of abbreviations used in this article is found in Table 3.1.

Table 3.1: *Abbreviations*

SP-1: specificity protein 1
CTRP3: C1q TNF Related Protein 3
LPS: Lipopolysaccharide
TLR: toll-like receptor
MCP-1: monocyte chemotactic protein 1
PPAR: peroxisome proliferator-activated receptor
pIgA: polymeric Immunoglobulin A
RANKL: Receptor activator of nuclear factor kappa-B ligand
TNF: Tumor necrosis factor
IL-6: Interleukin-6
AP-1: Activator protein 1
c-FOS: Fos proto-oncogene
Pit-1a: POU domain, class 1, transcription factor 1
C/EBP-α/β: CCAAT-enhancer-binding proteins-alpha/beta
MyoD: Myogenic Differentiation
c-JUN: Jun proto-oncogene, AP-1 transcription factor subunit
TY-IID: Transcription factor II D – “TATAA”
CREB: cAMP response element-binding protein
GATA-1: GATA-binding factor 1
SRY: Sex-determining region Y
Sox-5: SRY-related HMG-box 5
c-Myc: similar to myelocytomatosis viral oncogene
RXR: Retinoid X receptor
PGC-1α: Peroxisome proliferators activated receptor-γ co-activator-1α
NRF-1/NRF-2: nuclear respiratory factor 1/2
TFAM: mitochondrial transcription factor A
TBXAS1: thromboxane A synthase 1

HUVEC: Human umbilical vascular endothelial cells
ROS: Reactive oxygen species
TGF-β: Transforming growth factor beta

History of CTRP3

Initial discovery

CTRP3 was first discovered in 2001(43) in C3H10T1/2 mouse mesenchymal stem cells treated to induce chondrogenic differentiation. Because of its size and 23 Gly-X-Y repeats in the N-terminal collagen domain it was originally named CORS26 (Collagenous repeat-containing sequence 26 kDa protein). Later Wong *et al.* (2004) identified CTRP3 as a member of a family of highly conserved adiponectin paralogs designated as CTRPs and CORS26 was renamed CTRP3(76). Alternative names that have been used for CTRP3 are cartducin (1, 44) and cartonectin (56, 73), both due to the detection of CTRP3 expression in developing cartilage.

Structure

Analysis of the primary structure predicts that CTRP3 is a highly hydrophilic secreted protein, with an N-terminal hydrophobic signal peptide, and no transmembrane domains (43). Experimental work confirms that CTRP3 is a secreted protein and circulates in the blood, which indicates that the physiological function of CTRP3 occurs through endocrine mechanisms (51, 75). Additionally, CTRP3 has a series of N-terminal Collagenous repeats (Gly-X-Y), and a highly conserved C-terminal globular domain (76), thus placing CTRP3 within the expanding C1q TNF Superfamily (62) (Figure 3.1). CTRP3 shares sequence homology with adiponectin (38% in mouse and 36% in human), and is highly conserved (95.9% identity between human and mouse proteins) (36). Additionally, there are two splice variants of CTRP3 that have been identified. The longer splice variant, designated as CTRP3B, encodes an extra 73 N-terminal amino

acids due to the retention of intron 1. CTRP3B contains a highly conserved N-linked glycosylation site that is not present on the original splice variant, CTRP3A (51). At this time the functional significance of the splice variants of CTRP3 is unknown as research has focused almost exclusively on CTRP3A. Regardless, both CTRP3A and CTRP3B are secreted proteins which are detectable in human serum. Although only CTRP3A has been detected in mouse serum, both variants are expressed in mouse adipose tissue (51, 75). One of the reasons for the difficulty in detecting the CTRP3B variant is that unlike CTRP3A, CTRP3B degrades rapidly unless it forms a higher order oligomer with CTRP3A (51).

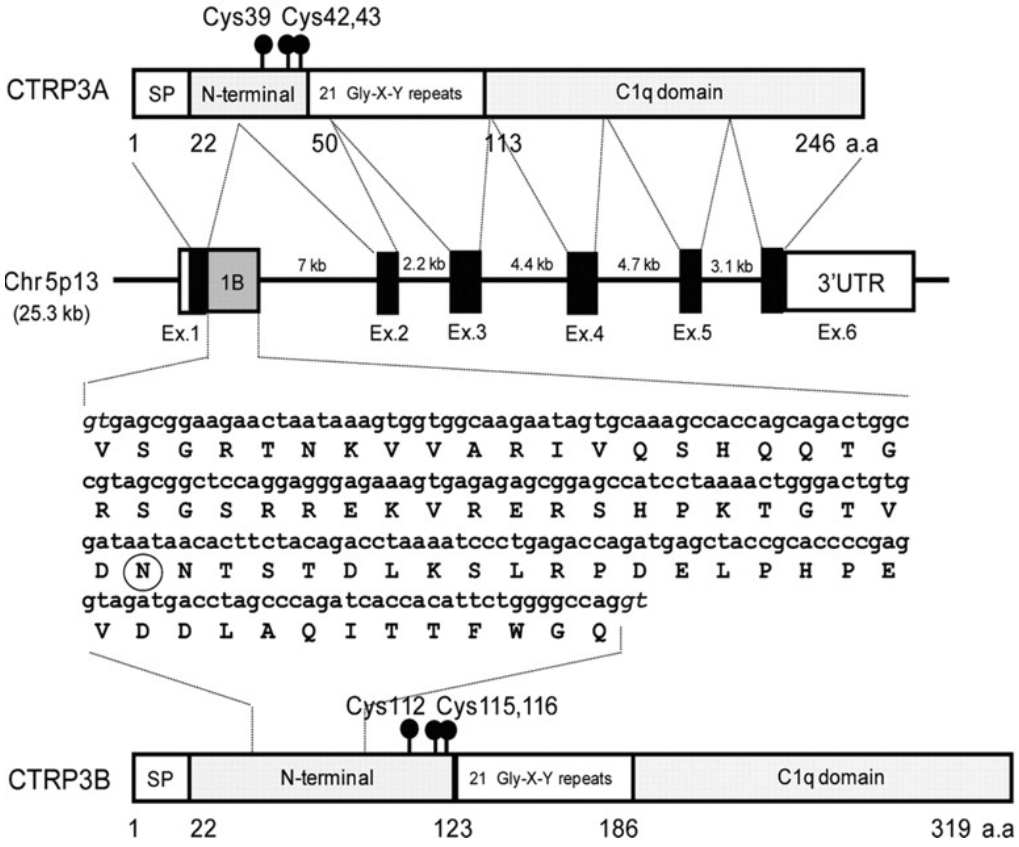

Figure 3.1: *Structural Overview of CTRP3.* Two splice variants were identified and designated as CTRP3A and CTRP3B. B, organization of the CTRP3A and CTRP3B genes and proteins.

The human CTRP3A gene is 25.3 kb in size, consists of six exons and five introns, and is located on chromosome 5p13. Exons 1, 2, 3, 4, 5, and 6 of the CTRP3A gene are 171, 112, 155, 130, 100, and 2,885 bp in size, respectively. The size of each intron is also indicated. Exon 1B (gray square) contains a 219-nucleotide sequence found in CTRP3B cDNA, coding for an extra 73 amino acid residues. A potential N-linked glycosylation site is circled. The consensus splice donors are shown in italic type. This figure was originally published in The Journal of Biological Chemistry (51) and image reproduced according to the copyright policy of the ASBMB.

CTRP3 is endogenously co-expressed in many tissues with other proteins within the C1q TNF superfamily. However, CTRP3 is unique as it does not form hetero-oligomeric complexes with adiponectin or any other CTRP protein (76). Most CTRP proteins will form hetero-oligomers with adiponectin or at least 1 other CTRP protein when coexpressed (75, 76). However, higher-order oligomers are the primary form by which CTRP3 is found circulating in either human or mouse serum, indicating that CTRP3 high-order oligomeric complexes occur solely between its two splice variants, CTRP3A and CTRP3B (51). While the significance of these posttranslational modifications and higher order structure formations have yet to be explored, it is likely that these modifications influence the function of CTRP3. Therefore, it is important to differentiate between functional studies and experimental findings gleaned from bacterial-produced compared with other types of recombinant CTRP3 protein. Bacterial-produced recombinant CTRP3 protein does not possess the potentially physiologically relevant post-translational modifications or multimeric structures, and may explain any observed lack of biological activity (19, 61).

Recently using the novel ligand-receptor capture method, and mammalian-cell expressed CTRP3, Li *et al*. (2016) (41) identified Lysosomal-associated membrane

protein 1 (LAMP-1) and Lysosome membrane protein 2 (LIMP II) as potential receptors for CTRP3. Although it remains to be determined whether either of these proteins directly mediate the intercellular effects of CTRP3 or act as co-receptors for a yet unidentified protein, both LAMP1 and LIMPII are widely expressed in a number of different tissues corresponding to the variety of functions attributed to CTRP3. A comprehensive list of *in vitro* functions documented for CTRP3 is listed in Table 3.2. CTRP3 may also act without directly initiating intracellular action but rather through inhibiting the binding of other ligands. For example, lipopolysaccharide (LPS) is a potent endotoxin that binds to Toll-like receptor 4 (TLR4) and promotes a cellular inflammatory response. However, even though CTRP3 does not bind directly to either LPS or TLR4, CTRP3 prevents their interaction through an unestablished mechanism (30).

Table 3.2: *Complete Summary of the In Vitro Functions of CTRP3*

Cell line	Citation	Type of treatment	Effect
N1511 (mouse chondrogenic progenitor)	Akiyama et al (2006)(1)	10 µg/ml [E. Coli produced His_6-tagged signal peptide removed]	Increased ERK ½, and Akt phosphorylation from 5 min-1 hour, but not JNK or p38 MAPK
MSS31 (mouse endothelial cells)	Akiyama (2) et al (2007)	1-5 µg/ml [E. Coli produced His_6-tagged signal peptide removed]	↑ Proliferation and migration, ↑ ERK1/2 & MAPK p38 within 15 minutes.
LM8 (mouse osteosarcoma cell line)	Akiyama et al (2009)(3)	2-10 µg/ml [E. Coli produced His_6-tagged signal peptide removed]	CTRP3 treatment ↑ proliferation and ↑ ERK1/2 phosphorylation with no effect on migration or p38, JNK1/2, or Akt phosporylation.
NOHS (mouse osteosarcoma cell line)	Akiyama et al (2009)(3)	2-10 µg/ml [E. Coli produced His_6-tagged signal peptide removed]	CTRP3 treatment ↑ proliferation and ↑ ERK1/2 phosphorylation with no effect on migration or p38, JNK1/2, or Akt.
Rat vascular smooth muscle cells (VSMCs)	Feng et al (2016)(15)	Human globular CTRP3 (Aviscera Bioscience) Catalog # not reported	CTRP3 promotes ATP synthesis, oxidative phosphorylation complex proteins, and

			ROS levels; whereas siRNA knockdown reduces ATP and oxidative phosphorylation complex proteins levels
Human primary colonic lamina propria fibroblasts (CLPF)	Hofmann et al 2011(21)	Recombinant CTRP-3 (High Five insect cells)	Significantly and dose-dependently reduced LPS-induced IL-8 secretion in CLPF within 8 hours after LPS exposure, whereas LPS-induced IL-6 and TNF release was not affected. CTRP-3 inhibited TGF-β production and the expression of CTGF and collagen I in CLPF, whereas collagen III expression remained unchanged.
RWPE-1 prostate cells (ATCC Number CRL-11609)	Hou Et al. 2015(23)	Mammalian expressed CTRP3 (3, 10, or 30 µg/ml)	Increased cell number in a dose dependent manner at 24-72 hours, and 10 µg/ml prevented apoptosis. Cytokeratin-19, GLRX3 and DDAH1 were upregulated and cytokeratin-17 and 14-3-3 sigma were downregulated proteins in CTRP3-treated cells.
bone marrow macrophages (BMM)	Kim et al (2015)(27)	Recombinant human CTRP3 was purchased from AdipoGen (Catalog number not reported)	↓ osteoclast differentiation from BMM treated with IL-1, $1,25(OH_2)D_3$, Receptor activator of nuclear factor kappa-B ligand (RANKL), further CTRP3 prevented mature osteoclasts from reabsorbing bone
Adipocyte (3T3-L1)	Kopp et al. 2010(30)	1-10 µg/ml Recombinant full length CTRP3 (H5 insect cells)	Suppressed LPS, lauric acid, TLR1/2, or TLR3 ligand-induced MCP-1 release. CTRP3 had no effect on TLR2/6 ligand-induced MCP-1 release. Further, siRNA knockdown of CTRP3 increased MCP-1 release and decreased adiponectin secretion and reduced lipid accumulation.
Primary Human monocytes	Kopp, A. et al.(2010)(30)	1 µg/ml Recombinant full length CTRP3 (H5 insect cells)	Suppressed LPS-induced MIF & CCL4 release in lean subjects, & MCP-1 in monocytes from both diabetic and leans subjects. Prevents

			Lauric acid induced release of IL-6 and TNF
Primary Human monocytes	Kopp, A. et al.(2010)(31)	1 µg/ml Recombinant full length CTRP3 (H5 insect cells)	↓ LPS-induced secretion of IL-6 in monocytes from control but not T2D. CTRP3 did not significantly affect TNF secretion.
Adipocyte (3T3-L1)	Li et al 2014(38)	Recombinant CTRP3 (uncited origin)	increased adipocyte glucose uptake and decreased TNF and IL6 secretion in insulin resistant 3T3-L1A
Adipocyte (3T3-L1)	Li et al 2014(39)	Mammalian expressed recombinant CTRP3 (250 ng/mL)	↑ the secretion of adiponectin, leptin, visfatin, and apelin with peak detectable effect at 12 hours (effects prevented by the addition of an AMPK inhibitor).
Adipocyte (3T3-L1)	Schmid et al (2012)(59)	siRNA knockdown of CTRP3	Reduced resistin secretion and lipolysis.
Adventitial fibroblasts	Lin et al (2014)(42)	CTRP3 protein (10 µg/ml) (source/type of CTRP3 was not reported)	CTRP3 prevents TGF-β1 induced fibroblasts phenotypic Conversion, proliferation, migration, collagen I expression, and connective tissue growth factor (all indicators of inappropriate of vascular remodeling and neointima formation).
HSC-2/8 (human chondrocytes)	Maeda et al (2006)(44)	10 µg/ml [E. Coli produced His_6-tagged signal peptide removed]	Increase proliferation
N1511 (mouse chondrogenic progenitor)	Maeda et al (2006)(44)	2-10 µg/ml [E. Coli produced His_6-tagged signal peptide removed]	Increase proliferation
TM3 mouse Leydig Cells	Otani et al (2012)(47)	Mammalian expressed full length (3-30 ug/ml)	Dose responsive ↑ testosterone production, ↑ steroidogenic acute regulatory protein mRNA and protein levels
Adipocyte (3T3-L1)	Schmid et al 2012(59)	siRNA knockdown of CTRP3	siRNA knockdown of CTRP3 reduced resistin secretion and lipolysis.
Adipocyte (3T3-L1)	Schmid et al 2013(58)	siRNA-mediated cellular knockdown of CTRP-3	siRNA-mediated cellular knockdown of CTRP-3 in adipocytes resulted in an upregulation of CTRP-5 expression.
Adipose tissue collected from control (n=3) or	Schmid et al. (2012)(59)		CTRP3 protein levels were higher in subcutaneous adipocytes from an obese compared with lean donor, no

diabetic (n=3) female donors)			differences were observed from visceral adipocytes. (Note: small sample size, n=3)
THP-1 (human - Acute Monocytic Leukemia cell line)	Weigert et al 2005(70)	1 µg/ml Recombinant full length CTRP3 (H5 insect cells)	Suppressed LPS induced: IL-6 & TNF mRNA and release.
Adipocyte (3T3-L1)	Wolfing et al (2008)(73)	10 ng/ml Recombinant full length CTRP3 (H5 insect cells)	increase adiponectin and resistin secretion but not promoter activity with no effect on IL-6 (no effect on human-derived adipocytes).
Primary cultured adult rat cardiac fibroblast (CF)	Wu et al 2015(77)	2 µg/ml Recombinant human gCTRP3 (Aviscera Bioscience; 00082-01-100; E. Coli expressed); also used siRNA knockdown of CTRP3	Inhibited TGF-β1α-induced α-SMA, SM22α, SM22α, collagen I, collagen III, and connective tissue growth factor (CTGF) expression [markers for myofibroblast differentiation]. Whereas, SiRNA knockdown of CTRP3 increased TGF-β1-induced α-smooth muscle actin (α-SMA) and smooth muscle 22α (SM22α) collagen I, collagen III, and CTGF expression. Further CTRP3 attenuated TGF-β1 induced-elevations in phosphor-Smad3 (Ser204).
Cardiomyocytes (adult mouse)	Yi et al (2012)(81)	Bacterial expressed globular domain of Mouse CTRP3	CTRP3 upregulated levels of phosphorylated Akt, HIF1α, and VEGF. Further cardiomyocyte hypoxia-induced apoptosis was attenuated with condition media from 3t3-L1A adipocytes, however this effect was abolished when the conditioned media came from 3T3-L1a cells treated with CTRP3 siRNA.
human umbilical vascular endothelial cells (HUVECs)	Yi et al (2012)(81)	Bacterial expressed globular domain of Mouse CTRP3	CTRP3 had no effect on tube formation, Akt phosphorylation or HIF1α or VEGF expression. These results suggest that the *in vivo* proangiogenic effect of CTRP3 is no through direct mechanisms on endothelial cells. Further, treatment of HUVECs cell with condition

			media from primary cardiomyocytes treated with CTRP3 significantly enhanced HUVEC tube formation.
Primary meckel's cartilage	Yokohama-Tamaki et al (2011)(82)	Knock-down of CTRP3 (antisense ogliodeoxynucleotide)	Caused severe curvature deformation and suppressed growth.
human mesangial cells (HMCs)	Zhang et al (2016)(86)	Full length human CTRP3 (PubMed No. NM_030945.2) adenovirus mediated overexpression	↓ pIgA-induce IL-6 and TGF-beta secretion from HMC cells.
Neonatal rat ventricular myocytes	Zhang et al 2016(85)	0.5 – 4 μg/ml Human recombinant globular and full-length CTRP3 (Aviscera Bioscience) Catalog # not reported	Both increased the expression of PGC-1α, nuclear respiratory factor 1&2, and markers of mitochondrial biogenesis
Human mesangial cells (HMCs)	Zhang et al (2016)(86)	Treated with Serum polymeric IgA (pIgA) from control or IgAN patients	pIgA markedly increased IL-6 and TGF-β in HMCs, which were suppressed after Ad-CTRP3 transfection.
Rat Cultured Carotid Arterial Rings	Zhou et al (2014)(90)	(1, 2, and 4 μg/mL) Recombinant human globular domain CTRP3 Aviscera Bioscience (00082-01-100, Santa Clara, CA)	CTRP3 Promotes Vascular Calcification in High-Phosphate Cultured Carotid Arterial Rings.
Rat vascular smooth muscle cells (VSMCs)	Zhou et al (2014)(90)	(1, 2, and 4 μg/mL) Recombinant human globular domain CTRP3 Aviscera Bioscience (00082-01-100, Santa Clara, CA)	CTRP3 Promotes β-Glycerophosphate–Induced VSMC Calcification *In Vitro* and promoted the phenotypic transition from contractile to osteogenic phenotype. CTRP3 increases mitochondrial Reactive oxygen species levels in VSMC.

Regulation

Analysis of the upstream untranslated region for CTRP3 identified a number of putative consensus sequences for transcription factor regulation of CTRP3 expression. The proximal region of the CTRP3 promoter is highly conserved between rodent and human (28), indicating that there are conserved functional regulation sites. These predicted regulatory sites include loci for the following transcription factors: specificity protein 1 (SP-1); Activator protein 1 (AP-1); Peroxisome proliferator-activated receptor

(PPAR); Fos proto-oncogene (c-FOS); POU domain, class 1, transcription factor 1 (Pit-1a); CCAAT-enhancer-binding proteins-alpha/beta (C/EBP-α/β); Myogenic Differentiation (MyoD); c-JUN; Transcription factor II D – "TATAA" box (TY-IID); cAMP response element-binding protein (CREB); GATA-binding factor 1 (GATA-1); Sex-determining region Y (SRY); SRY-related HMG-box 5 (Sox-5); similar to myelocytomatosis viral oncogene (c-Myc); and Retinoid X receptor (RXR) (53-55). However, to date, only a few transcription factors have been demonstrated to regulate CTRP3 expression experimentally: c-FOS, SP-1, c-JUN, and PPAR-gamma. Although CTRP3, SP-1 and PPAR-gamma are induced during adipocyte differentiation, promoter activity assays demonstrate that PPAR-gamma, SP-1, and c-FOS are all negative regulators of CTRP3 expression (53, 56). Electrophoretic mobility shift assays confirmed that both SP-1 and PPAR-gamma (but not SRY, c-FOS, C/EBPβ, or PPAR-alpha) bind to the promoter region for CTRP3. To date only the transcription factor c-Jun has been shown to be an unequivocal positive regulator for CTRP3 transcription (28). The transcription factor c-Jun is one of three Jun family proteins making up the activator protein-1 (AP-1) transcription factor group. Chromatin immunoprecipitation assay confirmed that c-Jun binds to the AP-1 region (-184/-177) of CTRP3 (28), whereas, other Jun and Fos members JunB, JunD, FosB, Fra-1 and Fra-2 were tested by a reporter gene assay and had no effect on CTRP3 promoter activity (28). Further, treatment of adipocytes, *in vitro*, or diet-induced obese rats, *in vivo*, with the glucagon-likepeptide-1 (GLP-1) receptor agonist, Exendin-4 (Ex-4), increased CTRP3 expression and circulating levels through activation of the Protein kinase A (PKA) pathway (37, 40). Briefly, the activation of GLP-1 receptor and, the PKA pathway activates a HOB1 motif

within the A1 activation domain of c-JUN and promotes c-JUN's binding to the AP-1 region (6). However, the regulation of CTRP3 under physiological conditions *in vivo* has not yet been established. Unlike most adipokines, circulating CTRP3 levels are increased with fasting (51), indicating that CTRP3 levels may be suppressed by either insulin or activated by glucagon signaling pathways. Further, CTRP3 levels are negatively associated with insulin and leptin levels in high fat fed mice (51). Taken together, these data show a potential reciprocal relationship between food intake and CTRP3. However, the clinical implications have yet to be explored, especially regarding the significance of the by-phasic regulation of CTRP3 and lipid metabolism.

Tissues expressed

A summary of cell lines, which express CTRP3, *in vitro*, are listed in Table 3.3. CTRP3 is not detectable in undifferentiated adipocytes, but can be detected at 4 days of differentiation (55, 56). These data match *in vivo* data which shows that CTPR3 is highly expressed in adipose tissue. In addition, CTRP3 is also detected during development, starting at mouse embryonic day 15 (43, 75, 76), in developing chondrocytes (43) and cartilage (44). These data have led to speculation that CTRP3 is essential for appropriate bone growth and development. This is supported by experimental evidence that demonstrates that CTRP3 stimulates the proliferation and differentiation of chondrogenic and osteogenic precursors, inhibits osteoclast activity, and is essential for appropriate bone formation *in vitro* (1, 27, 44, 82). However, a clinical association between abnormal development and deregulation of CTRP3 protein has yet to be documented. On the other hand, CTRP3 is highly expressed in both osteoscarcoma and chandroblastoma cell lines but not in the MC3T3-E1 mouse osteoblast-like non-

cancer cell line (3). These data have led to speculation that elevated CTRP3 level in adults may be a risk factor and/or biomarker for certain types of cancer, specifically osteoscarcoma, but again this hypothesis remains to be tested either *in vivo* or in a clinical population.

Table 3.3: *CTRP3 Expression In Vitro*

Cell Line	Reference	Finding
Adipose tissue collected from control (n=3) or diabetic (n=3) female donors	Schmid et al 2012(59)	CTRP3 protein levels were higher in subcutaneous adipocytes from an obese compared with lean donor, no differences were observed from visceral adipocytes. (Note: small sample size, n = 3)
N1511 (mouse chondrogenic progenitor)	Maeda et al 2006(44)	CTRP3 is induced w/ differentiation by TGF-beta
3T3-L1a (mouse pre-adipocyte)	Schaffler et al 2007(56)	Produce CTRP3 at day 4 differentiation and CTRP3 promoter activity was suppressed when treated with PPAR ligands: troglitazone (α/γ), fenofibrate (α), but not 15-Deoxy-Delta-12,14-prostaglandin J2.
3T3-L1a (mouse pre-adipocyte)	Li et al 2015(37)	Exendin-fragment 4 (Ex-4), a specific GLP-1 receptor agonist, specifically used to treat T2D, increased CTRP3 mRNA and protein whereas Ex-9 (and GLP-1 antagonist) or blocking activation of PKA (thr197) phosphorylation by H89, a selective antagonist of PKA, blocked Ex-4 induced increases in CTRP3. Neither H89 nor Ex-9 had any effect on CTRP3 alone.
3T3-L1a (mouse pre-adipocyte)	Schmid et al 2012(59)	CTRP3 is positively regulated by insulin, and inhibited by chronic LPS-exposure or Intracellular infection of adipocytes by S. aureus. Further, siRNA knockdown of CTRP3 reduced resistin secretion and lipolysis.
MC3T3-E1 (mouse osteoblast-like cell line; non-cancer)	Akiyama et al 2009(3)	Neither CTRP3 mRNA or protein was detected
Human mesangial cells (HMCs)	Zhang et al 2016(86)	polymeric IgA (pIgA) suppressed CTRP3 mRNA and protein whereas the IgA1 fractions (mIgA and pIgA) had no effect on CTRP3. Further, galactose-deficient IgA (gd-IgA; the type of IgA found in IgAN patients) suppressed CTRP3 mRNA levels even more than pIgA at identical concentrations (~60% compared with 30%).
LM8 (mouse osteosarcoma cell line)	Akiyama et al 2009(3)	CTRP3 mRNA and protein detected.
NOHS (mouse osteosarcoma cell line)	Akiyama et al 2009(3)	CTRP3 mRNA and protein detected.
Human omental adipose tissue explants	Tan et al 2013(65)	Metformin increased CTRP3 secretion.
TM3 mouse Leydig Cells	Otani et al 2012(47)	Express CTRP3

In adult mice CTRP3 is considered an adipokine, as it is predominantly expressed in adipose tissue (55, 56, 75), indicating that CTRP3 may have a functional role in energy storage and metabolism. However, CTRP3 is also expressed in the lung, kidneys, spleen, testis, and macrophages with moderate expression in heart, bone, small intestine, liver, kidney, skeletal muscle, and vascular smooth muscle cells (1, 43, 44, 47, 51, 54, 59, 75, 76, 90). Combined these data indicate that CTRP3 has a variety of factors which could contribute to its regulation and function. In the following sections we will detail the experimental evidence regarding the functional activity of CTRP3 in regards to metabolism, cardiovascular health, inflammation, and growth and development.

Metabolism, Metabolic disease and CTRP3

Overview

CTRP3 has been documented to have a variety of effects on metabolism. The complete overview of *in vitro* effects is listed in Table 3.2. Briefly, CTRP3 increases adipokine secretion, attenuates inflammatory signaling, promotes proliferation, increases cellular differentiation, and increases hepatic lipid oxidation (39, 41, 50, 51, 58). Whereas, the *in vivo* the effects of CTRP3 are less well examined. The summary of all animal experiments and CTRP3 are listed in Table 3.4. For example, in rodents an acute injection with recombinant CTRP3 protein decreases serum glucose levels for up to 8-hours with no change to insulin levels (51). The chronic transgenic overexpression of CTRP3 had not effect upon glucose levels, which demonstrates the development of a potential compensatory mechanism (51). On the other hand, both transgenic overexpression and daily administration of CTRP3 were effective in attenuating high fat

diet-induced hepatic insulin resistance and hepatic steatosis (50). Conversely, hepatic triglycerides were elevated in high fat-fed CTRP3 Knockout mice when compared to high fat-fed wild-type mice (71). Considered together, these data suggest that the metabolic effects of CTRP3 are specific to the liver, as no changes to metabolism were observed in skeletal muscle in any experimental (*in vivo* or *in vitro*) model examined. Interestingly, neither transgenic overexpression nor genetic deletion of CTRP3 resulted in a measurable metabolic effect in mice fed a low fat diet (50, 71), which indicates that CTRP3 may function specifically to help regulate metabolism in response to elevated lipid consumption.

Table 3.4: *Metabolic Effects of CTRP3 In Vivo*

Model	Reference	Results
Male rats HFD+low dose Streptozotocin	Li et al 2014(40)	CTRP3 mRNA increased between birth and 10 weeks of age. Insulin resistance or T2D decreased CTRP3 (Protein &mRNA) and treatment with Ex-4 slightly increased CTRP3.
CTRP3 Knockout and collagen-induced arthritis model	Murayama et al (2014)(46)	↑ severe histopathological changes.
Transgenic CTRP3 overexpression with low or high fat diet	Petersen et al (2016)(48)	LF-diet; ↑ the circulating levels of CCL11, CXCl9, CXCL10, CCL17, CX3CL1, CCL22, AND Scd30. HF-Diet: ↓ circulating levels of IL-5, TNF-α, sVEGF2, and sVEGFR3, and ↑ circulating levels soluble gp130.
Acute injection of CTRP3	Peterson et al (2010)(50)	↓glucose, ↑pAkt and hepatic gluconeogenesis (specifically PEPCK and G6Pase.
Transgenic CTRP3 overexpression with low or high fat diet	Peterson et al (2012)(51)	No metabolic effect LF-diet; On HF-diet: mild shift to lipid oxidation, ↓ hepatic triglyceride synthesis, ↓ hepatic stenosis, ↑ insulin sensitivity. ↓ circulating TNF, IL5 and cholesterol levels and more than doubled soluble gp130 (sgp130) levels (an inhibitor of IL-6).
Viral suspension consisting of $1x10^{\wedge 9}$ genomic copies of the lentivirus-CTRP3 (Lenti-CTRP3)	Wang et al (2016)(67)	Attenuates Brain Injury after Intracerebral Hemorrhage via AMPK-Dependent Pathway in Rat.

CTRP3 Knockout fed a high fat diet	Wolf et al (2016)(71)	No differences in metabolic factors between KO and WT, however the liver was smaller with a higher triglyceride content.
Mouse model of myocardial infarction (MI); Adenovirus mediated overexpression of human full-length CTRP3	Yi et al 2012(81)	MI reduced adipocyte CTRP3 mRNA and plasma protein levels. Whereas, Replenishment of CTRP3 after MI Improves Survival, Cardiac Function, promotes angiogenesis,

Regardless, the clinical implications of these effects have yet to be explored, as the reported associations between obesity and/or type 2 diabetes (T2D) with CTRP3 levels are contradictory in the literature. The summary finding of all cross sectional human studies, which examine CTRP3 levels, are listed in Table 3.5. Briefly, CTRP3 levels are reported to be elevated (12), not different (16, 66), or reduced (5, 14, 52, 65, 72, 83) with obesity and/or T2D. In most reports circulating CTRP3 levels are higher in women than in men (10, 14, 72, 83), with one exception (52). Further complicating the relationship between CTRP3 levels and human health, Wager *et al*. (2016) (66) reported that CTRP3 levels are elevated with obesity in male but are reciprocally reduced with obesity in female subjects. This contradictory gender dependent association of obesity and circulating CTRP3 levels provides some explanation regarding the conflicting data in the literature, as almost all the reported studies combined varying proportions of male and female subjects within each experimental group. Nevertheless, these data demonstrate that there is a gender specific regulation and function of CTRP3 that needs to be explored in more detail. Further, all of these studies have examined the total amount of CTRP3 with no attention being given to the different splice variants or in the multimeric structures of the circulating CTRP3. This is worth noting as high molecular weight adiponectin is thought to be the active form (20,

32), and similarly the different splice variants and multimeric structure may also contribute to the function of CTRP3. Lastly, the associations between circulating CTRP3 levels (splice variants and multimeric structures) and hepatic steatosis in human subjects have not been explored even though animal experiments have shown a specific hepatic effect of both CTRP3A and CTRP3B (51).

Table 3.5: *Cross-Sectional Studies Regarding CTRP3 Levels*

Population (Male:Female)	**Reference**	**Result**
Newly diagnosed T2D (25:22) vs Control (35:28)	Ban et al 2014(5)	CTRP3 levels were lower in T2D (150 ng/ml) vs control (249 ng/ml). CTRP3 was negatively associated with C-reactive protein levels and positively associated with insulin levels in control subjects. No associations were observed in T2D.
126 singleton live births (67:59)	Chen et al. 2016(9)	CTRP3 was positively correlated with Ponderal index (a measurement of thinness) and birth weight.
Control (40:79), prediabetic (40:71), or T2D (54:65)	Choi et al 2012(12)	Overall: CTRP3 levels were positively correlated with Total cholesterol, fasting blood glucose, AST and ALT, Creatinine, and C-reactive protein levels, and negatively correlated with estimated glomerular filtration rate. CTRP3 increased significantly with T2D (Normal 273, prediabetes 482, and T2D 516 ng/ml).
453 nondiabetic Korean adults (137:316)	Choi et al. 2013(10)	CTRP3 levels were higher in women than men. Independently associated with age, sex, and triglyceride, LDL cholesterol, adiponectin, and retinol-binding protein 4 (RBP4) levels.
362 Korean adults: with acute coronary syndrome (49:20), stable angina pectoris (58:27), or control subjects (137:71)	Choi et al. 2014(11)	CTRP-3 levels were lower in patients with acute coronary syndrome or stable angina pectoris compared to control subjects. CTRP-3 levels negatively associated with glucose and C-reactive protein positively associated with HDL-cholesterol and adiponectin.
Newly diagnosed obese and hypertensive patients (124:83)	Deng et al 2015(14)	Regardless of groups women had higher CTRP3 levels than men. Both obesity and High blood pressure were associated with lower CTRP3 levels, there was no further reduction in obesity combined with High BP
Obese (33:39) and T2D (34:35)	Flehmig et al 2014(16)	No difference in CTRP3 levels with obesity or T2D. Of the 69 T2D, 46 were taking metformin and CTRP3 levels were increased with metformin (267 vs 343 ng/mL).
COPD patients (50:23) and healthy controls (29:25)	Li et al 2015(34)	CTRP3 levels (COPD 950 ng/mL; Control 820 ng/mL) had no correlation to lung function. No association between CTRP-3 and CRP, TNF-α, or adiponectin.
Lean (25:20), obese (19:24), T2D (17:24), and Obese+T2D (22:23)	Qu et al 2015(52)	No difference in CTRP3 between men and women (397.51 ± 122.67 vs 416.17 ± 131.24 ng/mL,). CTRP3 levels were reduced in obese and T2D and further reduced in obese+T2D. CTRP3 levels were negatively associated with IL-6 levels, HOMA-IR, and HbA1c.

Women with Polycystic ovary syndrome (PCOS)	Tan et al. 2013(65)	CTRP3 levels were lower in women with PCOS (200 ng/ml) compared with control (330 ng/ml); Metformin intervention increased CTRP3 levels to (272 ng/ml). BMI, Insulin, LDL, Triglycerides, CRP and Carotid intima-media thickness were all negatively associated with CTRP3 levels. TNF levels were not associated with CTRP3
Lean (20:40) and obese (6:44)	Wolf et al 2015(72)	CTRP3 was inversely associated with BMI and triglyceride levels. Men had significantly lower CTRP3 levels compared to women (397.7 vs. 432 ng/mL, $p<0.01$).
Control (61:22) vs. metabolic syndrome (32:12)	Yoo et al. 2013(83)	CTRP3 concentrations exhibit a significant negative association with cardiometabolic risk factors and positive association with adiponectin.
16 patients diagnosed with IgA nephropathy (IgAN) compared to 12 controls	Zhang et al 2016(86)	CTRP3 levels were lower in patients with IgAN (TGF-β and IL-6 levels were elevated in these patients).
Patients with symptoms requiring heart catheterization to diagnosis obstructive CAD (52:48)	Wagner et al 2016(66)	No association between obstructive coronary artery disease and CTRP3 levels. CTRP3 levels were higher in lean female than males. CTRP3 levels increased with obesity in males, but decreased with obesity in female patients.

Human studies

To date very few experimental intervention studies have been performed with human subjects. The first, Wurm *et al*. (2007) (78) examined circulating CTRP3 levels before and 2 hours after a glucose load (n=20, 14 males and 6 females) and observed no change. However, this study occurred before there were reliable ELISA's developed for CTRP3 and examined CTRP3 levels solely though immunoblot analysis. Further complicating the results from this study is that although they reported the supplier (R&D Systems) they did not include the catalog number for the antibody used and they reported band migration of 50 kDa for CTRP3 on a denaturing SDS-PAGE. CTRP3 has a predicted and gel migration ~30 kDa and although the posttranslational modifications for CTRP3 could result in a higher than predicted migration pattern on an SDS gel, this has not been observed by other researchers (1, 43, 51, 70, 75). Indeed, the antibody for human CTRP3 from R&D Systems (R and D Systems Cat# AF7925, RRID:AB_2619735) also reports detecting a band at ~30 kDa. Moreover, using an

ELISA based method Ban *et al*. (2014) observed that in type 2 diabetic patients CTRP3 levels decreased from ~150 to 50 ng/ml in response to a 2-hour oral glucose load (5). In light of these data and the progress within the past 9 years in CTRP3 antibody and ELISA development, the effects of glucose on CTRP3 levels in a healthy human subject population should be reexamined. In addition, due to the potential role of CTRP3 in lipid metabolism, experiments should also examine the effects of acute lipid loading on circulating CTRP3 levels.

Only one study has examined the effects of exercise on circulating CTRP3 levels in human subjects. Briefly, Choi *et al*. (2013) examine changes to circulating CTRP3 levels after a 3-month exercise program (45 min cardio/20 min resistance 5x/week) in 76 obese Korean females. (10) They found that CTRP3 levels decreased by ~15% (444 ng/ml to 374 ng/ml) after exercise intervention. The exercise training program also resulted in ~9% loss in body weight, so it is unclear if the change in CTRP3 levels were due to exercise or the reduction in body fat. The effects of acute exercise or exercise training on CTRP3 levels in a healthy human population or in the absence of weight loss have not been investigated.

Lastly, Tan *et al*. (2013) (65) reported that women with polycystic ovary syndrome had lower levels of CTRP3 than control subjects. Polycystic ovary syndrome is an endocrine system disorder associated with obesity, diabetes, dyslipidemia, and cardiovascular complications and Metformin is a common medication used in the treatment of insulin resistance, obesity and type 2 diabetes. CTRP3 levels were restored with Metformin treatment along with general improvement in insulin sensitivity.

CTRP3 and Cardiovascular Disease

Cardiovascular disease (CVD) is the leading cause of death in the world, accounting for 30% of all deaths. (17) The identification of novel biomarkers indicating the progression, or signaling pathways which can be exploited as a treatment, for CVD is an ongoing interest for combating this disease. It is well established that obesity is a leading risk factor for CVD (63), however very little attention has been given to the endocrine function of adipose tissue and its role in CVD. In both cell culture and animal models CTRP3 has been shown to be protective following heart attack (myocardial infarction, MI) or stroke (intracerebral hemorrhage, ICH) (11, 42, 67, 77, 80, 81, 83, 89). Table 3.6 contains the complete summary of the treatment effects of CTRP3 treatment as it related to CVD. Specifically, CTRP3 stimulates mitochondrial biogenesis in cardiac tissue and promotes vascular relaxation (85,89), whereas immediately following an MI there is a significant decrease of adipose tissue CTRP3 mRNA and circulating CTRP3 protein levels (77, 81). In animal models of MI exogenous CTRP3 pretreatment (adenovirus-delivered or recombinant CTRP3) increases survival, improves postevent cardiac function, and prevents pathological remodeling (77, 81). Progressive remodeling after myocardial infarction (MI) is a leading cause of morbidity and mortality associated with MI. Specifically Transforming growth factor beta (TGF-β) has been reported to be involved in ventricular remodeling by promoting myocardial fibrosis (88). However, CTRP3 attenuates TGF-β1-induced signaling and pathogenic remodeling post-MI both *in vivo* and *in vitro* (77). Regarding stroke recovery, preconditioning with CTRP3 reduced cerebral edema, reduced blood-brain barrier damage, improved neurological

function, and reduced oxidative stress following ICH (67,80). Collectively, these data illustrate the potential of CTRP3 and CTRP3-mediated signaling pathways as a prospective post-MI/ICH treatment targets.

Table 3.6: *Summary of Cardiovascular Effects of CTRP3 Treatment*

Model	Reference	Treatment/Measurement	Effect
MSS31 (mouse endothelial cells(79))	Akiyama (2) et al (2007)	1-5 μg/ml [E. Coli produced His_6-tagged signal peptide removed]	↑ Proliferation and migration, ↑ ERK1/2 & MAPK p38 within 15 minutes.
Rat vascular smooth muscle cells (VSMCs)	Feng et al 2016(15)	Recombinant human globular CTRP3 (Aviscera Bioscience, no catalog # provided), or siRNA knockdown of CTRP3	CTRP3 increase ATP synthesis and oxidative phosphorylation complex proteins, reversed with knockdown. CTRP3 increases mitochondrial ROS.
Rat vascular smooth muscle cells (VSMCs)	Feng et al 2016(15)	Recombinant human globular domain CTRP3 (Aviscera Bioscience, no catalog # provided)	CTRP3 increases mitochondrial Reactive oxygen species levels in VSMC.
Adventitial fibroblasts	Lin et al 2014(42)	CTRP3 protein (10 μg/ml) (source/type of CTRP3 was not reported)	CTRP3 prevents TGF-β1 induced fibroblasts phenotypic conversion, proliferation, migration, and collagen I expression.
Primary cultured adult rat cardiac fibroblast (CF)	Wu et al 2015(77)	2 μg/ml Recombinant human gCTRP3 (Aviscera Bioscience; 00082-01-100; E. Coli expressed); also used siRNA knockdown of CTRP3	CTRP3 inhibited TGF-β1 induced markers for myofibroblast differentiation and TGF-β1 induced- phosphorylation of Smad3. Whereas, CTRP3 knockdown increased TGF-β1 induced markers for myofibroblast differentiation.
Rat intracerebral hemorrhage (ICH)	Yang et al 2016(80)	+/- lentivirus or recombinant CTRP3 (80 μg/kg, Chimerigen, USA),	Reduced cerebral edema and blood-brain barrier damage and improved neurological functions and reduced oxidative stress via PKA signaling pathway
Cardiomyocytes (adult mouse)	Yi et al 2012(81)	Bacterial expressed globular domain of Mouse CTRP3, and condition media from 3T3-L1a cell +/- CTRP3 siRNA.	CTRP3 upregulated levels of phosphorylated Akt, HIF1α, and VEGF. Cardiomyocyte hypoxia-induced apoptosis was attenuated with condition media from 3t3-L1A adipocytes, abolished with CTRP3 siRNA.
HUVEC	Yi et al 2012(81)	Bacterial expressed globular domain of mouse CTRP3	Condition media from primary cardiomyocytes treated with CTRP3 significantly enhanced HUVEC tube formation. No direct effect of CTRP3
Mouse - myocardial infarction (MI)	Yi et al 2012(81)	Adenovirus or bacterial expressed globular domain of mouse CTRP3	MI reduced CTRP3 levels, CTRP3 treatment improved survival rate, restored cardiac function, increased revascularization, and reduced fibrosis

Neonatal rat ventricular myocytes	Zhang et al 2016(85)	0.5 – 4 μg/ml Human recombinant globular and full-length CTRP3 (Aviscera Bioscience, no catalog #)	CTRP3 increased AMPK activated transcription factors and restored hypoxia-reoxygenation injury induced reduction in sirtuin1, PGC-1α, NRF-1, complex III and ATP content.
Aortic rings from C57BL/6 mice	Zheng et al 2011(89)	mammalian expressed CTRP3 (1, 3, & 10 μg/ml)	3 and 10 (but not 1) μg/ml of mammalian expressed CTRP3 caused significant vasorelaxation.
Rat Cultured Carotid Arterial Rings	Zhou et al 2014(90)	(1-4 μg/mL) human globular CTRP3 (Aviscera Bioscience, 00082-01-100)	CTRP3 Promotes Vascular Calcification in High-Phosphate Cultured Carotid Arterial Rings.
Rat vascular smooth muscle cells (VSMCs)	Zhou et al 2014(90)	(1-4 μg/mL) human globular CTRP3 (Aviscera Bioscience, 00082-01-100)	CTRP3 Promotes β-Glycerophosphate–Induced VSMC Calcification and mitochondrial Reactive oxygen species levels in VSMC.
Mouse: Adenine-induced chronic renal failure (CRF)	Zhou et al 2014(90)	CTRP3 levels measured by ELISA and RT-qPCR or Adenovirus encoding full-length human CTRP3	Protein CTRP3 levels increased but adipose mRNA expression was reduced with CRF. CTRP3 Increased Vascular Calcification.

CTRP3 is also demonstrated to play a large role in angiogenesis and endothelial cell proliferation. (2, 23, 45, 81) For example, during the recovery period following rat carotid artery balloon-injury model CTRP3 expression increases dramatically (35). Interestingly CTRP3 may not act directly on the endothelial cells, but through indirect pathways mediated by cardiac or smooth muscles cells. Direct treatment of Human Umbilical Vein Endothelial Cells (HUVEC) with CTRP3 had no direct effect on capillary-like structures formation (tube formation), Akt phosphorylation or hypoxia-inducible factor 1, alpha subunit (HIF-1α) or Vascular endothelial growth factor (VEGF) expression. (81) However, conditioned media from primary cardiomyocytes treated with CTRP3 induced HUVEC tube formation, indicating the presence of CTRP3-induced cardiomyocyte-secreted paracrine factors. (81) However, the direct effect of CTRP3 on HUVEC cells cannot be completed ruled out as Yi *et al*. (2012) (81) used bacterial expressed CTRP3 directly on HUVEC cells and used mammalian expressed CTRP3 *in vivo*. This discrepancy may indicate a post-

translational modification is required for CTRP3-induced effects on vascular endothelium.

As shown in table 3.6, very few studies have examined the association between CVD and circulating CTRP3 levels in a human patient population. Specifically, Wagner *et al*. (66) observed no association between the presence of CVD and CTRP3 levels among patients with symptoms requiring catherization for detecting the presence of coronary artery blockage. Whereas, Deng *et al*. 2015 (14), observed that both obesity and high blood pressure were associated with lower CTRP3 levels and Choi *et al*. 2014 (11) reported that CTRP-3 concentrations in patients with acute coronary syndrome or stable angina pectoris were significantly decreased compared to control subjects. Further, CTRP3 concentrations have been shown to exhibit a significant negative association with many cardiometabolic risk factors (11, 83). As CTRP3 levels decrease with obesity, at least in men (66), the lower levels of CTRP3 may contribute to the impaired mitochondrial biogenesis in cardiac cells and increase the susceptibility/severity of an MI event. On the other hand, excessive sustained elevation of CTRP3 may also be detrimental to cardiovascular health as CTRP3 as promotes vascular and aortic ring calcification (90), increase vascular calcification promotes arterial hardening and the development of arteriosclerosis. Regardless of the associations between CTRP3-mediated signaling and CVD appear promising and need to be investigated in more detail.

Inflammation

Metabolic syndrome is defined as a cluster of risk factors which directly increase the risk of CVD, T2D, and all-cause mortality (4, 26). One of the major defining risk factors for metabolic syndrome is a chronic state of low-grade inflammation state marked by elevated circulating pro-inflammatory cytokines (TNF, IL-6, and C-reactive protein). The adipose tissue immune response plays a major role in the development of the chronic pro-inflammatory state (22, 26). Whereas, CTRP3 is a potential anti-inflammatory mediator, and is negatively associated with the pro-inflammatory cytokines TNF, IL-6, and C-reactive protein (5, 11, 12, 14, 48, 50, 52, 65, 83). In animal models diet-induced obesity results in decreased CTRP3 levels concurrent with an elevation in TNF and IL-6 (50). Similarly, diet-induced obese CTRP3-knockout mice have an enhanced elevation of IL-6 and TNF levels (71). Further, transgenic overexpression of CTRP3 attenuates the high-fat diet induce rise in cytokine levels and more than doubles circulating soluble gp130 (sgp130) levels (50). Circulating sgp130 is a potent inhibitor of inflammatory cytokines such as IL-6 (24). On another note, although essential for regulating platelet aggregation, excessive levels of the cytokine thromboxane A2 are associated with the development of insulin resistance and arteriosclerosis (18), and are elevated in both human and mouse models of obesity (33). However, loss of Thromboxane synthase (TBXAS), the enzyme necessary to produce thromboxane A2, markedly enhances insulin sensitivity concurrent with the up-regulation of CTRP3, as well as other adipokines (CTRP9, CTRP12) (33). CTRP3 has also demonstrated potential as a treatment for a specific inflammatory disorder, IgA nephropathy (IgAN). IgAN is a kidney disorder caused by deposits of the protein immunoglobulin A (IgA)

inside the glomeruli of kidney and excessive mesangial cell activation. In patients with IgAN CTRP3 levels are significantly reduced and the cytokines IL-6 and TGF-β are elevated (86). Treatment of isolated adult human mesangial cells (HMCs) with CTRP3 reduced IL-6 and TGF-*β* production and inhibited HMC activation (86). Combined these data demonstrate the potential of CTRP3 in the treatment of inflammatory disorders. The summary finding of all studies examining the connection between inflammation and CTRP3 are listed in Table 3.7.

Table 3.7: *CTRP3 and Inflammation*

Model	Reference	Type of treatment	Effect
Human primary colonic lamina propria fibroblasts (CLPF)	Hofmann et al 2011(21)	Recombinant CTRP-3 (High Five insect cells)	Significantly and dose-dependently reduced LPS-induced IL-8 secretion in CLPF within 8 hours after LPS exposure, whereas LPS-induced IL-6 and TNF release was not affected. CTRP-3 inhibited TGF-β production and the expression of CTGF and collagen I in CLPF, whereas collagen III expression remained unchanged.
Primary Human monocytes	Kopp et al 2010(30)	1 µg/ml Recombinant full length CTRP3 (H5 insect cells)	Suppressed LPS-induced MIF & CCL4 release in lean subjects, & MCP-1 in monocytes from both diabetic and leans subjects. Prevents Lauric acid induced release of IL-6 and TNF
Primary Human monocytes	Kopp et al 2010(31)	1 µg/ml Recombinant full length CTRP3 (H5 insect cells)	↓ LPS-induced secretion of IL-6 in monocytes from control but not T2D. CTRP3 did not significantly affect TNF secretion.
Adipocyte (3T3-L1)	Li et al 2014(38)	Recombinant CTRP3 (uncited origin)	Decreased TNF and IL6 secretion in insulin resistant 3T3-L1A.
Transgenic CTRP3 overexpression and CTRP3 Knockout	Peterse n et al 2016 (48)	Response to sublethal dose of LPS challenge	No effect on IL-1β, IL-6, TNF-α, or MIP-2 induction.
LPS (1 µg i.p.) into male mice +/- CTRP3	Schmid et al. 2014 (60)	Recombinant CTRP-3 (H5 insect cells)	Intraperitoneal injection (but not IV) injection of CTRP-3 significantly reduced LPS-induced IL-6 and levels MIP-2.

16 patients diagnosed with IgA nephropathy (IgAN) compared to 12 controls	Zhang et al 2016 (86)		CTRP3 levels were lower in patients with IgAN (TGF-B and IL-6 levels were elevated in the patients).
THP-1 (human - Acute Monocytic Leukemia cell line)	Weigert et al 2005 (70)	1 µg/ml Recombinant full length CTRP3 (H5 insect cells)	Suppressed LPS induced: IL-6 & TNF expression and secretion.

Lipopolysaccharide (LPS), is a well-established endotoxin used as a model of systemic immune response, *in vivo*. In cell culture models LPS inhibits adipose tissue differentiation, induces insulin resistance, and prevents the expression of CTRP3 (59). Whereas, CTRP3 has been shown to specifically block the binding of LPS to its receptor TLR4 (13, 30) and inhibit the inflammatory response (30). Further, in animal models intraperitoneal injection (IP) injection of CTRP3 (0.4ug/g body weight) significantly reduced LPS-induced (IP) inflammatory response (65). Although intravenous administration of CTRP3 was unable to prevent LPS-induced inflammation, this is thought to be a dose related limitation and future studies are ongoing to determine the clinically relevant levels of CTRP3 administration needed to inhibit a systematic immune response. Further, CTRP-3 potently inhibited LPS-induced IL-6 in monocytes isolated from healthy subjects but not in monocytes derived from a subject with T2D (31, 70). Similarly, the anti-inflammatory effects of CTRP3 have also been observed in isolated primary human colonic fibroblasts (21). Combined, these data show promise for the use of CTRP3 and CTRP3-mediated pathways as a potential anti-inflammatory mediator. However, neither chronic CTRP3 deficiency nor overexpression altered the inflammatory response to a sublethal challenge to LPS (48), indicating that

CTRP3 levels need to be regulated transiently to demonstrate an anti-inflammatory effect. Regardless, the potential use of CTRP3 as an inhibitor of inflammation needs to be examined in more detail.

Growth, Reproduction, and Tumorigenesis

CTRP3 has been linked to normal and pathogenic cellular proliferation, growth and development. CTRP3 has been consistently shown to stimulate the proliferation of chondrogenic precursors, chondrocytes, and osteocytes, *in vitro*, through activation of ERK1/2 and PI3K pathways (1, 3, 27, 44, 82). During early development CTRP3 is detected in developing chondrocytes (43) and cartilage (44) which has led to the hypothesis that CTRP3 is essential for normal cartilage and bone development. In support of this CTRP3 is appears to be essential for proper mandible formation through perichondrium maintenance and new cartilage formation (82). However, the role of CTRP in development may be dispensatory as CTRP3-knockout animals do not demonstrate a growth phenotype indicating a possible compensatory mechanism during development. However, CTRP3-knockout mice do exhibit increased susceptibility to collagen-induced arthritis, indicating CTRP3 may be important for the maintenance and repair of cartilage tissue (46). However, elevated CTRP3 may also be detrimental as CTRP3 is highly secreted from and increases growth rates of osteosarcoma and chondroblastoma tumor cell lines indicating that CTRP3 may be linked to these types of cancers (54). However, no cancers have been reported in CTRP3 transgenic overexpressing mice, although this has not been specifically examined. Lastly, CTRP3 is specifically expressed in the testosterone producing interstitial Leydig cells and treatment of TM3 mouse Leydig cells with CTRP3 increased testosterone production

(47). Although these findings may shed some light on the discrepancy between male and female in circulating CTRP3 levels, the overall clinical significance has yet to be explored.

SUMMARY AND CONCLUSION

Adipose tissue secretes numerous adipokines that contribute to a wide array of biological processes. CTRP3, is a novel and unique member of the adipokine superfamily which appears to have unique roles in a variety of tissue: hepatic lipid metabolism, cardiovascular response to ischemia, and increases chondrocyte proliferation and differentiation. CTRP3 can function in an autocrine, paracrine, and endocrine manner and there are many aspects of CTRP3's regulation and function that have yet to be explored. In addition, CTRP3 has been consistently linked to activation of the PKA signaling pathway, regardless of the tissue/treatment paradigm examined (37, 47, 80). This review should serve as a basis for the design of future experimental studies specifically examining: (i) the regulation of CTRP3 in response to food intake or exercise, (ii) associations between circulating CTRP3 levels, including the two different splice variants (CTRP3A and CTRP3B), and hepatic steatosis or osteoscarcoma in clinical population, and (iii) the associations between the different CTRP3 isoforms (CTRP3A and CTRP3B) and multimeric structures in clinical populations, (iv) the potential use of CTRP3 as an inhibitor of inflammation, and (v) whether the putative receptors, LAMP-1 and LIMPII are directly responsible for the intracellular effects of CTRP3 or at as co-receptors for a yet unidentified protein. Finally, the gender-specific regulation of CTRP3 needs to be explored in more detail (splice variants and multimeric

structures) especially in regards to the association between CTRP3 and human diseases such as non-alcoholic fatty liver disease, T2D, and metabolic syndrome.

REFERENCES

1. **Akiyama H, Furukawa S, Wakisaka S, and Maeda T**. Cartducin stimulates mesenchymal chondroprogenitor cell proliferation through both extracellular signal-regulated kinase and phosphatidylinositol 3-kinase/Akt pathways. *FEBS J* 273: 2257-2263, 2006.

2. **Akiyama H, Furukawa S, Wakisaka S, and Maeda T**. CTRP3/cartducin promotes proliferation and migration of endothelial cells. *Mol Cell Biochem* 304: 243-248, 2007.

3. **Akiyama H, Furukawa S, Wakisaka S, and Maeda T**. Elevated expression of CTRP3/cartducin contributes to promotion of osteosarcoma cell proliferation. *Oncol Rep* 21: 1477-1481, 2009.

4. **Alberti KG, and Zimmet PZ**. Definition, diagnosis and classification of diabetes mellitus and its complications. Part 1: diagnosis and classification of diabetes mellitus provisional report of a WHO consultation. *Diabet Med* 15: 539-553, 1998.

5. **Ban B, Bai B, Zhang M, Hu J, Ramanjaneya M, Tan BK, and Chen J**. Low serum cartonectin/CTRP3 concentrations in newly diagnosed type 2 diabetes mellitus: *in vivo* regulation of cartonectin by glucose. *PLoS One* 9: e112931, 2014.

6. **Bannister AJ, Brown HJ, Sutherland JA, and Kouzarides T**. Phosphorylation of the c-Fos and c-Jun HOB1 motif stimulates its activation capacity. *Nucleic Acids Res* 22: 5173-5176, 1994.

7. **Byerly MS, Petersen PS, Ramamurthy S, Seldin MM, Lei X, Provost E, Wei Z, Ronnett GV, and Wong GW**. C1q/TNF-related protein 4 (CTRP4) is a unique secreted protein with two tandem C1q domains that functions in the hypothalamus to modulate food intake and body weight. *J Biol Chem* 289: 4055-4069, 2014.

8. **Byerly MS, Swanson R, Wei Z, Seldin MM, McCulloh PS, and Wong GW**. A central role for C1q/TNF-related protein 13 (CTRP13) in modulating food intake and body weight. *PLoS One* 8: e62862, 2013.

9. **Chen NN, He JR, Li WD, Kuang YS, Yuan MY, Liu XD, Zhang HZ, Hu SP, Xia HM, and Qiu X**. C1q and tumor necrosis factor-related protein 3 is present in human cord blood and is associated with fetal growth. *Clin Chim Acta* 453: 67-70, 2016.

10. **Choi HY, Park JW, Lee N, Hwang SY, Cho GJ, Hong HC, Yoo HJ, Hwang TG, Kim SM, Baik SH, Park KS, Youn BS, and Choi KM**. Effects of a combined aerobic and resistance exercise program on C1q/TNF-related protein-3 (CTRP-3) and CTRP-5 levels. *Diabetes Care* 36: 3321-3327, 2013.

11. **Choi KM, Hwang SY, Hong HC, Choi HY, Yoo HJ, Youn BS, Baik SH, and Seo HS**. Implications of C1q/TNF-related protein-3 (CTRP-3) and progranulin in patients with acute coronary syndrome and stable angina pectoris. *Cardiovasc Diabetol* 13: 14, 2014.

12. **Choi KM, Hwang SY, Hong HC, Yang SJ, Choi HY, Yoo HJ, Lee KW, Nam MS, Park YS, Woo JT, Kim YS, Choi DS, Youn BS, and Baik SH**. C1q/TNF-related protein-3 (CTRP-3) and pigment epithelium-derived factor (PEDF) concentrations in patients with type 2 diabetes and metabolic syndrome. *Diabetes* 61: 2932-2936, 2012.

13. **Compton SA, and Cheatham B**. CTRP-3: blocking a toll booth to obesity-related inflammation. *Endocrinology* 151: 5095-5097, 2010.

14. **Deng W, Li C, Zhang Y, Zhao J, Yang M, Tian M, Li L, Zheng Y, Chen B, and Yang G**. Serum C1q/TNF-related protein-3 (CTRP3) levels are decreased in obesity and hypertension and are negatively correlated with parameters of insulin resistance. *Diabetol Metab Syndr* 7: 33, 2015.

15. **Feng H, Wang JY, Zheng M, Zhang CL, An YM, Li L, and Wu LL**. CTRP3 promotes energy production by inducing mitochondrial ROS and up-expression of PGC-1alpha in vascular smooth muscle cells. *Exp Cell Res* 341: 177-186, 2016.

16. **Flehmig G, Scholz M, Kloting N, Fasshauer M, Tonjes A, Stumvoll M, Youn BS, and Bluher M**. Identification of adipokine clusters related to parameters of fat mass, insulin sensitivity and inflammation. *PLoS One* 9: e99785, 2014.

17. **Gaziano T, Reddy KS, Paccaud F, Horton S, and Chaturvedi V**. Cardiovascular Disease. In: *Disease Control Priorities in Developing Countries*, edited by Jamison DT, Breman JG, Measham AR, Alleyne G, Claeson M, Evans DB, Jha P, Mills A, and Musgrove P. Washington (DC): 2006.

18. **Graziani F, Biasucci LM, Cialdella P, Liuzzo G, Giubilato S, Della Bona R, Pulcinelli FM, Iaconelli A, Mingrone G, and Crea F**. Thromboxane production in morbidly obese subjects. *Am J Cardiol* 107: 1656-1661, 2011.

19. **Hada Y, Yamauchi T, Waki H, Tsuchida A, Hara K, Yago H, Miyazaki O, Ebinuma H, and Kadowaki T**. Selective purification and characterization of adiponectin multimer species from human plasma. *Biochem Biophys Res Commun* 356: 487-493, 2007.

20. **Hirose H, Yamamoto Y, Seino-Yoshihara Y, Kawabe H, Saito I.** Serum high-molecular-weight adiponectin as a marker for the evaluation and care of subjects with metabolic syndrome and related disorders. J Atheroscler Thromb 17: 1201-1211, 2010.

21. **Hofmann C, Chen N, Obermeier F, Paul G, Buchler C, Kopp A, Falk W, and Schaffler A**. C1q/TNF-related protein-3 (CTRP-3) is secreted by visceral adipose tissue and exerts antiinflammatory and antifibrotic effects in primary human colonic fibroblasts. *Inflamm Bowel Dis* 17: 2462-2471, 2011.

22. **Hotamisligil GS, Shargill NS, and Spiegelman BM**. Adipose expression of tumor necrosis factor-alpha: direct role in obesity-linked insulin resistance. *Science* 259: 87-91, 1993.

23. **Hou Q, Lin J, Huang W, Li M, Feng J, and Mao X**. CTRP3 Stimulates Proliferation and Anti-Apoptosis of Prostate Cells through PKC Signaling Pathways. *PLoS One* 10: e0134006, 2015.

24. **Jostock T, Mullberg J, Ozbek S, Atreya R, Blinn G, Voltz N, Fischer M, Neurath MF, and Rose-John S**. Soluble gp130 is the natural inhibitor of soluble interleukin-6 receptor transsignaling responses. *Eur J Biochem* 268: 160-167, 2001.

25. **Kambara T, Ohashi K, Shibata R, Ogura Y, Maruyama S, Enomoto T, Uemura Y, Shimizu Y, Yuasa D, Matsuo K, Miyabe M, Kataoka Y, Murohara T, and Ouchi N**. CTRP9 protein protects against myocardial injury following ischemia-reperfusion through AMP-activated protein kinase (AMPK)-dependent mechanism. *J Biol Chem* 287: 18965-18973, 2012.

26. **Kaur J**. A comprehensive review on metabolic syndrome. *Cardiol Res Pract* 2014: 943162, 2014.

27. **Kim JY, Min JY, Baek JM, Ahn SJ, Jun HY, Yoon KH, Choi MK, Lee MS, and Oh J**. CTRP3 acts as a negative regulator of osteoclastogenesis through AMPK-c-Fos-NFATc1 signaling *in vitro* and RANKL-induced calvarial bone destruction in *vivo*. *Bone* 79: 242-251, 2015.

28. **Kim MJ, Park EJ, Lee W, Kim JE, and Park SY**. Regulation of the transcriptional activation of CTRP3 in chondrocytes by c-Jun. *Mol Cell Biochem* 368: 111-117, 2012.

29. **Klonisch T, Glogowska A, Thanasupawat T, Burg M, Krcek J, Pitz M, Jaggupilli A, Chelikani P, Wong GW, and Hombach-Klonisch S**. Structural commonality of C1q Tumor Necrosis Factor-related proteins and their potential to activate RXFP1 signaling pathways in cancer cells. *Br J Pharmacol* 2016.

30. **Kopp A, Bala M, Buechler C, Falk W, Gross P, Neumeier M, Scholmerich J, and Schaffler A**. C1q/TNF-related protein-3 represents a novel and endogenous lipopolysaccharide antagonist of the adipose tissue. *Endocrinology* 151: 5267-5278, 2010.

31. **Kopp A, Bala M, Weigert J, Buchler C, Neumeier M, Aslanidis C, Scholmerich J, and Schaffler A**. Effects of the new adiponectin paralogous protein CTRP-3 and of LPS on cytokine release from monocytes of patients with type 2 diabetes mellitus. *Cytokine* 49: 51-57, 2010.

32. **Lara-Castro C, Luo N, Wallace P, Klein RL, Garvey WT.** Adiponectin multimeric complexes and themetabolic syndrome trait cluster. Diabetes 55: 249-259, 2006.

33. **Lei X, Li Q, Rodriguez S, Tan SY, Seldin MM, McLenithan JC, Jia W, and Wong GW**. Thromboxane synthase deficiency improves insulin action and attenuates adipose tissue fibrosis. *Am J Physiol Endocrinol Metab* 308: E792-804, 2015.

34. **Li D, Wu Y, Tian P, Zhang X, Wang H, Wang T, Ying B, Wang L, Shen Y, and Wen F**. Adipokine CTRP-5 as a Potential Novel Inflammatory Biomarker in Chronic Obstructive Pulmonary Disease. *Medicine (Baltimore)* 94: e1503, 2015.

35. **Li JM, Zhang X, Nelson PR, Odgren PR, Nelson JD, Vasiliu C, Park J, Morris M, Lian J, Cutler BS, and Newburger PE**. Temporal evolution of gene expression in rat carotid artery following balloon angioplasty. *J Cell Biochem* 101: 399-410, 2007.

36. **Li W, Cowley A, UludagM,Gur T,McWilliam H, Squizzato S, Park YM, Buso N, LopezR.**The EMBL-EBI bioinformatics web and programmatic tools framework. Nucleic Acids Res 43: W580-W584, 2015.

37. **Li X, Jiang L, Yang M, Wu Y, Sun S, and Sun J**. GLP-1 receptor agonist increases the expression of CTRP3, a novel adipokine, in 3T3-L1 adipocytes through PKA signal pathway. *J Endocrinol Invest* 38: 73-79, 2015.

38. **Li X, Jiang L, Yang M, Wu YW, Sun JZ, and Sun SX**. CTRP3 improves the insulin sensitivity of 3T3-L1 adipocytes by inhibiting inflammation and ameliorating insulin signalling transduction. *Endokrynol Pol* 65: 252-258, 2014.

39. **Li X, Jiang L, Yang M, Wu YW, Sun SX, and Sun JZ**. CTRP3 modulates the expression and secretion of adipokines in 3T3-L1 adipocytes. *Endocr J* 61: 1153-1162, 2014.

40. **Li X, Jiang L, Yang M, Wu YW, Sun SX, and Sun JZ**. Expression of CTRP3, a novel adipokine, in rats at different pathogenic stages of type 2 diabetes mellitus and the impacts of GLP-1 receptor agonist on it. *J Diabetes Res* 2014: 398518, 2014.

41. **Li Y, Ozment T, Wright GL, and Peterson JM**. Identification of Putative Receptors for the Novel Adipokine CTRP3 Using Ligand-Receptor Capture Technology. *Plos One* 11: e0164593, 2016.

42. **Lin S, Ma S, Lu P, Cai W, Chen Y, and Sheng J**. Effect of CTRP3 on activation of adventitial fibroblasts induced by TGF-beta1 from rat aorta *in vitro*. *Int J Clin Exp Pathol* 7: 2199-2208, 2014.

43. **Maeda T, Abe M, Kurisu K, Jikko A, and Furukawa S**. Molecular cloning and characterization of a novel gene, CORS26, encoding a putative secretory protein and its possible involvement in skeletal development. *J Biol Chem* 276: 3628-3634, 2001.

44. **Maeda T, Jikko A, Abe M, Yokohama-Tamaki T, Akiyama H, Furukawa S, Takigawa M, and Wakisaka S**. Cartducin, a paralog of Acrp30/adiponectin, is induced during chondrogenic differentiation and promotes proliferation of chondrogenic precursors and chondrocytes. *J Cell Physiol* 206: 537-544, 2006.

45. **Maeda T, and Wakisaka S**. CTRP3/cartducin is induced by transforming growth factor-beta1 and promotes vascular smooth muscle cell proliferation. *Cell Biol Int* 34: 261-266, 2010.

46. **Murayama MA, Kakuta S, Maruhashi T, Shimizu K, Seno A, Kubo S, Sato N, Saijo S, Hattori M, and Iwakura Y**. CTRP3 plays an important role in the development of collagen-induced arthritis in mice. *Biochem Biophys Res Commun* 443: 42-48, 2014.

47. **Otani M, Kogo M, Furukawa S, Wakisaka S, and Maeda T**. The adiponectin paralog C1q/TNF-related protein 3 (CTRP3) stimulates testosterone production through the cAMP/PKA signaling pathway. *Cytokine* 58: 238-244, 2012.

48. **Petersen PS, Wolf RM, Lei X, Peterson JM, and Wong GW**. Immunomodulatory roles of CTRP3 in endotoxemia and metabolic stress. *Physiol Rep* 4: 2016.

49. **Peterson JM, Aja S, Wei Z, and Wong GW**. CTRP1 protein enhances fatty acid oxidation via AMP-activated protein kinase (AMPK) activation and acetyl-CoA carboxylase (ACC) inhibition. *J Biol Chem* 287: 1576-1587, 2012.

50. **Peterson JM, Seldin MM, Wei Z, Aja S, and Wong GW**. CTRP3 attenuates diet-induced hepatic steatosis by regulating triglyceride metabolism. *Am J Physiol Gastrointest Liver Physiol* 305: G214-224, 2013.

51. **Peterson JM, Wei Z, and Wong GW**. C1q/TNF-related protein-3 (CTRP3), a novel adipokine that regulates hepatic glucose output. *J Biol Chem* 285: 39691-39701, 2010.

52. **Qu H, Deng M, Wang H, Wei H, Liu F, Wu J, and Deng H**. Plasma CTRP-3 concentrations in Chinese patients with obesity and type II diabetes negatively correlate with insulin resistance. *J Clin Lipidol* 9: 289-294, 2015.

53. **Schaffler A, Ehling A, Neumann E, Herfarth H, Paul G, Tarner I, Gay S, Buechler C, Scholmerich J, and Muller-Ladner U**. Role of specificity protein-1, PPARgamma, and pituitary protein transcription factor-1 in transcriptional regulation of the murine CORS-26 promoter. *Biochim Biophys Acta* 1678: 150-156, 2004.

54. **Schaffler A, Ehling A, Neumann E, Herfarth H, Paul G, Tarner I, Gay S, Scholmerich J, and Muller-Ladner U**. Genomic organization, promoter, amino acid sequence, chromosomal localization, and expression of the human gene for CORS-26 (collagenous repeat-containing sequence of 26-kDa protein). *Biochim Biophys Acta* 1630: 123-129, 2003.

55. **Schaffler A, Ehling A, Neumann E, Herfarth H, Tarner I, Gay S, Scholmerich J, and Muller-Ladner U**. Genomic organization, chromosomal localization and adipocytic expression of the murine gene for CORS-26 (collagenous repeat-containing sequence of 26 kDa protein). *Biochim Biophys Acta* 1628: 64-70, 2003.

56. **Schaffler A, Weigert J, Neumeier M, Scholmerich J, and Buechler C**. Regulation and function of collagenous repeat containing sequence of 26-kDa protein gene product "cartonectin". *Obesity (Silver Spring)* 15: 303-313, 2007.

57. **Scherer PE, Williams S, Fogliano M, Baldini G, and Lodish HF**. A novel serum protein similar to C1q, produced exclusively in adipocytes. *Journal of Biological chemistry* 270: 26746-26749, 1995.

58. **Schmid A, Kopp A, Aslanidis C, Wabitsch M, Muller M, and Schaffler A**. Regulation and function of C1Q/TNF-related protein-5 (CTRP-5) in the context of adipocyte biology. *Exp Clin Endocrinol Diabetes* 121: 310-317, 2013.

59. **Schmid A, Kopp A, Hanses F, Bala M, Muller M, and Schaffler A**. The novel adipokine C1q/TNF-related protein-3 is expressed in human adipocytes and regulated by metabolic and infection-related parameters. *Exp Clin Endocrinol Diabetes* 120: 611-617, 2012.

60. **Schmid A, Kopp A, Hanses F, Karrasch T, and Schaffler A**. C1q/TNF-related protein-3 (CTRP-3) attenuates lipopolysaccharide (LPS)-induced systemic inflammation and adipose tissue Erk-1/-2 phosphorylation in mice *in vivo*. *Biochem Biophys Res Commun* 452: 8-13, 2014.

61. **Seldin MM, Tan SY, and Wong GW**. Metabolic function of the CTRP family of hormones. *Rev Endocr Metab Disord* 15: 111-123, 2014.

62. **Shapiro L, and Scherer PE**. The crystal structure of a complement-1q family protein suggests an evolutionary link to tumor necrosis factor. *Current Biology* 8: 335-340, 1998.

63. **Smith SC, Jr.** Multiple risk factors for cardiovascular disease and diabetes mellitus. *Am J Med* 120: S3-S11, 2007.

64. **Su H, Yuan Y, Wang XM, Lau WB, Wang Y, Wang X, Gao E, Koch WJ, and Ma XL**. Inhibition of CTRP9, a novel and cardiac-abundantly expressed cell survival molecule, by TNFalpha-initiated oxidative signaling contributes to exacerbated cardiac injury in diabetic mice. *Basic Res Cardiol* 108: 315, 2013.

65. **Tan BK, Chen J, Hu J, Amar O, Mattu HS, Adya R, Patel V, Ramanjaneya M, Lehnert H, and Randeva HS**. Metformin increases the novel adipokine cartonectin/CTRP3 in women with polycystic ovary syndrome. *J Clin Endocrinol Metab* 98: E1891-1900, 2013.

66. **Wagner RM, Sivagnanam K, Clark WA, and Peterson JM**. Divergent relationship of circulating CTRP3 levels between obesity and gender: a cross-sectional study. *PeerJ* 4: e2573, 2016.

67. **Wang S, Zhou Y, Yang B, Li L, Yu S, Chen Y, and Zhu J**. C1q/Tumor Necrosis Factor-Related Protein-3 Attenuates Brain Injury after Intracerebral Hemorrhage via AMPK-Dependent Pathway in Rat. *Front Cell Neurosci* 10: 237, 2016.

68. **Wei Z, Peterson JM, Lei X, Cebotaru L, Wolfgang MJ, Baldeviano GC, and Wong GW**. C1q/TNF-related protein-12 (CTRP12), a novel adipokine that improves insulin sensitivity and glycemic control in mouse models of obesity and diabetes. *J Biol Chem* 287: 10301-10315, 2012.

69. **Wei Z, Peterson JM, and Wong GW**. Metabolic regulation by C1q/TNF-related protein-13 (CTRP13): activation OF AMP-activated protein kinase and suppression of fatty acid-induced JNK signaling. *J Biol Chem* 286: 15652-15665, 2011.

70. **Weigert J, Neumeier M, Schaffler A, Fleck M, Scholmerich J, Schutz C, and Buechler C**. The adiponectin paralog CORS-26 has anti-inflammatory properties and is produced by human monocytic cells. *FEBS Lett* 579: 5565-5570, 2005.

71. **Wolf RM, Lei X, Yang ZC, Nyandjo M, Tan SY, and Wong GW**. CTRP3 deficiency reduces liver size and alters IL-6 and TGFbeta levels in obese mice. *Am J Physiol Endocrinol Metab* 310: E332-345, 2016.

72. **Wolf RM, Steele KE, Peterson LA, Magnuson TH, Schweitzer MA, and Wong GW**. Lower Circulating C1q/TNF-Related Protein-3 (CTRP3) Levels Are Associated with Obesity: A Cross-Sectional Study. *PLoS One* 10: e0133955, 2015.

73. **Wolfing B, Buechler C, Weigert J, Neumeier M, Aslanidis C, Schoelmerich J, and Schaffler A**. Effects of the new C1q/TNF-related protein (CTRP-3)

"cartonectin" on the adipocytic secretion of adipokines. *Obesity (Silver Spring)* 16: 1481-1486, 2008.

74. **Wong GW, Krawczyk SA, Kitidis-Mitrokostas C, Ge G, Spooner E, Hug C, Gimeno R, and Lodish HF**. Identification and characterization of CTRP9, a novel secreted glycoprotein, from adipose tissue that reduces serum glucose in mice and forms heterotrimers with adiponectin. *FASEB J* 23: 241-258, 2009.

75. **Wong GW, Krawczyk SA, Kitidis-Mitrokostas C, Revett T, Gimeno R, and Lodish HF**. Molecular, biochemical and functional characterizations of C1q/TNF family members: adipose-tissue-selective expression patterns, regulation by PPAR-gamma agonist, cysteine-mediated oligomerizations, combinatorial associations and metabolic functions. *Biochem J* 416: 161-177, 2008.

76. **Wong GW, Wang J, Hug C, Tsao TS, and Lodish HF**. A family of Acrp30/adiponectin structural and functional paralogs. *Proc Natl Acad Sci U S A* 101: 10302-10307, 2004.

77. **Wu D, Lei H, Wang JY, Zhang CL, Feng H, Fu FY, Li L, and Wu LL**. CTRP3 attenuates post-infarct cardiac fibrosis by targeting Smad3 activation and inhibiting myofibroblast differentiation. *J Mol Med (Berl)* 93: 1311-1325, 2015.

78. **Wurm S, Neumeier M, Weigert J, Schaffler A, and Buechler C**. Plasma levels of leptin, omentin, collagenous repeat-containing sequence of 26-kDa protein (CORS-26) and adiponectin before and after oral glucose uptake in slim adults. *Cardiovasc Diabetol* 6: 7, 2007.

79. **Yanai N, Satoh T, and Obinata M**. Endothelial cells create a hematopoietic inductive microenvironment preferential to erythropoiesis in the mouse spleen. *Cell Struct Funct* 16: 87-93, 1991.

80. **Yang B, Wang S, Yu S, Chen Y, Li L, Zhang H, and Zhao Y**. C1q/tumor necrosis factor-related protein 3 inhibits oxidative stress during intracerebral hemorrhage via PKA signaling. *Brain Res* 2016.

81. **Yi W, Sun Y, Yuan Y, Lau WB, Zheng Q, Wang X, Wang Y, Shang X, Gao E, Koch WJ, and Ma XL**. C1q/tumor necrosis factor-related protein-3, a newly identified adipokine, is a novel antiapoptotic, proangiogenic, and cardioprotective molecule in the ischemic mouse heart. *Circulation* 125: 3159-3169, 2012.

82. **Yokohama-Tamaki T, Maeda T, Tanaka TS, and Shibata S**. Functional analysis of CTRP3/cartducin in Meckel's cartilage and developing condylar cartilage in the fetal mouse mandible. *J Anat* 218: 517-533, 2011.

83. **Yoo HJ, Hwang SY, Hong HC, Choi HY, Yang SJ, Choi DS, Baik SH, Bluher M, Youn BS, and Choi KM**. Implication of progranulin and C1q/TNF-related

protein-3 (CTRP3) on inflammation and atherosclerosis in subjects with or without metabolic syndrome. *PLoS One* 8: e55744, 2013.

84. **Yuasa D, Ohashi K, Shibata R, Mizutani N, Kataoka Y, Kambara T, Uemura Y, Matsuo K, Kanemura N, Hayakawa S, Hiramatsu-Ito M, Ito M, Ogawa H, Murate T, Murohara T, and Ouchi N**. C1q/TNF-related protein-1 functions to protect against acute ischemic injury in the heart. *FASEB J* 30: 1065-1075, 2016.

85. **Zhang CL, Feng H, Li L, Wang JY, Wu D, Hao YT, Wang Z, Zhang Y, and Wu LL**. Globular CTRP3 promotes mitochondrial biogenesis in cardiomyocytes through AMPK/PGC-1alpha pathway. *Biochim Biophys Acta* 1861: 3085-3094, 2016.

86. **Zhang R, Zhong L, Zhou J, and Peng Y**. Complement-C1q TNF-Related Protein 3 Alleviates Mesangial Cell Activation and Inflammatory Response Stimulated by Secretory IgA. *Am J Nephrol* 43: 460-468, 2016.

87. **Zhang Y, Proenca R, Maffei M, Barone M, Leopold L, and Friedman JM**. Positional cloning of the mouse obese gene and its human homologue. *Nature* 372: 425-432, 1994.

88. **Zhao M, Zheng S, Yang J, Wu Y, Ren Y, Kong X, Li W, and Xuan J**. Suppression of TGF-beta1/Smad signaling pathway by sesamin contributes to the attenuation of myocardial fibrosis in spontaneously hypertensive rats. *PLoS One* 10: e0121312, 2015.

89. **Zheng Q, Yuan Y, Yi W, Lau WB, Wang Y, Wang X, Sun Y, Lopez BL, Christopher TA, Peterson JM, Wong GW, Yu S, Yi D, and Ma XL**. C1q/TNF-related proteins, a family of novel adipokines, induce vascular relaxation through the adiponectin receptor-1/AMPK/eNOS/nitric oxide signaling pathway. *Arterioscler Thromb Vasc Biol* 31: 2616-2623, 2011.

90. **Zhou Y, Wang JY, Feng H, Wang C, Li L, Wu D, Lei H, Li H, and Wu LL**. Overexpression of c1q/tumor necrosis factor-related protein-3 promotes phosphate-induced vascular smooth muscle cell calcification both *in vivo* and *in vitro*. *Arterioscler Thromb Vasc Biol* 34: 1002-1010, 2014.

CHAPTER 4

IDENTIFICATION OF PUTATIVE RECEPTORS FOR THE NOVEL ADIPOKINE CTRP3 USING LIGAND-RECEPTOR CAPTURE TECHNOLOGY

Li Y [1], Ozment T [2], Wright GL [1], and Peterson JM [1,3].

[1] Department of Biomedical Sciences, Quillen College of Medicine, East Tennessee State University, Johnson City, TN [2] Department of Internal Medicine, Quillen College of Medicine, East Tennessee State University, Johnson City, TN [3] Department of Health Sciences, College of Public Health, East Tennessee State University, Johnson City, TN

This work has been published in Li et al., PLoS ONE, 11(10), 2016

ABSTRACT

C1q/TNF Related Protein 3 (CTRP3) is a member of a family of secreted proteins that exert a multitude of biological effects. Our initial work identified CTRP3's promise as an effective treatment for Nonalcoholic fatty liver disease (NAFLD). Specifically, we demonstrated that mice fed a high fat diet failed to develop NAFLD when treated with CTRP3. The purpose of this current project is to identify putative receptors which mediate the hepatic actions of CTRP3. We used Ligand-receptor glycocapture technology with TriCEPS™-based ligand-receptor capture (LRC-TriCEPS; Dualsystems Biotech AG). The LRC-TriCEPS experiment with CTRP3-FLAG protein as ligand and insulin as a control ligand was performed on the H4IIE rat hepatoma cell line. Initial analysis demonstrated efficient coupling of TriCEPS to CTRP3. Further, flow cytometry analysis (FACS) demonstrated successful oxidation and crosslinking of CTRP3-TriCEPS and Insulin-TriCEPS complexes to cell surface glycans. Demonstrating the utility of TriCEPS under these conditions, the insulin receptor was identified in the control dataset. In the CTRP3 treated cells a total enrichment of 261 peptides was observed. From these experiments 5 putative receptors for CTRP3 were identified with

two reaching statistical significance: Lysosomal-associated membrane protein 1 (LAMP-1) and Lysosome membrane protein 2 (LIMP II). Follow-up Co-immunoprecipitation analysis confirmed the association between LAMP1 and CTRP3 and further testing using a polyclonal antibody to block potential binding sites of LAMP1 prevented CTRP3 binding to the cells. The LRC-TriCEPS methodology was successful in identifying potential novel receptors for CTRP3. The identification of the receptors for CTRP3 is an important prerequisites for the development of small molecule drug candidates, of which none currently exist, for the treatment NAFLD.

INTRODUCTION

Since the discovery of leptin by Zhang *et al*. (1) many secreted bioactive molecules have been identified which originate from adipose tissue. Thus far, over 260 unique adipose tissue derived secreted proteins/peptides have been identified, collectively termed adipokines (2-5). Efforts to identify such metabolic regulators have led to the discovery of a family of secreted proteins, designated as C1q/TNF-Related Proteins, with 15 unique proteins currently identified (CTRP1-15) (6-14). C1q family proteins are characterized by a distinctive ‘globular domain’ of about 140 amino acids (the gC1q domain) (14). The CTRP proteins, adiponectin, TNF-alpha, as well as other proteins with the C1q domain are collectively referred to as the C1q/TNF superfamily (14-18). Proteins within the C1q/TNF superfamily share some structural similarities, but may have apposing functions (18). To date, many unique functions have been identified for the CTRP proteins encompassing regulatory roles in metabolism, inflammation and cell proliferation (6, 9, 15-29). Of these proteins our lab has identified a liver specific role for CTRP3 in preventing Nonalcoholic fatty liver disease (NAFLD) (29).

Adiponectin, the most widely studied member of the C1q/TNF superfamily, increases lipid oxidation in liver and skeletal muscle (16, 30-32). Unlike adiponectin or other C1q TNF related proteins, we observed no direct effect of CTRP3 on skeletal muscle *in vitro* or *in vivo* (9, 29). This implies that CTRP3 works through a novel receptor, as the three identified receptors for adiponectin are all present in skeletal muscle (33-35). In further support of this hypothesis both CTRP3 and adiponectin decrease hepatic TAG accumulation, however adiponectin reduces hepatic triglyceride levels largely through activation of AMP-activated protein kinase (AMPK) pathways (32), whereas CTRP3 did not affect AMPK phosphorylation status (9, 29). The finding of divergent downstream signaling pathways also argues that CTRP3 has a receptor distinct from adiponectin. Combined, these data indicate that CTRP3 is a distinct member of the C1q/TNF superfamily and functions through a unique receptor in liver. The receptor and the mechanism(s) responsible for the CTRP3-induced reduction in hepatic TAG accumulation remain unexplored.

LRC-TriCEPS™ is promising, novel technology recently described in Nature Protocols and Nature Biotechnology (36, 37). First published by the lab of Bernd Wollscheid, TriCEPS™ is a chemoproteomic reagent coupled to a ligand of interest (CTRP3) that acts to covalently link the ligand to the cell-based receptor (36). This linkage protects the ligand-receptor conjugate from the subsequent digestion steps and peptide level purification via the biotin tag on the TriCEPS™ molecule. The TriCEPS™ and the ligand are subsequently released through specific enzymatic cleavage and the receptor peptides are collected and analyzed by Liquid chromatography-tandem mass spectrometry (LC-MS/MS). The LRC-TriCEPS™ technique has been validated through

successful detection of known receptors, however, using this technology to identify receptors for novel proteins is still in its infancy (36, 37).

The purpose of this study was to determine if we could successful use the LRC-TriCEPS™ to identify novel potential receptors which mediate the hepatic effects of CTRP3. In brief, we were able to identify five potential novel receptors using the LRC-TriCEPS™ technique.

EXPERIMENTAL PROCEDURES

Cell culture. HEK-293T cells (Thermo fisher, GripTite 293 MSR Cell Line Cat # R79507) were cultured in Dulbecco's Modification of Eagle's Medium (DMEM) with 4.5 g/L glucose without L-glutamine and sodium pyruvate (Corning, Cat# 15-017) supplemented with 5% (v/v) fetal bovine serum (HyCloneTM, Cat# SH30088.03) and with antibiotic/antimycotic Solution (Corning, Cat# 30-004-CI). HEK-293T cells were used for transfection and protein purification protocols. H4IIE cells (H-4-II-E rat hepatoma cells, ATCC® cat# CRL-1548™, RRID:CVCL_0284) were cultured in DMEM containing 1 g/L glucose, L-glutamine, and sodium pyruvate (Corning Cat# 10-014) supplemented with 10% (v/v) fetal bovine serum (HyCloneTM, cat# SH30088.03) and with antibiotic/antimycotic Solution (Corning, Cat# 30-004-CI). H4IIE rat hepatoma cells are a well-established *in vitro* model of hepatocytes, useful for metabolic research as this cell line mirrors the liver-like, insulin regulated glucose and lipid metabolism found in the liver (38-40). Further, the CTRP3 amino acid sequence is highly conserved throughout vertebrate evolution with only 4 amino acids differing between the mouse and rat orthologs and a 95% homogeneity between mouse and human (6, 9). Therefore,

we expect that the receptor and metabolic effects of CTRP3 established in H4IIE cell line *in vitro* will provide insight to the actions of CTRP3 *in vivo*.

Protein purification. C-terminal FLAG-Tagged mouse CTRP3 and CTRP1 were produced as described previously (9, 41). Briefly, transient transfections were performed on HEK-293T cells using calcium phosphate according to standard protocols (42). At 48 h after transfection, cells were washed and then cultured in serum-free Opti-MEM I medium (Invitrogen, Cat# 51985034) supplemented with vitamin C (0.1 mg/ml; Fisher Scientific Company, Cat# FLBP351). Supernatants were collected three times, every 48 h, pooled and purified using an anti-FLAG affinity gel according to the manufacturer's protocol (Biotool.com, Cat# B23101), and eluted with 150 µg/ml FLAG peptide (Sigma, Cat# F4799). Dialysis was performed on purified proteins with 20 mM Hepes buffer (pH 8.0) containing 135 mM NaCl in a 10 kDa cut-off Slide-A-Lyzer dialysis cassette (Thermo Fisher Scientific, Cat# 88252).

Immunofluorescence. For visualization H4IIE hepatocytes were grown to confluence on Millicell EZ SLIDE (Millipore Cat# PEZGS0816) in standard growth medium. The cells treated with recombinant FLAG tagged CTRP3, CTRP1, or vehicle for 1 hr. Afterwards the cells were washed in phosphate buffered saline (PBS; 137 mM NaCl, 10 mM Phosphate, 2.7 mM KCl, ph 7.2) fixed in 4% formaldehyde diluted in PBS for 10 minutes at 37°C, washed with PBS, and then blocked in 5% Normal goat serum (diluted in PBS). The cells were then incubated with rabbit anti-FLAG (Cell Signaling Technology Cat# 14793; RRID: AB_2572291) followed by fluorochrome-conjugated secondary antibody (Cell Signaling Technology Cat# 4412 RRID: AB_1904025). Cells

were then mounted with an anti-fade mounting medium with DAPI (DAPI Fluoromount-G®; SouthernBiotech Cat# 0100-20), and immunofluorescence was visualized [Zeiss Observer.Z1].

Fatty acid oxidation. H4IIE hepatocytes were allowed to adhere to 24-well culture plates XF24 cell culture microplate (Seahorse Bioscience, Cat# 100777-004) after seeding for 2 days, according to standard protocols (Seahorse Bioscience). Cells were pre-incubated with 5 µg/ml CTRP3 or vehicle for 1 H then transferred into XF assay medium (Seahorse Bioscience, Cat# 100965-000) supplemented with 0.5mM sodium pyruvate and 5mM glucose before being placed into the XF24 Extracellular Flux Analyzer (Seahorse Bioscience XF24). The dosage of recombinant CTRP3 was selected based on our previous experimental observations (9), and is well within the common dosages reported within the literature of 2-30 µg/ml (9, 29, 43, 44). Sensor cartridge of XF24 extracellular flux assay kit (Seahorse Bioscience, Cat# 100850-001) is hydrated by loading 1ml XF calibrant (Seahorse Bioscience, Cat# 100840-000) into each well in utility plate and incubating at 37°C overnight in a non-CO_2 incubator. 200 uM palmitate conjugated to bovine serum albumin (BSA) or fatty acid free BSA (served as a vehicle control) was added in XF24 cell culture microplate at time-points indicated. A 1 mM working stock of palmitate (Sigma Cat# P5585) conjugated to 0.17 mM fatty acid free BSA (Sigma Cat# A8806) was prepared according to established protocols (Seahorse Bioscience). Briefly, 50 ml of a BSA solution (0.34 mM BSA, 150 mM NaCl, pH 7.4) was heated to 37°C and 40 ml of a palmitate solution (2.98 mM palmitate, 150 mM NaCL), heated to 70°C, and was added in 5 mL increments. The combined solution was incubated at 37°C for 1 H under constant agitation, afterwards the pH was

adjusted to 7.4 and the final volume was adjusted to 100 mL with 150 mM NaCl. Aliquots were stored until use at -20°C in glass vials.

Flow Cytometry. H4IIE hepatocytes were grown to confluence in 6-well plates (Corning Costar® Cat# 3516) and then treated with/without recombinant CTRP3-FLAG for indicated times. The cells were then collected in PBS, fixed in 4% formaldehyde, and then incubated with rabbit anti-FLAG antibody (Cell Signaling Technology, Cat# 14793; RRID: AB_2572291) followed by fluorochrome-conjugated secondary antibody (Cell Signaling Technology, Cat# 4412; RRID:AB_1904025). Next cells were suspended in buffer (0.5% Bovine Serum Albumin in PBS) and analyzed for mean fluorescent intensity (MFI) by using a FACScalibur flow cytometer with (CellQuest software, BD Biosciences). Except for the quality control step for LRC-TriCEPS (see below), all FACS experiments were performed three separate times in triplicate for each experiment. For blocking experiments cells were co-incubated with polyclonal Lysosomal-associated membrane protein 1 (LAMP-1) antibody (Santa Cruz Biotechnology Cat# sc-8098, RRID:AB_2134494)

TriCEPS™-based ligand-receptor capture (LRC-TriCEPS). In conjunction with Dualsystems Biotech AG, TriCEPS™-based ligand-receptor capture (LRC-TriCEPS; Dualsystems Biotech, cat# P05201) was utilized to identify the putative receptor for CTRP3 according to manufacturers directions. Briefly, 300 µg recombinant CTRP3-FLAG protein or Insulin (control ligand) was dissolved in 150 µl HEPES buffer (25 mM, pH 8.2) and 1.5 µl of the TriCEPS™ reagent was added to each sample and incubated for 2 H at 20°C under constant gentle agitation. After incubation 1µl of each sample was

removed to complete a Dot blot experiment as a quality control to test for efficient TriCEPS™ coupling to the ligands (data not shown). Three separate 50 mL tubes each containing 2x108 H4IIE Hepatocytes in PBS (pH 6.5) were washed and cooled to 4°C, all subsequent steps were performed at 4°C. 200 µl was collected from each tube and labeled as non-oxidized cells. Next, to mildly oxidize the cell surface proteins 1.5 mM NaIO4 was added to each tube and cells were incubated at 4°C in the dark for 15 min under gentle rotation. The cells were then washed twice at 300 x g for 5 min and then resuspended in 20 ml PBS (pH 6.5). An aliquot of ~80 µl was collected from each tube and labeled as oxidized cells. The cells were then evenly divided into 6 separate tubes and 50 µl of either TriCEPS™-coupled insulin or TriCEPS™-coupled CTRP3 was added to each tube and incubated for 90 min at 4°C under constant gentle agitation. An aliquot of ~80 µl was collected from each tube and the collected samples (non-oxidized cells, oxidized cells, insulin cells and CTRP3-FLAG cells) were analyzed by FACS to test for the crosslinking efficiency of the TriCEPS™-ligand complexes to the cell surface glycans using fluorochrome conjugated streptavidin (Thermo Fisher Scientific Inc. eBioscience Cat# 11-4317). After completion of the coupling reaction, the cells were collected and the cell pellet was sent to Dualsystems for LC-MS/MS analysis.

LC-MS/MS analysis. The samples were analyzed on a Thermo LTQ Orbitrap XL spectrometer fitted with an electrospray ion source. The samples were measured in data dependent acquisition mode in a 60 min gradient using a 10cm C18. The six individual samples in the dataset were analyzed with a statistical ANOVA model. This model assumes that the measurement error follows Gaussian distribution and views individual features as replicates of a protein's abundance and explicitly accounts for this

redundancy. It tests each protein for differential abundance in all pairwise comparisons of ligand and control samples and reports the *p*-values. Next, *p*-values are adjusted for multiple comparisons to control the experiment-wide false discovery rate (FDR). The adjusted p-value obtained for every protein is plotted against the magnitude of the fold enrichment between the two experimental conditions. Proteins are considered significant if FC>2 and adj. *p*-value<0.05.

Co-Immnunoprecipitation (Co-IP) and Immunoblot Analysis. H4IIE hepatocytes were grown to confluence in 6-well plates (Corning Costar® Cat# 3516) and then treated overnight with/without recombinant CTRP3-FLAG overnight. The cells were then washed with PBS and collected in Non-denaturing lysis buffer (20 mM Tris HCl pH 8, 137 mM NaCl, 10% glycerol, 1% Nonidet P-40, 2 mM EDTA). Cells were incubated with constant agitation for 30 minutes at 37°C and then centrifuged at 10,000xg at 4°C for 10 minutes and the supernatant was collected and protein concentration was determined via Bradford assay (Pierce Coomassie Plus Cat# 23238). Equal amounts of protein were diluted to 500 µl final volume and used for immunoprecipitation according to manufactures directions (Bimake, Anti-DYKDDDDK(Flag) Affinity Gel Cat# B23101). Total protein homogenate or immunoprecipitate were loaded and separated on a 12% Mini-Protean® TGXTM gel (Bio-Rad, Cat#456-1046) and transferred to nitrocellulose membranes (0.45 µm, Bio-Rad Cat#1620115). Membranes were blocked in 2% non-fat milk and probed with primary antibodies overnight at 4°C (Anti-LAMP1, Abcam Cat# ab24170, RRID:AB_775978; or Anti-LIMPII, Abcam Cat# ab176317, RRID: AB_2620169) followed horseradish peroxidase (HRP)-conjugated goat anti-rabbit secondary antibody (Thermo Fisher Scientific Cat# 31460, RRID:AB_228341).

Membranes were incubated with HRP Substrate (Millipore Immobilon Cat# WBKLS0100) and chemiluminescence was then visualized with FuorChem® M imager (ProteinSimple). Precision Plus Protein™ Dual Color Standards molecular weight markers were used in all immunoblot analysis (BioRad Cat#161-0374).

Statistical Analysis. For analysis of flow cytometry and fatty acid oxidation, data from each experiment were normalized to the control and the combined data from the three independent replicates was combined and analyzed with a one-way ANOVA (flow cytometry) or repeated measure ANOVA (fatty acid oxidation) followed by Tukey's multiple comparisons test Post hoc analysis. Statistics analysis were completed by Graphpad Prizm version 6.

RESULTS

CTRP3 binds and has a physiological effect on hepatoma cells

Immunohistochemical analysis was used to demonstrate that recombinant CTRP3, but not CTRP1 binds to H4IIE hepatocytes *in vitro* (Figure 4.1). Confirmatory experiments using flow cytometry demonstrated a 200% increase in mean fluorescent intensity (MFI) when cells were treated with recombinant FLAG tagged CTRP3 and probed with anti-FLAG antibodies, compared with vehicle, and fluorochrome-conjugated secondary antibody alone treatments (Figure 4.2C). Interestingly, only a subset (~20%) of H4IIE cells stained positive for CTRP3 binding. This may indicate that CTRP3 receptor surface expression is transient. For instance, it may be yoked to the cell cycle or some other parameter of cellular circumstance.

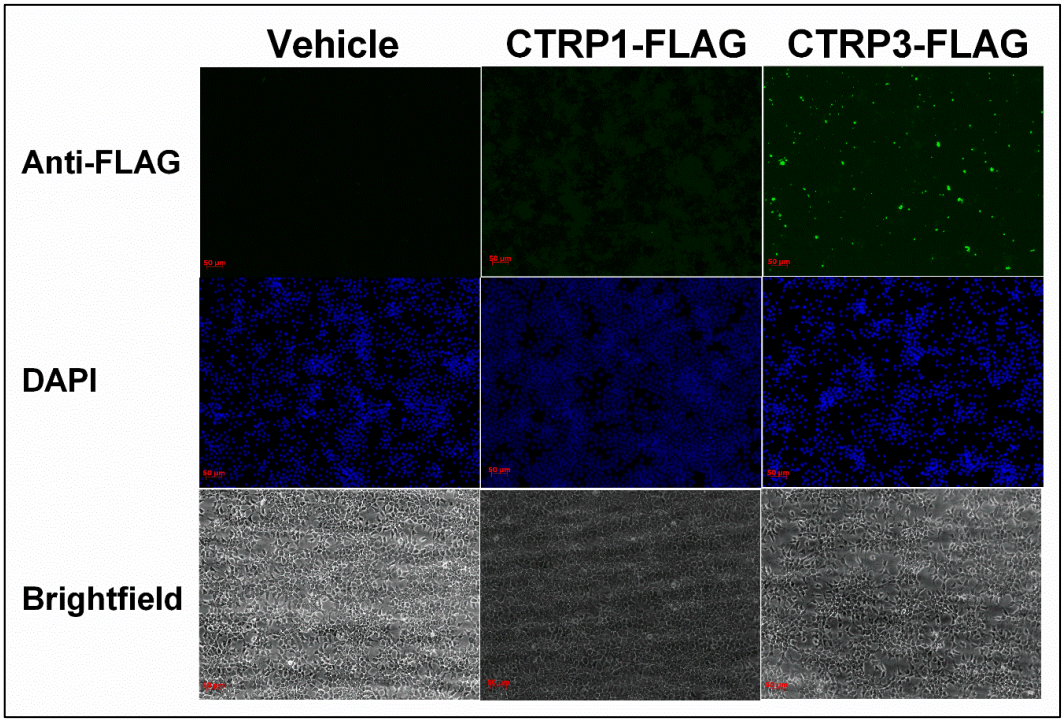

Figure 4.1: *CTRP3 Binds to Hepatocytes In Vitro*. H4IIE hepatocytes were plated on Millicell EZ SLIDE (Millipore) and allowed to adhere for 48 H in standard growth medium. The cells were treated with recombinant FLAG tagged CTRP3, CTRP1, or vehicle the cells were then incubated with rabbit anti-FLAG primary antibody followed by fluorochrome-conjugated secondary antibody. Cells were then mounted with an anti-fade mounting medium with DAPI, and immunofluorescence was visualized.

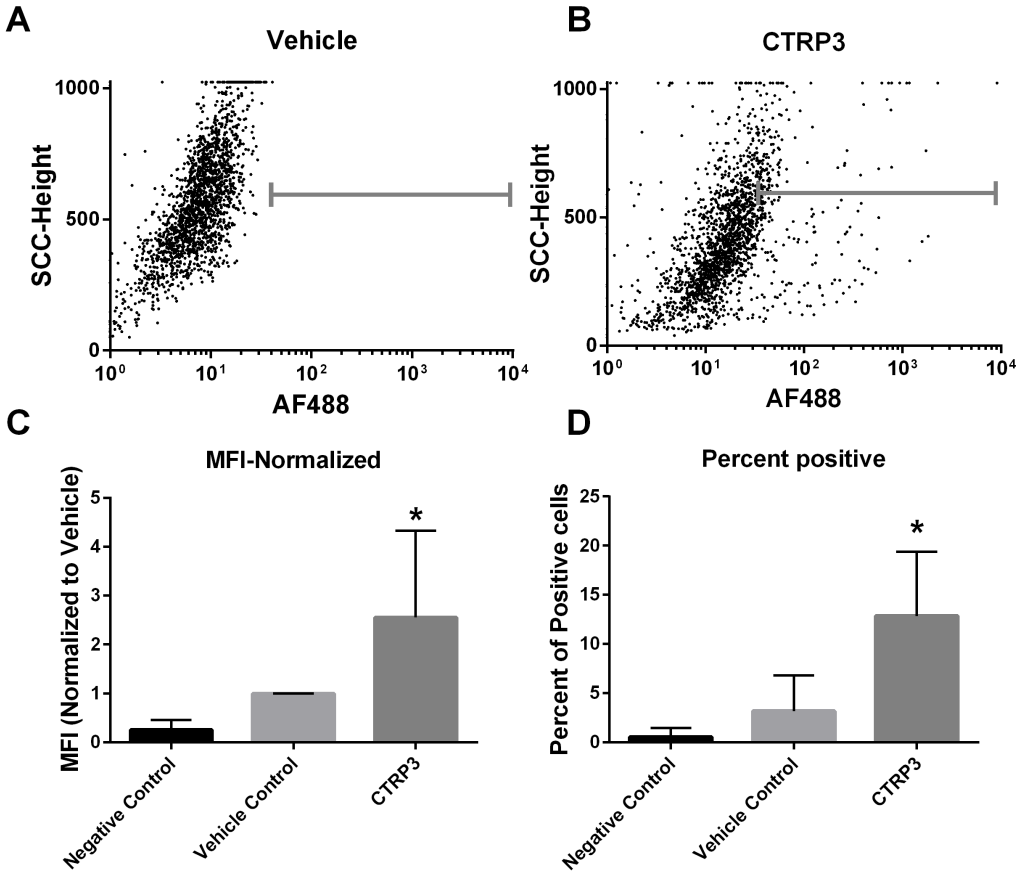

Figure 4.2: *CTRP3 Binds to Hepatocytes in Vitro.* H4IIE hepatocytes were grown in standard media and then treated for 1 H ± CTRP3-FLAG (5 µg/ml). The cells were then washed and collected in PBS, fixed in 4% formaldehyde, and then incubated with rabbit anti-FLAG antibody followed by fluorochrome-conjugated secondary antibody and analyzed for mean fluorescent intensity (MFI) by flow cytometry. Representative image (20% of points shown) of raw flow data from vehicle treated (A) or CTRP3-FLAG treated (B). C, the MFI ± CTRP3 normalized to vehicle for each independent replicate. D, Percent of the cells that were positive for each experiment. Data for figures C & D are from 3 independent replicates performed on different days with separate lots of recombinant CTRP3-FLAG protein with each replicate performed in triplicate and reported as mean ± SD. * P < vs. 0.0001 vehicle.

The next series of experiments examined the effects of CTRP3 on hepatocyte oxygen consumption to determine if the binding of CTRP3 to the hepatocytes resulted in a physiological effect. Pre-treatment with recombinant CTRP3 (5 µg/ml) had no effect

on lipid oxidation in hepatocytes under standard conditions. However, in the presence of an excess of free fatty acids (200 μM palmitate) there was 24% increase in total oxygen consumption in the CTRP3 pre-treated cells, indicating greater FFA utilization (Figure 4.3).

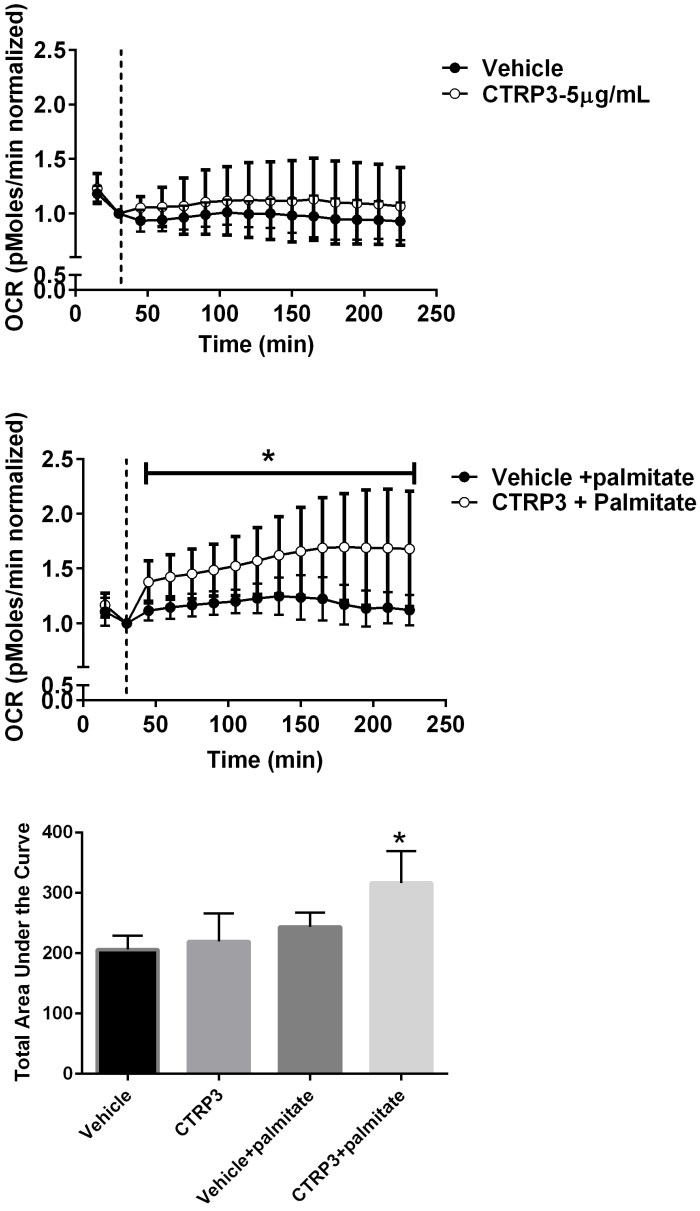

Figure 4.3: *CTRP3 Increases Oxygen Consumption.* Cells were pre-incubated with 5 µg/ml recombinant CTRP3 or vehicle for 1 H before being placed into the XFe24 Extracellular Flux Analyzer (Seahorse Bioscience) and oxygen consumption rate (OCR) was determined. OCR was measured in the absence (A) or after the addition of 200 µM palmitate (B) added at 15 minutes (vertical line). C, Area under the curve was calculated (mean OCR value at each interval*time) for each treatment. Data represents the mean ± SD. Data is pooled from 3 independent experiments each performed in triplicate, *P < 0.05 vs. vehicle + palmitate.

TriCEPS™-based ligand-receptor capture (LRC-TriCEPS)

An experiment with CTRP3-FLAG protein as a ligand and insulin as a control ligand was performed on the H4IIE rat hepatoma cell line. Control experiments to assess the technical quality were performed in parallel. Briefly, flow cytometry showed successful oxidation and crosslinking of CTRP3-TriCEPS and Insulin-Triceps to the cell surface glycans (Figure 4.4A). LC-MS/MS analysis showed a total enrichment of glycopeptides of 11% (261 peptides). Under these conditions, INSR (insulin receptor) could be identified and quantified in the control dataset. From these experiments 5 putative receptors for CTRP3 were identified with two reaching statistical significance: Lysosomal-associated membrane protein 1 (LAMP-1) and Lysosome membrane protein 2 (LIMP II) (Table 4.1 and Figure 4.4B) As LAMP1 was the promising candidate further experiments were carried out focusing on LAMP1.

Table 4.1: Table 8TriCEPS™-Based Ligand-Receptor Capture (LRC-TriCEPS)
TriCEPS™-Based Ligand-Receptor Capture (LRC-TriCEPS)

Uniprot identifier	***Protein***	***Number of peptides***	***log2FC***	***adj.pvalue***
P14562	LAMP1	4	1.00	5.79E-05
P27615	LIMPII	2	1.06	0.035
P16391	HA12	3	0.53	0.046
D3ZQ57	D3ZQ57	2	0.50	0.046
Q66HD0	ENPL	2	1.13	0.072

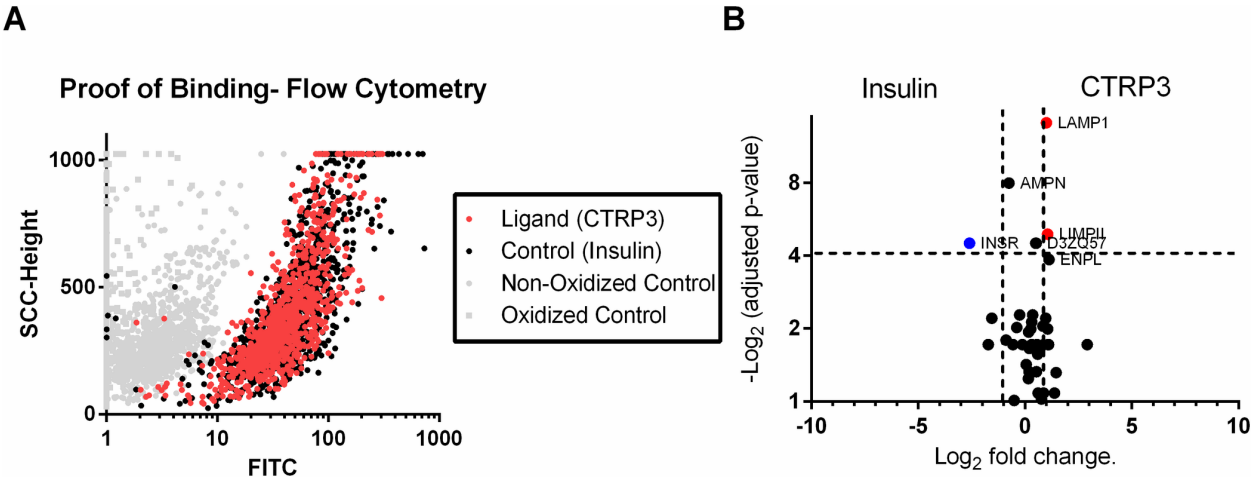

Figure 4.4: *H4IIE Rat Hepatoma Cells Were Treated With TriCEPs Conjugated to Insulin or CTRP3*. A, The binding of ligands to cell surface receptors was detected by Steptavidin FITC (The TriCEPS™ reagent contains biotin) and analyzed for mean fluorescent intensity (MFI). Representative image (20% of points shown) of raw flow data from vehicle treated. B, The samples were analyzed by Mass spectrometry (Dualsystems Biotech, AG) and the adjusted p-value (ANOVA, adjusted for multiple comparisons) for the differential abundance of each protein was plotted against the magnitude of the fold enrichment between insulin and CTRP3 samples. Proteins are considered significant if fold change >2 and P<0.05. Two proteins (LAMP1 and LIMPII) were statistically significant.

LAMP1 antibody prevents CTRP3 binding

To follow up the LRC-TriCEPS experiment we repeated the FACS experiments with the addition of a polyclonal antibody to LAMP1 in an attempt to disrupt the binding of CTRP3. The co-incubation of H4IIE cells with recombinant CTRP3 and anti-LAMP1 polyclonal antibody was found to significantly attenuate the binding of CTRP3 to H4IIE cells (Figure 4.5E and F).

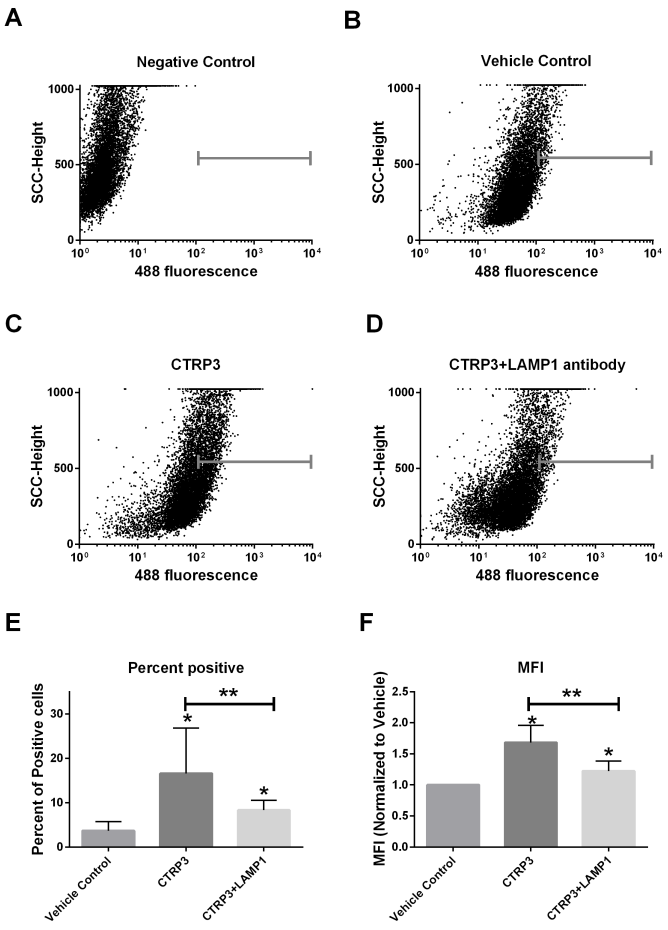

Figure 4.5: *Blocking LAMP1 Suppresses CTRP3 Binding.* H4IIE hepatocytes were grown to confluence in standard media and then treated for overnight ± CTRP3-FLAG (2.5 µg/well) and ± polyclonal LAMP1 antibody (10 µg/well, to block potential CTRP3 binding sites). The cells were then washed and collected in PBS, fixed in 4% formaldehyde, and then incubated with rabbit anti-FLAG antibody followed by fluorochrome-conjugated secondary antibody and analyzed for mean fluorescent intensity (MFI) by flow cytometry. A-D, Representative flow data from H4IIE hepatocytes. A MFI >100 was taken as positive and is indicated in the flow plots with a gray bar. A, pooled cells with no primary antibody (isotype or negative control). B, cell incubated with vehicle, C, recombinant CTRP3-FLAG protein, or D, co-incubated with recombinant CTRP3-FLAG protein plus poly-clonal anti-LAMP1. E, Percent of the cells that were positive from each experiment. F, the MFI ± CTRP3 normalized to vehicle for each independent replicate. Data for figures E & F are from 3 independent replicates performed on different days with separate lots of recombinant CTRP3-FLAG protein with each independent replicate performed in triplicate and reported as mean ± SD. * $P < 0.001$ vs. vehicle; ** $P < 0.001$ vs. CTRP3+LAMP1.

CTRP3 Co-IP

We found that treatment with CTRP3 did not affect LAMP1 protein concentration in total lysate (Figure 4.6C). To determine whether CTRP3 interacted with LAMP1 protein a Co-IP assay was performed. Immunoblot analysis was able to successfully identify LAMP1 in the CTRP3 Co-precipitate and not in the FLAG peptide or buffer only treated cells, further supporting the hypothesis that CTRP3 and LAMP1 associate *in vivo* (Figure 4.6D).

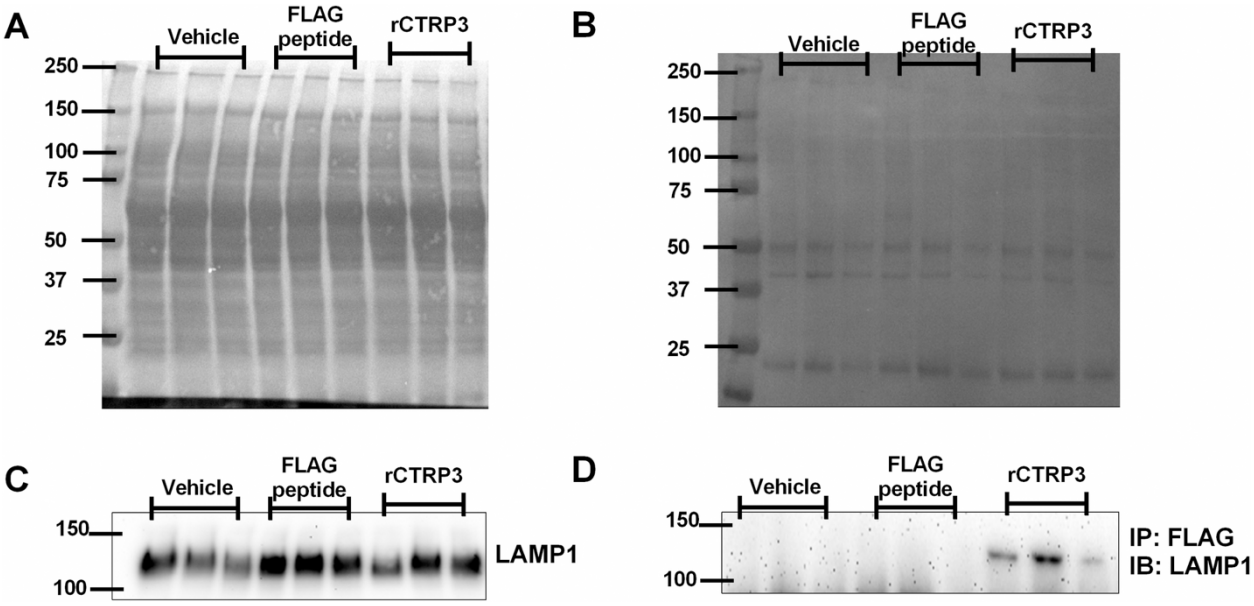

Figure 4.6: *Co-Immnunoprecipitation (Co-IP) and Immunoblot Analysis.* H4IIE cells were treated overnight with vehicle, FLAG peptide, or recombinant FLAG tagged CTRP3 (rCTRP3). Total protein homogenate (A & C) or immunoprecipitate (B & D) were separated by SDS-page gel and transferred to nitrocellulose membrane. A & B, after immunoblot total protein was visualized by brief incubation with Ponceau S staining solution (5% acetic acid & 0.1% Ponceau S). C, LAMP1 in total protein homogenate was similar between treatments. D, Co-IP results

showing LAMP1 binds to CTRP3. Samples were immunoprecipated with anti-FLAG Affinity Gel followed by immunoblotting with antibodies against LAMP1.

DISCUSSION

Summary of Findings

We successful showed using two different techniques that recombinant purified mammalian-expressed CTRP3 protein binds to the H4IIE hepatoma cells. Further, using real-time oxygen consumption data we demonstrate that pre-conditioning cells with CTRP3 increased oxygen consumption rates. Because electrons produced by free fatty acid (FFA) beta-oxidation enter the electron transport chain at the level of complex 2 while those derived from glucose enter at complex 1, a switch from glucose to FFA utilization is accompanied by higher oxygen consumption rates (45, 46). Theoretically, the switch from glucose to FFA should cause ~30% increase in OCR (46, 47), if ATP turnover remains unchanged. The ~24% increase observed in oxygen consumption supports previous findings that CTRP3 increases FFA oxidation in hepatocytes (29). Lastly, the LRC-TriCEPS experiments successfully identified and quantified statistically two proteins as targets for CTRP3: LAMP1 and LIMPII. Additionally, 3 other potential candidates were identified, and although there were not statistically quantified they were reported as putative receptors (Table 4.1). Follow-up experiments with an anti-LAMP1 polyclonal antibody partially attenuated the binding of CTRP3 to the cells and Co-IP experiments further confirmed that LAMP1 associates with CTRP3.

Study Limitations

Although we were successfully able to identify potential proteins which act as the receptor to mediate the effects of CTRP3 there are some study limitations that need to be addressed. This study used an immortalized cell line as a model for hepatocytes.

H4IIE cells were chosen because they are a commonly used liver cell culture line that maintains characteristics of intact liver cells and we have shown previously that CTRP3 had a physiological response in these cells (i.e. reduced neutral lipid accumulation (29)). Further, the LRC-TriCEPS protocol requires isolated cells and isolation of hepatocytes from intact liver requires enzymatic dissociation which by definition disrupts cell surface proteins. Future visualization and co-localization studies using intact liver will need to be performed. Additionally, binding and lipid oxidation experiments with primary hepatocytes also need to be performed. Lastly, the identification of putative receptors that are not exclusively expressed in hepatocytes still leaves open the possibility that the liver-specific *in vivo* effects of CTRP3 (29) are mediated through indirect mechanisms and not necessarily through direct actions of CTRP3 on hepatocytes.

Hepatic function of CTRP3

Previous work has shown that the novel adipokine CTRP3 has a potent biological effect on the liver (9, 29). Briefly, both transgenic overexpression of CTRP3 and daily administration of recombinant CTRP3 reduced diet-induced hepatic triglyceride accumulation (29). Further, acute injections of recombinant CTRP3 significantly lowered hepatic gluconeogenesis up to 8 H post injection (9). However, the mechanism by which CTRP3 attenuates hepatic triglyceride levels or gluconeogenesis is unknown. Due to the similarity of CTRP3 and other members of the CTRP family to adiponectin it has been suggested that the actions of all members of the CTRP family are mediated through the adiponectin receptors: T-cadherin, and adiponectin receptors 1 and 2 (35, 48). However, our previous work suggests that CTRP3 works through a

novel mechanism, as unlike adiponectin, CTRP3 did not increase hepatic AMPK phosphorylation (9, 29, 32). Moreover, we observed no effect of CTRP3 treatment in skeletal muscle, which has all three of the known receptors for adiponectin (9, 33, 34). Lastly, we have shown that CTRP3 but not CTRP1 binds to hepatocytes *in vitro* (Figure 4.2), which supports our hypothesis that CTRP3 is a distinctive member of the C1q/TNF superfamily and functions through a unique receptor.

Functions of LAMP1 and LIMPII

LAMP1 [Uniprot identifier P14562 (Figure 4.7)] is also known as 120 kDa lysosomal membrane glycoprotein (LGP-120) and CD107 antigen-like family member A (CD107a). LAMP1 was initially characterized as a type 1 integral lysosomal membrane glycoprotein that is found in a wide variety of tissues (including the liver) and is commonly used as a lysosomal marker (49, 50). However more recently it has been reported that LAMP1 also shuttles to the plasma membrane, indicating that it could act as a cell surface receptor (51, 53). Further, ~5% of the total LAMP1 protein is located on the plasma membrane due to lysosomal fusion (51, 54). The transient nature of LAMP1 plasma membrane associate could explain why, in a theoretically homologous cell culture population, only about 15–20% of the cells appeared to be positive for CTRP3 binding (Figure 4.1 and 4.2). Regardless, we were able to show that pretreatment with CTRP3 was sufficient to induce a significant increase in oxygen consumption. Although LAMP1, in addition to LAMP2, account for ~50% of lysosomal membrane proteins (49) the exact function for LAMP1 remains elusive, as LAMP1 knockout mice do not appear to have any functional or structural abnormality (49, 52). Currently, it is believed that LAMP1 is partly responsible for maintaining lysosomal integrity and function (49), and

plasma membrane expression of LAMP1 may play a role in tumor cell differentiation and metastasis (49). The potential role of LAMP1 in mediating hepatic lipid oxidation has not been explored.

A

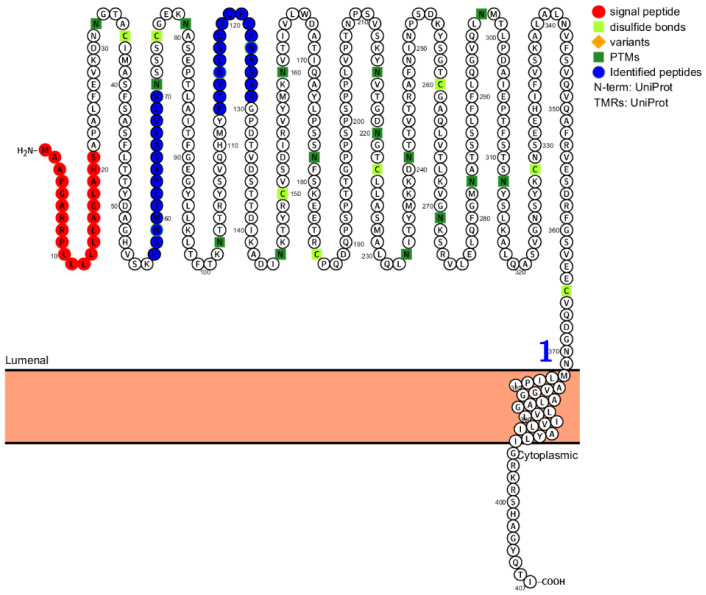

B

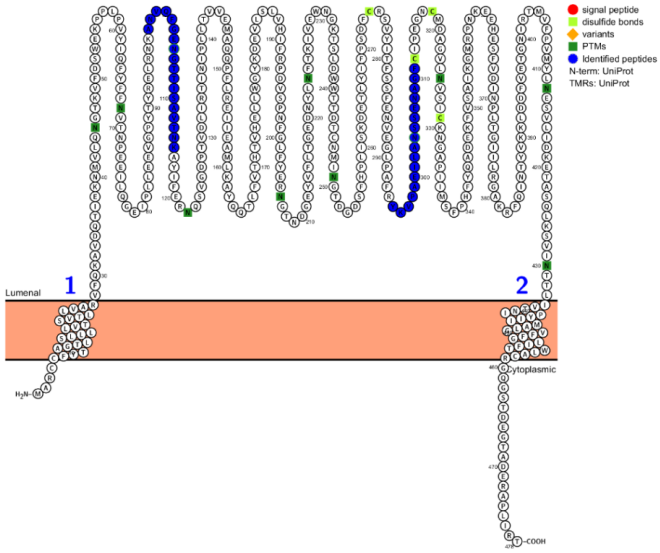

Figure 4.7: *Protter Visualization of Identified Peptide*. The identified peptides of LAMP1 (A) and LIMP II (B) are visualized with Protter [62]. Identified peptide sequences are signified by blue circles.

Lysosome membrane protein 2 (LIMPII, Uniprot identifier P27615) is also known as Scavenger receptor class B member 2 (SCRB2), 85 kDa lysosomal membrane sialoglycoprotein (LGP85), and as CD36 antigen-like 2. LIMPII was first discovered in a rat liver lysosomal fraction (55) and accounts for ~4% of all lysomal proteins (56). Although the presence of LIMPII on the plasma membrane of hepatocytes has not been examined, LIMPII has been shown to be essential in the cell-to-cell adhesion of the plasma membrane of cardiac myocytes (intercalated discs) (57). Although the exact function in metabolism for LIMPII is unknown the closely related protein Scavenger receptor class B member 3 (SCARB3, also known asCD36/FAT) has been implicated in hepatic insulin resistance (58, 59) and immunity (60), both functions implicated with CTRP3. Like SCARB3, LIMPII has been shown to bind to the adhesive glycoprotein thrombospondin-1 (56), which may help mediate cell-to-cell interactions. LIMPII is primarily expressed in the liver, placenta, adrenal cortex and adrenal gland (50) and has already been implicated as an internal receptor responsible for shuttling the enzyme glucocerebrosidase to the lysosome. Glucocerebrosidase metabolizes the sphingolipid glucocerebroside, and when deficient results in Gaucher disease (or the excessive accumulation of the lipid molecule glucocerebroside in cells (i.e. hepatocytes) (61).

Although lacking known cellular signaling functions, both LAMP1 and LIMPII are expressed in hepatic cells, where they are potentially positioned to interact with CTRP3. Further, both of these proteins can be found on the cell surface however, they may act as a co-receptor for an as-yet-unidentified signaling receptor through which CTRP3 transmits metabolic signals.

SUMMARY AND CONCLUSION

Previous work has shown that the novel adipokine CTRP3 has a potent biological effect on the liver (9, 29). However, the mechanism by which CTRP3 attenuates hepatic triglyceride levels is unknown. The purpose of this study was to determine if we could successfully use the relatively new methodological approach, LRC-TriCEPS™ method, to identify potential receptors, which mediate the biological effects of CTRP3. We have successfully identified two potential novel receptors using the LRC-TriCEPS™ technique: LAMP1 and LIMPII. Although, the intracellular signaling mechanism remains unknown the identification of the receptors for CTRP3 and other members of this family is an important prerequisite of the development of small molecule drug candidates that work through CTRP3 receptors to exert effects beneficial to human health.

REFERENCES

1. **Zhang Y, Proenca R, Maffei M, Barone M, Leopold L, Friedman JM.** Positional cloning of the mouse obese gene and its human homologue. *Nature.* 1994;372(6505):425-32.

2. **Conde J, Scotece M, Gomez R, Lopez V, Gomez-Reino JJ, Lago F, *et al*.** Adipokines: biofactors from white adipose tissue. A complex hub among inflammation, metabolism, and immunity. *Biofactors.* 2011;37(6):413-20.

3. **Pardo M, Roca-Rivada A, Seoane LM, Casanueva FF.** Obesidomics: contribution of adipose tissue secretome analysis to obesity research. *Endocrine.* 2012;41(3):374-83.

4. **Alvarez-Llamas G, Szalowska E, de Vries MP, Weening D, Landman K, Hoek A, *et al*.** Characterization of the human visceral adipose tissue secretome. *Mol Cell Proteomics.* 2007;6(4):589-600.

5. **Lehr S, Hartwig S, Lamers D, Famulla S, Muller S, Hanisch FG, *et al*.** Identification and validation of novel adipokines released from primary human adipocytes. *Mol Cell Proteomics.* 2012;11(1):M111 010504.

6. **Wong GW, Wang J, Hug C, Tsao TS, Lodish HF.** A family of Acrp30/adiponectin structural and functional paralogs. *Proc Natl Acad Sci.* 2004;101(28):10302-7.

7. **Seldin MM, Peterson JM, Byerly MS, Wei Z, Wong GW.** Myonectin (CTRP15), a novel myokine that links skeletal muscle to systemic lipid homeostasis. *J Biol Chem.* 2012;287(15):11968-80.

8. **Peterson JM, Seldin MM, Tan SY, Wong GW.** CTRP2 overexpression improves insulin and lipid tolerance in diet-induced obese mice. *PLoS One.* 2014;9(2):e88535.

9. **Peterson JM, Wei Z, Wong GW.** C1q/TNF-related protein-3 (CTRP3), a novel adipokine that regulates hepatic glucose output. *J Biol Chem.* 2010;285(51):39691-701.

10. **Byerly MS, Swanson R, Wei Z, Seldin MM, McCulloh PS, Wong GW.** A central role for C1q/TNF-related protein 13 (CTRP13) in modulating food intake and body weight. *PLoS One.* 2013;8(4):e62862.

11. **Wei Z, Peterson JM, Lei X, Cebotaru L, Wolfgang MJ, Baldeviano GC, *et al*.** C1q/TNF-related protein-12 (CTRP12), a novel adipokine that improves insulin sensitivity and glycemic control in mouse models of obesity and diabetes. *J Biol Chem.* 2012;287(13):10301-15.

12. **Wei Z, Peterson JM, Wong GW.** Metabolic regulation by C1q/TNF-related protein-13 (CTRP13): activation OF AMP-activated protein kinase and suppression of fatty acid-induced JNK signaling. *J Biol Chem.* 2011;286(18):15652-65.

13. **Wei Z, Seldin MM, Natarajan N, Djemal DC, Peterson JM, Wong GW.** C1q/tumor necrosis factor-related protein 11 (CTRP11), a novel adipose stroma-derived regulator of adipogenesis. *J Biol Chem.* 2013;288(15):10214-29.

14. **Wong GW, Krawczyk SA, Kitidis-Mitrokostas C, Revett T, Gimeno R, Lodish HF.** Molecular, biochemical and functional characterizations of C1q/TNF family members: adipose-tissue-selective expression patterns, regulation by PPAR-gamma agonist, cysteine-mediated oligomerizations, combinatorial associations and metabolic functions. *Biochem J.* 2008;416(2):161-77.

15. **Davis KE, Scherer PE.** Adiponectin: no longer the lone soul in the fight against insulin resistance? *Biochemical Journal.* 2008;416(2):e7-e9.

16. **Pajvani UB, Du X, Combs TP, Berg AH, Rajala MW, Schulthess T, *et al*.** Structure-function studies of the adipocyte-secreted hormone Acrp30/adiponectin implications for metabolic regulation and bioactivity. *J Biol Chem.* 2003;278(11):9073-85.

17. **Scherer PE, Williams S, Fogliano M, Baldini G, Lodish HF.** A novel serum protein similar to C1q, produced exclusively in adipocytes. *J Biol Chem.* 1995;270(45):26746-9.

18. **Shapiro L, Scherer PE.** The crystal structure of a complement-1q family protein suggests an evolutionary link to tumor necrosis factor. *Current Biology.* 1998;8(6):335-40.

19. **Lasser G, Guchhait P, Ellsworth JL, Sheppard P, Lewis K, Bishop P, *et al*.** C1qTNF-related protein-1 (CTRP-1): a vascular wall protein that inhibits collagen-induced platelet aggregation by blocking VWF binding to collagen. *Blood.* 2006;107(2):423-30.

20. **Wong GW, Krawczyk SA, Kitidis-Mitrokostas C, Ge G, Spooner E, Hug C, *et al*.** Identification and characterization of CTRP9, a novel secreted glycoprotein, from adipose tissue that reduces serum glucose in mice and forms heterotrimers with adiponectin. *FASEB J.* 2009;23(1):241-58.

21. **Compton SA, Cheatham B.** CTRP-3: blocking a toll booth to obesity-related inflammation. *Endocrinology.* 2010;151(11):5095-7.

22. **Yokohama-Tamaki T, Maeda T, Tanaka TS, Shibata S.** Functional analysis of CTRP3/cartducin in Meckel's cartilage and developing condylar cartilage in the fetal mouse mandible. *J Anat.* 2011;218(5):517-33.

23. **Enomoto T, Ohashi K, Shibata R, Higuchi A, Maruyama S, Izumiya Y, *et al*.** Adipolin/C1qdc2/CTRP12 protein functions as an adipokine that improves glucose metabolism. *J Biol Chem.* 2011;286(40):34552-8.

24. **Otani M, Kogo M, Furukawa S, Wakisaka S, Maeda T.** The adiponectin paralog C1q/TNF-related protein 3 (CTRP3) stimulates testosterone production through the cAMP/PKA signaling pathway. *Cytokine.* 2012;58(2):238-44.

25. **Seldin MM, Tan SY, Wong GW.** Metabolic function of the CTRP family of hormones. *Rev Endocr Metab Disord.* 2014;15(2):111-23.

26. **Lin S, Ma S, Lu P, Cai W, Chen Y, Sheng J.** Effect of CTRP3 on activation of adventitial fibroblasts induced by TGF-beta1 from rat aorta *in vitro*. *Int J Clin Exp Pathol.* 2014;7(5):2199-208.

27. **Petersen PS, Wolf RM, Lei X, Peterson JM, Wong GW.** Immunomodulatory roles of CTRP3 in endotoxemia and metabolic stress. *Physiol Rep.* 2016;4(5).

28. **Li Y, Geng X, Wang H, Cheng G, Xu S.** CTRP9 Ameliorates Pulmonary Arterial Hypertension Through Attenuating Inflammation and Improving Endothelial Cell Survival and Function. *J Cardiovasc Pharmacol.* 2016;67(5):394-401.

29. **Peterson JM, Seldin MM, Wei Z, Aja S, Wong GW.** CTRP3 attenuates diet-induced hepatic steatosis by regulating triglyceride metabolism. *Am J Physiol Gastrointest Liver Physiol.* 2013;305(3):G214-24.

30. **Xu A, Wang Y, Keshaw H, Xu LY, Lam KS, Cooper GJ.** The fat-derived hormone adiponectin alleviates alcoholic and nonalcoholic fatty liver diseases in mice. *The Journal of clinical investigation*. 2003;112(1):91-100.

31. **Asterholm IW, Scherer PE.** Enhanced metabolic flexibility associated with elevated adiponectin levels. *The American journal of pathology.* 2010;176(3):1364-76.

32. **Tomas E, Tsao T-S, Saha AK, Murrey HE, cheng Zhang C, Itani SI, *et al*.** Enhanced muscle fat oxidation and glucose transport by ACRP30 globular domain: Acetyl–CoA carboxylase inhibition and AMP-activated protein kinase activation. *Proc Natl Acad Sci.* 2002;99(25):16309-13.

33. **Yamauchi T, Kamon J, Ito Y, Tsuchida A, Yokomizo T, Kita S, *et al.*** Cloning of adiponectin receptors that mediate antidiabetic metabolic effects. *Nature.* 2003;423(6941):762-9.

34. **Hug C, Wang J, Ahmad NS, Bogan JS, Tsao T-S, Lodish HF.** T-cadherin is a receptor for hexameric and high-molecular-weight forms of Acrp30/adiponectin. *Proc Natl Acad Sci.* 2004;101(28):10308-13.

35. **Hug C, Wang J, Ahmad NS, Bogan JS, Tsao TS, Lodish HF.** T-cadherin is a receptor for hexameric and high-molecular-weight forms of Acrp30/adiponectin. *Proc Natl Acad Sci.* 2004;101(28):10308-13.

36. **Frei AP, Moest H, Novy K, Wollscheid B.** Ligand-based receptor identification on living cells and tissues using TRICEPS. *Nature protocols.* 2013;8(7):1321-36.

37. **Frei AP, Jeon O-Y, Kilcher S, Moest H, Henning LM, Jost C, *et al*.** Direct identification of ligand-receptor interactions on living cells and tissues. *Nature biotechnology.* 2012;30(10):997-1001.

38. **Granner D, Andreone T, Sasaki K, Beale E.** Inhibition of transcription of the phosphoenolpyruvate carboxykinase gene by insulin. *Nature.* 1983;305(5934):549-51.

39. **Wolfla CE, Ross RA, Crabb DW.** Induction of alcohol dehydrogenase activity and mRNA in hepatoma cells by dexamethasone. *Arch Biochem Biophys.* 1988;263(1):69-76.

40. **Hectors TL, Vanparys C, Pereira-Fernandes A, Knapen D, Blust R.** Mechanistic evaluation of the insulin response in H4IIE hepatoma cells: new endpoints for toxicity testing? *Toxicol Lett.* 2012;212(2):180-9.

41. **Peterson JM, Aja S, Wei Z, Wong GW.** CTRP1 protein enhances fatty acid oxidation via AMP-activated protein kinase (AMPK) activation and acetyl-CoA carboxylase (ACC) inhibition. *J Biol Chem.* 2012;287(2):1576-87.

42. **Kingston RE, Chen CA, Okayama H.** Calcium phosphate transfection. *Curr Protoc Immunol.* 2001;Chapter 10:Unit 10 3.

43. **Hou Q, Lin J, Huang W, Li M, Feng J, Mao X.** CTRP3 Stimulates Proliferation and Anti-Apoptosis of Prostate Cells through PKC Signaling Pathways. *PLoS One.* 2015;10(7):e0134006.

44. **Maeda T, Jikko A, Abe M, Yokohama-Tamaki T, Akiyama H, Furukawa S, *et al*.** Cartducin, a paralog of Acrp30/adiponectin, is induced during chondrogenic differentiation and promotes proliferation of chondrogenic precursors and chondrocytes. *J Cell Physiol.* 2006;206(2):537-44.

45. **Leverve X, Batandier C, Fontaine E.** Choosing the right substrate. *Novartis Found Symp.* 2007;280:108-21; discussion 21-7, 60-4.

46. **Lodish HF.** *Molecular cell biology.* 7th ed. New York: W.H. Freeman and Co.; 2013. xxxiii, 1154-58.

47. **Ferrick DA, Neilson A, Beeson C.** Advances in measuring cellular bioenergetics using extracellular flux. *Drug Discov Today.* 2008;13(5-6):268-74.

48. **Yamauchi T, Kamon J, Ito Y, Tsuchida A, Yokomizo T, Kita S, *et al*.** Cloning of adiponectin receptors that mediate antidiabetic metabolic effects. *Nature.* 2003;423(6941):762-9.

49. **Eskelinen EL.** Roles of LAMP-1 and LAMP-2 in lysosome biogenesis and autophagy. *Mol Aspects Med.* 2006;27(5-6):495-502.

50. **Su AI, Wiltshire T, Batalov S, Lapp H, Ching KA, Block D, *et al*.** A gene atlas of the mouse and human protein-encoding transcriptomes. *Proc Natl Acad Sci.* 2004;101(16):6062-7.

51. **Lippincott-Schwartz J, Fambrough DM.** Cycling of the integral membrane glycoprotein, LEP100, between plasma membrane and lysosomes: kinetic and morphological analysis. *Cell.* 1987;49(5):669-77.

52. **Andrejewski N, Punnonen EL, Guhde G, Tanaka Y, Lullmann-Rauch R, Hartmann D, *et al*.** Normal lysosomal morphology and function in LAMP-1-deficient mice. *J Biol Chem.* 1999;274(18):12692-701.

53. **Rodriguez A, Webster P, Ortego J, Andrews NW.** Lysosomes behave as Ca^{2+}-regulated exocytic vesicles in fibroblasts and epithelial cells. *J Cell Biol.* 1997;137(1):93-104.

54. **Kima PE, Burleigh B, Andrews NW.** Surface-targeted lysosomal membrane glycoprotein-1 (Lamp-1) enhances lysosome exocytosis and cell invasion by Trypanosoma cruzi. *Cell Microbiol.* 2000;2(6):477-86.

55. **Lewis V, Green SA, Marsh M, Vihko P, Helenius A, Mellman I.** Glycoproteins of the lysosomal membrane. *J Cell Biol.* 1985;100(6):1839-47.

56. **Crombie R, Silverstein R.** Lysosomal integral membrane protein II binds thrombospondin-1. Structure-function homology with the cell adhesion molecule CD36 defines a conserved recognition motif. *J Biol Chem.* 1998;273(9):4855-63.

57. **Schroen B, Leenders JJ, van Erk A, Bertrand AT, van Loon M, van Leeuwen RE, *et al*.** Lysosomal integral membrane protein 2 is a novel component of the cardiac intercalated disc and vital for load-induced cardiac myocyte hypertrophy. *J Exp Med.* 2007;204(5):1227-35.

58. **Corpeleijn E, van der Kallen CJ, Kruijshoop M, Magagnin MG, de Bruin TW, Feskens EJ, *et al*.** Direct association of a promoter polymorphism in the CD36/FAT fatty acid transporter gene with Type 2 diabetes mellitus and insulin resistance. *Diabet Med.* 2006;23(8):907-11.

59. **Glazier AM, Scott J, Aitman TJ.** Molecular basis of the Cd36 chromosomal deletion underlying SHR defects in insulin action and fatty acid metabolism. *Mamm Genome.* 2002;13(2):108-13.

60. **Silverstein RL, Febbraio M.** CD36, a scavenger receptor involved in immunity, metabolism, angiogenesis, and behavior. *Sci Signal.* 2009;2(72):re3.

61. **Gonzalez A, Valeiras M, Sidransky E, Tayebi N.** Lysosomal integral membrane protein-2: a new player in lysosome-related pathology. *Mol Genet Metab.* 2014;111(2):84-91.

CHAPTER 5

SUMMARY & FUTURE DIRECTIONS

HIF-1α

The studies described in the proceeding chapters provided insight into the cellular mechanisms by which HIF-1α and CTRP3 mediate metabolic changes to combat stress. HIF-1α remodels metabolism to confer ischemic cardioprotection. In the present studies, enhanced glycolytic flux in HIF-1α hearts *ex vivo* was indicated by significantly higher ^{13}C-labeled lactic acid accumulation as ischemia progressed (0 to 30 mins). Additionally, phosphorylation of glycogen synthase was significantly upregulated by HIF-1α. Because phosphorylation deactivates GS, this favors glycogenolysis in the ischemic heart. These findings are consistent with our previous data that lactate released into the perfusate was significantly elevated following ischemia of HIF-1α heart at 30 mins (J. Wu et al. 2013). In spite of the increase of glycolytic flux, paradoxically, we found that ^{13}C-labeled glycogen (glucose reserves) levels were maintained at pre-ischemic levels in HIF-1α hearts for up to 30 mins of ischemia, whereas glycogen levels were depleted after 5 mins of ischemia in WT hearts. In addition, the rate of ^{13}C-Glucose incorporation into glycogen is maintained at pre-ischemic levels in HIF-1α hearts for up to 30 mins of ischemia while becoming undetectable in WT hearts. Combined these findings suggest that HIF-1α is responsible for an unexpected source of glucose that contributes to the glucose:glycogen turnover during no-flow ischemia in heart. Further, our experiments demonstrated that HIF-1α triggers myocardial gluconeogenesis in response to ischemia. Specifically, we observed gluconeogenetic intermediates [m+3] isotopologues such as glucose-6-phosphate, fructose-6-phosphate,

and fructose 1,6-bisphosphate were only present in the HIF-1α ischemic hearts. The only theoretical source of the [m+3] molecules is from catabolism of the U-$^{13}C_6$ glucose (all six carbons are ^{13}C-labeled) and the derived metabolites combining with endogenous unlabeled glucose-derived metabolites (Consult Figure. 2.3).

Taken together, our data indicates that HIF-1α triggers active myocardial gluconeogenesis to enhance glucose:glycogen turnover and subsequent ATP production in response to ischemic stress. We surmise that the glycolytic ATP production provides energy in a compartmentalized fashion for ionic sarcolemmal function (i.e. Na^+-K^+ pump), thus promoting cellular ionic homeostasis. Without maintaining cellular ionic homeostasis, the cell membrane integrity would quickly degrade and the cell would die. Therefore, these studies identify a novel cardioprotective mechanism for cardiomyocytes exposed to prolonged ischemic stress.

These results also suggest that the steps of gluconeogenesis that is induced by HIF-1α, is the point where pyruvate is converted to OAA via pyruvate carboxylase (PC) for anaplerotic carboxylation rather than at the pyruvate dehydrogenase (PDH) reaction. This warrants further investigation.

We have previously described several metabolic pathways upregulated by HIF-1α possibly contribute to the energetic supply for gluconeogenesis in this model. For example, HIF-1α induces fumarate respiration allowing the cardiomyocyte to use fumarate as a terminal electron acceptor instead of O_2 to sustain anaerobic mitochondrial polarization. In another alternative pathway leading to the synthesis of major metabolic end product succinate under anaerobic conditions, GTP is produced

from the conversion of α-ketoglutarate to succinate via substrate level phosphorylation (Hochachka et al. 1975). Our data show higher GTP levels in HIF-1α hearts at 30 min of ischemia, compared to WT.

Future Studies with HIF-1α

Taken together, we show that HIF-1α-induced gluconeogenesis in myocardia could contribute to the ischemic cardioprotection. Work on the very large metabolomics dataset will continued. Specific gluconeogenesis inhibitors exist. Future studies will utilize these these inhibitors to establish that the maintenance of glycolysis and glycogen reserves in HIF-1α hearts is dependent upon glyconeogenesis. Loss of ischemic tolerance of the HIF-1α heart upon the blockade of gluconeogenesis would establish the cardioprotective role of this pathway. In addition, the use of ^{13}C labeled glucogenic amino acids will be employed to probe the carbon backbone source of the synthesized glucose in the HIF-1α hearts.

CTRP3

Although, we initially proposed that CTRP3 would also be cardioprotective, our studies indicate that CTRP3 overexpression does not promote cardiofunctional recovery and tissue viability in ischemic mouse heart. These data suggest that CTRP3 does not confer specific protective effect in myocardia, at least in this *ex vivo* model of hypoxic injury. However, CTRP3 transgenic mice failed to develop high fat diet-induced hepatic steatosis (Peterson et al. 2013). To pursue this further we investigated the CTRP3 specific effects in the lipid-overloaded hepatocyte.

As a polypeptide adipokine, after being released from adipocytes into blood, CTRP3 must reach the liver and bind to a receptor in hepatocytes to exert its regulative effects on hepatic lipid metabolism and inflammation. Our first set of experiments led to the successful identification of putative CTRP3 receptors, LAMP-1 and LIMP II, which may mediate hepatic metabolism. Further, we demonstrated that in the presence of excess fatty acids CTRP3 significantly enhance fatty acid utilization by hepatocytes. Thus, here CTRP3-induced fatty acids oxidation protects H4IIE hepatocytes against potential metabolic stress from lipid accumulation.

Future Studies with CTRP3

The specific function of LAMP1 is unknown and LAMP1 knockout animals do not present with an observable phenotype when fed standard chow diet (Andrejewski et al. 1999). Experiments with high-fat feeding with LAMP1 knockout animals have not been performed, and we propose that the loss of LAMP1 will ameliorate the hepato-protective effect of CTRP3. Further, as LAMP1 is not exclusive to hepatocytes (LAMP1 is also found on macrophages) CTRP3 may act through blocking lipid-induced inflammation on the macrophages and hepatocytes. Therefore, future studies should be performed to identify whether CTRP3 binds directly to macrophages as well. Lastly, as there is no known intracellular signaling pathway initiated by LAMP1 it could be that the binding of CTRP3 to LAMP1 is essential for inhibiting the binding of ligand to a separate receptor. In support of this CTRP3 has been shown to block lipopolysaccharides (LPS) from activating the Toll-like receptor 4 in isolated macrophages, even though CTRP3 did not bind directly to either the Toll-like receptor 4 or LPS (Kopp et al. 2010). Future

studies should be performed with macrophages and hepatocytes from LAMP1 knockout animals to test this potential mechanism.

Conclusion

Both HIF-1α and CTRP3 regulate metabolism and offer tissue specific protection to various stressors.

REFERENCES

Ahmed MH, Barakat S, Almobarak AO. 2012. Nonalcoholic fatty liver disease and cardiovascular disease: Has the time come for cardiologists to be hepatologists? J Obes. Epub 483135.

Andrejewski N, Punnonen EL, Guhde G, Tanaka Y, Lüllmann-Rauch R, Hartmann D, Von Figura K, Saftig P. 1999. Normal lysosomal morphology and function in LAMP-1-deficient mice. J Biol Chem. 274*,* 12692–12701.

Ballestri S, Nascimbeni F, Romagnoli D, Lonardo A. 2016. The independent predictors of non-alcoholic steatohepatitis and its individual histological features.: Insulin resistance, serum uric acid, metabolic syndrome, alanine aminotransferase and serum total cholesterol are a clue to pathogenesis and candidate targets for treatment. Hepatol Res. 46, 1074–1087.

Bertout JA, Patel SA, Simon MC. 2008. The impact of O_2 availability on human cancer. Nat Rev Cancer. 8, 967–975.

Cai Z, Zhong H, Bosch-Marce M, Fox-Talbot K, Wang L, Wei C, Trush MA, Semenza GL. 2008. Complete loss of ischaemic preconditioning-induced cardioprotection in mice with partial deficiency of HIF-1α. Cardiovasc Res. 77, 463–470.

Carmeliet P, Dor Y, Herbert JM, Fukumura D, Brusselmans K, Dewerchin M, Neeman M, Bono F, Abramovitch R, Maxwell P, et al. 1998. Role of HIF-1alpha in hypoxia-mediated apoptosis, cell proliferation and tumour angiogenesis. Nature. 394, 485–490.

Corcoran SE, O'Neill LAJ. 2016. HIF1α and metabolic reprogramming in inflammation. J Clin Invest. 126, 3699–3707.

Cramer T, Yamanishi Y, Clausen BE, Förster I, Pawlinski R, Mackman N, Haase VH, Jaenisch R, Corr M, Nizet V, et al. 2003. HIF-1α is essential for myeloid cell-mediated inflammation. Cell. 112, 645–657.

Dames SA, Martinez-Yamout M, De Guzman RN, Dyson HJ, Wright PE. 2002. Structural basis for Hif-1 /CBP recognition in the cellular hypoxic response. Proc Natl Acad Sci. 99, 5271–5276.

Elkins JM, Hewitson KS, McNeill LA, Seibel JF, Schlemminger I, Pugh CW, Ratcliffe PJ, Schofield CJ. 2003. Structure of factor-inhibiting hypoxia-inducible factor (HIF) reveals mechanism of oxidative modification of HIF-1α. J Biol Chem. 278, 1802–1806.

Forsythe JA, Jiang BH, Iyer N V, Agani F, Leung SW, Koos RD, Semenza GL. 1996.

Activation of vascular endothelial growth factor gene transcription by hypoxia-inducible factor 1. Mol Cell Biol. 16, 4604–4613.

Freedman SJ, Sun Z-YJ, Poy F, Kung AL, Livingston DM, Wagner G, Eck MJ. 2002. Structural basis for recruitment of CBP/p300 by hypoxia-inducible factor-1 . Proc Natl Acad Sci. 99, 5367–5372.

Gerber HP, Condorelli F, Park J, Ferrara N. 1997. Differential transcriptional regulation of the two vascular endothelial growth factor receptor genes. Flt-1, but not Flk-1/KDR, is up-regulated by hypoxia. J Biol Chem. 272, 23659–23667.

Guo Y, Jones WK, Xuan YT, Tang XL, Bao W, Wu WJ, Han H, Laubach VE, Ping P, Yang Z, et al. 1999. The late phase of ischemic preconditioning is abrogated by targeted disruption of the inducible NO synthase gene. Proc Natl Acad Sci U S A. 96, 11507–11512.

Hewitson KS, McNeill LA, Riordan M V., Tian YM, Bullock AN, Welford RW, Elkins JM, Oldham NJ, Bhattacharya S, Gleadle JM, et al. 2002. Hypoxia-inducible factor (HIF) asparagine hydroxylase is identical to factor inhibiting HIF (FIH) and is related to the cupin structural family. J Biol Chem. 277, 26351–26355.

Huang LE, Gu J, Schau M, Bunn HF. 1998. Regulation of hypoxia-inducible factor 1 is mediated by an O_2-dependent degradation domain via the ubiquitin-proteasome pathway. Proc Natl Acad Sci. 95, 7987–7992.

Hochachka PW, Owen TG, Allen JF, Whittow GC. 1975. Multiple end products of anaerobiosis in diving vertebrates. Comp. Biochem. Physiol. Part B Comp. Biochem. 50, 17–22.

Ivan M, Kondo K, Yang H, Kim W, Valiando J, Ohh M, Salic A, Asara JM, Lane WS, Kaelin J. 2001. HIFα targeted for VHL-mediated destruction by proline hydroxylation: Implications for O_2 sensing. Science. 292, 464–468.

Iyer NV, Kotch LE, Agani F, Leung SW, Laughner E, Wenger RH, Gassmann M, Gearhart JD, Lawler a M, Yu a Y, et al. 1998. Cellular and developmental control of O_2 homeostasis by hypoxia-inducible factor 1 alpha. Genes Dev. 12, 149–162.

Jaakkola P, Mole DR, Tian YM, Wilson MI, Gielbert J, Gaskell SJ, Von Kriegsheim A, Hebestreit HF, Mukherji M, Schofield CJ, et al. 2001. Targeting of HIF-α to the von Hippel-Lindau ubiquitylation complex by O_2-regulated prolyl hydroxylation. Science. 292, 468–472.

Jung F, Palmer L a, Zhou N, Johns R a. 2000. Hypoxic regulation of inducible nitric oxide synthase via hypoxia inducible factor-1 in cardiac myocytes. Circ Res. 86, 319–325.

Kopp A, Bala M, Buechler C, Falk W, Gross P, Neumeier M, Schölmerich J, Schäffler A. 2010. C1q/TNF-related protein-3 represents a novel and endogenous lipopolysaccharide antagonist of the adipose tissue. Endocrinology. 151, 5267–5278.

Lando D, Peet DJ, Gorman JJ, Whelan DA, Whitelaw ML, Bruick RK. 2002. FIH-1 is an asparaginyl hydroxylase enzyme that regulates the transcriptional activity of hypoxia-inducible factor. Genes Dev. 16, 1466–1471.

Lando D, Peet DJ, Whelan DA, Gorman JJ, Whitelaw ML. 2002. Asparagine hydroxylation of the HIF transactivation domain: A hypoxic switch. Science. 295, 858–861.

Li J-M, Zhang X, Nelson PR, Odgren PR, Nelson JD, Vasiliu C, Park J, Morris M, Lian J, Cutler BS, et al. 2007. Temporal evolution of gene expression in rat carotid artery following balloon angioplasty. J Cell Biochem. 101, 399–410.

Li Y, Wright GL, Peterson JM. 2017. C1q/TNF-related protein 3 (CTRP3) function and regulation. Compr Physiol. 7, 863–878.

Liu Y, Cox SR, Morita T, Kourembanas S. 1995. Hypoxia regulates vascular endothelial growth factor gene expression in endothelial cells: Identification of a 5’ enhancer. Circ Res. 77, 638–643.

Mahon PC, Hirota K, Semenza GL. 2001. FIH-1: A novel protein that interacts with HIF-1α and VHL to mediate repression of HIF-1 transcriptional activity. Genes Dev. 15, 2675–2686.

Maxwell PH, Wlesener MS, Chang GW, Clifford SC, Vaux EC, Cockman ME, Wykoff CC, Pugh CW, Maher ER, Ratcliffe PJ. 1999. The tumour suppressor protein VHL targets hypoxia-inducible factors for oxygen-dependent proteolysis. Nature. 399, 271–275.

Murry CE, Jennings RB, Reimer KA. 1986. Preconditioning with ischemia: A delay of lethal cell injury in ischemic myocardium. Circulation. 74, 1124–1136.

Ockaili R. 2005. HIF-1 activation attenuates postischemic myocardial injury: role for heme oxygenase-1 in modulating microvascular chemokine generation. AJP Hear Circ Physiol. 289, 542–548.

Perla F, Prelati M, Lavorato M, Visicchio D, Anania C. 2017. The Role of Lipid and Lipoprotein Metabolism in Non-Alcoholic Fatty Liver Disease. Children. 4, 46.

Peterson JM, Seldin MM, Wei Z, Aja S, Wong GW. 2013. CTRP3 attenuates diet-induced hepatic steatosis by regulating triglyceride metabolism. AJP Gastrointest

Liver Physiol. 305, 214–224.

Peterson JM, Wei Z, Wong GW. 2010. C1q/TNF-related protein-3 (CTRP3), a novel adipokine that regulates hepatic glucose output. J Biol Chem. 285, 39691–39701.

Rosenberg JH, Werner JH, Moulton MJ, Agrawal DK. 2018. Current Modalities and Mechanisms Underlying Cardioprotection by Ischemic Conditioning. J Cardiovasc Transl Res. Online ISSN 1937–5395.

Salceda S, Caro J. 1997. Hypoxia-inducible factor 1α (HIF-1α) protein is rapidly degraded by the ubiquitin-proteasome system under normoxic conditions. Its stabilization by hypoxia depends on redox-induced changes. J Biol Chem. 272, 22642–22647.

Sarkar K, Cai Z, Gupta R, Parajuli N, Fox-Talbot K, Darshan MS, Gonzalez FJ, Semenza GL. 2012. Hypoxia-inducible factor 1 transcriptional activity in endothelial cells is required for acute phase cardioprotection induced by ischemic preconditioning. Proc Natl Acad Sci. 109, 10504–10509.

Seagroves TN, Ryan HE, Lu H, Wouters BG, Knapp M, Thibault P, Laderoute K, Johnson RS. 2001. Transcription factor HIF-1 is a necessary mediator of the pasteur effect in mammalian cells. Mol Cell Biol. 21, 3436–3444.

Semenza GL. 2003. Targeting HIF-1 for cancer therapy. Nat Rev Cancer. 3, 721–732.

Semenza GL, Jiang BH, Leung SW, Passantino R, Concordat JP, Maire P, Giallongo A. 1996. Hypoxia response elements in the aldolase A, enolase 1, and lactate dehydrogenase a gene promoters contain essential binding sites for hypoxia-inducible factor 1. J Biol Chem. 271, 32529–32537.

Semenza GL, Wang GL. 1992. A nuclear factor induced by hypoxia via *de novo* protein synthesis binds to the human erythropoietin gene enhancer at a site required for transcriptional activation. Mol Cell Biol. 12, 5447–5454.

Vink A, Schoneveld AH, Lamers D, Houben AJS, van der Groep P, van Diest PJ, Pasterkamp G. 2007. HIF-1alpha expression is associated with an atheromatous inflammatory plaque phenotype and upregulated in activated macrophages. Atherosclerosis. 195, e69–75.

Wang GL, Jiang BH, Rue EA, Semenza GL. 1995. Hypoxia-inducible factor 1 is a basic-helix-loop-helix-PAS heterodimer regulated by cellular O2 tension. Proc Natl Acad Sci. 92, 5510–5514.

Wang GL, Semenza GL. 1995. Purification and characterization of Hypoxia-inducible Factor 1. J Biol Chem. 270, 1230–1237.

Wang GL, Semenza GL. 1996. Molecular basis of hypoxia-induced erythropoietin expression. Curr Opin Hematol. 3, 156–162.

Wolf RM, Lei X, Yang Z-C, Nyandjo M, Tan SY, Wong GW. 2016. CTRP3 deficiency reduces liver size and alters IL-6 and TGFβ levels in obese mice. Am J Physiol - Endocrinol Metab. 310, 332–345.

Wong GW, Wang J, Hug C, Tsao T-S, Lodish HF. 2004. A family of Acrp30/adiponectin structural and functional paralogs. Proc Natl Acad Sci. 101, 10302–10307.

Wu D, Lei H, Wang JY, Zhang CL, Feng H, Fu FY, Li L, Wu LL. 2015. CTRP3 attenuates post-infarct cardiac fibrosis by targeting Smad3 activation and inhibiting myofibroblast differentiation. J Mol Med. 93, 1311–1325.

Wu J, Bond C, Chen P, Chen M, Li Y, Shohet RV, Wright G. 2015. HIF-1α in the heart: Remodeling nucleotide metabolism. J Mol Cell Cardiol. 82, 194–200.

Wu J, Chen P, Li Y, Ardell C, Der T, Shohet R, Chen M, Wright GL. 2013. HIF-1alpha in heart: protective mechanisms. Am J Physiol Heart Circ Physiol. 305, 821–828.

Yi W, Sun Y, Yuan Y, Lau WB, Zheng Q, Wang X, Wang Y, Shang X, Gao E, Koch WJ, et al. 2012. C1q/tumor necrosis factor-related protein-3, a newly identified adipokine, is a novel antiapoptotic, proangiogenic, and cardioprotective molecule in the ischemic mouse heart. Circulation. 125, 3159–3169.

Zhang CL, Feng H, Li L, Wang JY, Wu D, Hao YT, Wang Z, Zhang Y, Wu LL. 2017. Globular CTRP3 promotes mitochondrial biogenesis in cardiomyocytes through AMPK/PGC-1α pathway. Biochim Biophys Acta - Gen Subj. 1861, 3805–3094.

VITA

YING LI

Education	PhD in Biomedical Sciences, East Tennessee State University, Johnson City, TN 2018 MS in Neuroscience, Soochow University, Suzhou, China 2009 MD in Medicine, Yan'an University, Yan'an, China 2005
Professional Experience	Graduate Research Assistant Department of Biomedical Sciences, Quillen College of Medicine, East Tennessee State University, Johnson City, TN, 2014 – 2018 Research Technician Department of Biomedical Sciences, Quillen College of Medicine, East Tennessee State University, Johnson City, TN, 2010 – 2014 Graduate Teaching Assistant Department of Physiology, College of Medicine, Soochow University, Suzhou, China, 2007 – 2008
Selected Publications	1. Trogen, G., Bacon, J., Li, Y., Wright, G. L., Degroat, A., Hagood, K. L., Warren, Z., Forsman, A., Clark, W. A. & Peterson, J. M. (2018). Transgenic overexpression of C1q/TNF-related protein 3 (CTRP3) prevents alcohol-induced hepatic triglyceride accumulation. American Journal of Physiology-Endocrinology and Metabolism. (Accepted) 2. Li, Y., Wright, G. L., & Peterson, J. M. (2017). C1q/TNF-related protein 3 (CTRP3) function and regulation. Comprehensive Physiology, 7(3):863–878. 3. Li, Y., Ozment, T., Wright, G. L., & Peterson, J. M. (2016). Identification of putative receptors for the novel adipokine CTRP3 using ligand-receptor capture technology. PLoS ONE, 11(10).

4. Beaumont, E., Wright, G. L., Southerland, E. M., Li, Y., Chui, R., KenKnight, B. H., … Ardell, J. L. (2016). Vagus nerve stimulation mitigates intrinsic cardiac neuronal remodeling and cardiac hypertrophy induced by chronic pressure overload in guinea pig. American Journal of Physiology - Heart and Circulatory Physiology, 310(10), H1349–H1359.

5. Wu, J., Bond, C.E., Chen, P., Chen, M., Li, Y., Shohet, R. V., & Wright, G. L. (2015). HIF-1α in the heart: Remodeling nucleotide metabolism. Journal of Molecular and Cellular Cardiology, 82, 194–200.

Awards

Travel Scholarship, Resource Center for Stable Isotope Resolved Metabolomics, University of Kentucky, KY, 2017